Molecular Insights Into the SERCA – Phospholamban Regulatory Axis

by

Gareth Peter Armanious

A thesis submitted in partial fulfillment of the requirements for the degree of

Doctor of Philosophy

Department of Biochemistry

University of Alberta

©Gareth Peter Armanious, 2023

Abstract

The movement of calcium across the membranes of the sarcoplasmic reticulum (SR) is crucial in the muscle's contraction-relaxation cycle. When calcium enters the cytosol of a muscle cell from the SR, it initiates muscle contraction, while its removal by the sarco(endo)plasmic reticulum calcium ATPase (SERCA) induces muscle relaxation. SERCA's activity is regulated by Phospholamban (PLN), which can reversibly inhibit its apparent calcium affinity. This inhibition is reversed by phosphorylation of PLN through the action of protein kinase A (PKA). The significance of SERCA in heart disease has been highlighted through the discovery of hereditary mutations in the cytoplasmic and transmembrane domains of PLN. These variants, such as Arg9-Cys, Arg9-Leu, Arg9-His, deletion of Arg14 (R14-del), and truncation at Leu39 (Leu39-X) have been associated with heart disease. This thesis aims to offer valuable insights into the mechanisms of PLN variants and their ability to influence SERCA activity, in addition to probing the fundamental interactions and regulatory action of PLN on SERCA.

I examined how mutations in distinct regions of PLN important for phosphorylation, interaction with SERCA, and membrane anchoring impact the SERCA-PLN regulatory axis. In addition, I explored the fundamental ability of PLN to influence SERCA activity and how this inhibitory effect is achieved. While there are well- known disease-associated and disease-causing variants of PLN, there are many variants of uncertain significance (VUS) which have not been characterized. I sought to proactively assess PLN residue significance in the regulation of SERCA and characterize newly identified and uncharacterized PLN variants. Additionally, despite multiple crystal structures of SERCA that represent various conformations throughout the calcium transport cycle, the structure and function of PLN throughout the entirety of the SERCA transport cycle has gaps in our understanding of the mode of interaction and how PLN

exerts control on SERCA. Using sequential alanine, truncation, and selective mutagenesis of PLN, and steady-state vs. pre-steady-state SERCA activity measurements, I was able to reveal mechanistic insight into how hereditary mutations alter regulation of SERCA in addition to uncovering key residues of WT PLN of critical importance for SERCA regulation.

Using sequential truncation and alanine mutations, I discovered that PLN C-terminal residues are critical determinants of the regulatory control of SERCA, with truncation of only 1 C-terminal residue resulting in a 50% loss of regulatory control over SERCA, compared to a complete loss of function in the case of Leu39-truncation. Truncation of two or more C-terminal residues resulted in a complete loss of function akin to the PLN-null effect observed with Leu39-truncation PLN. I conclude that PLN C-terminal residues are critical for localization, oligomerization, and regulatory function. In particular, the PLN C terminus is an important determinant of the quaternary structure of the SERCA regulatory complex.

With respect to investigation of how PLN regulates SERCA, I evaluated the effects of PLN on calcium translocation and ATP hydrolysis by SERCA under conditions that mimic environments in sarcoplasmic reticulum membranes. I observed that PLN altered ATP-dependent calcium translocation by SERCA within the first transport cycle. Using pre-steady-state charge (calcium) translocation and steady-state ATPase activity under different substrate conditions (various calcium and/or ATP concentrations) promoting distinct conformational states of SERCA, we found that the effect of PLN on SERCA depends on substrate preincubation conditions. The results indicated that PLN can establish an inhibitory interaction with multiple SERCA conformational states with distinct effects on SERCA's kinetic properties. Moreover, I noted multiple modes of interaction between SERCA and PLN and observed that once a particular mode of

association is engaged it persists throughout the SERCA transport cycle and multiple turnover events, providing insights into the physiological role of PLN and its regulatory effect on SERCA transport activity.

Lastly, I focused on novel missense variants in PLN, an Ala15-Thr variant found in a 4-year-old female and a Pro21-Thr variant found in a 60 -year-old female, both with a family history and clinical diagnosis of dilated cardiomyopathy. Both patients also harboured a Val896-Met variant in cardiac myosin binding protein. The PLN variants caused defects in the function, phosphorylation, and dephosphorylation of PLN, and we classified these variants as potentially pathogenic. While the cardiac myosin binding protein variant Val896-Met has been previously classified as benign, it has the potential to be a low-risk susceptibility variant. My studies provide new evidence for missense variants previously classified as benign or VUS.

Preface

Part of the Chapter 1 introduction has been prepared for publication in The Springer Nature Singapore Pte Ltd. *Membrane Protein Complexes: Structure and Function,* Subcellular Biochemistry (Chapter 8 The SarcoEndoplasmic Reticulum Calcium ATPase) and has been revised for incorporation in the present thesis. Chapter 2 research was originally published in The Journal of Biological Chemistry and has been revised for incorporation in the present thesis to reflect all my own original work. Chapter 3 research was originally published in The Journal of Biological Chemistry and has been revised for incorporation in the present thesis to reflect all my own original work. Chapter 4 has been prepared for publication and submitted. All in vitro work is my own, with a collaborating lab performing in silico analysis by contributing the final molecular dynamics simulations. A clarifying statement precedes each chapter to denote specifics of contributions.

Acknowledgements

I would like to thank Dr. Howard Young for his mentorship. Your guidance and shared experiences have been invaluable. Thank you for being a great leader. Special thanks to my graduate committee members for challenging my knowledge and perspective throughout my research, providing feedback, and aiding in shaping my graduate program. Thank you to all of the members of the Young lab, it has been a pleasure to be trained by more experienced members, and to learn with the entirety of the Young lab. I would also like to thank my family and friends for their relentless support.

Table of Contents

List of Tables

List of Figures

List of Abbreviations

SR	Sarcoplasmic reticulum
ER	Endoplasmic reticulum
SERCA	Sarco(endo)plasmic reticulum calcium ATPase
PLN	Phospholamban
SLN	Sarcolipin
PKA	Protein kinase A
PKA-c	Catalytic subunit of PKA
DCM	Dilated cardiomyopathy
RyR	Ryanodine receptor
PMCA	Plasma membrane calcium ATPase
NCX	Sodium calcium exchanger
ATP	Adenosine triphosphate
ADP	Adenosine diphosphate
AMP	Adenosine monophosphate
cAMP	Cyclic adenosine monophosphate
P-domain	Phosphorylation domain
A-domain	Actuator domain
N-domain	Nucleotide binding domain
PDB	Protein data bank accession number
AMP-PCP	5'-adenylyl (beta,gamma-methylene)diphosphonate
SDS-PAGE	Sodium dodecyl sulfate polyacrylamide gel electrophoresis
FRET	Förster resonance energy transfer
NMR	Nuclear magnetic resonance

CaMKII	calcium/calmodulin-dependent protein kinase II
Akt	Protein kinase B
PP-1	Protein phosphatase-1
AKAP	A kinase anchoring protein
SNP	Single nucleotide polymorphism
K_{Ca}	Apparent calcium affinity
V_{max}	Maximal activity
n_H	Hill coefficient (cooperativity)
EYPC	Egg yolk phosphatidylcholine
EYPA	Egg yolk phosphatidic acid
MALDI-TOF	Matrix-assisted laser desorption/ionisation-time of flight
TCA	Trichloroacetic acid
[γ-^{32}P] ATP	Adenosine 5'-[γ-32P] triphosphate
IPTG	Isopropyl β-D-1-thiogalactopyranoside

List of Amino Acid Abbreviations

Full Name	Abbreviation (3 Letter)	Abbreviation (1 Letter)
Alanine	Ala	A
Arginine	Arg	R
Asparagine	Asn	N
Aspartate	Asp	D
Aspartate or Asparagine	Asx	B
Cysteine	Cys	C
Glutamate	Glu	E
Glutamine	Gln	Q
Glutamate or Glutamine	Glx	Z
Glycine	Gly	G
Histidine	His	H
Isoleucine	Ile	I
Leucine	Leu	L
Lysine	Lys	K
Methionine	Met	M
Phenylalanine	Phe	F
Proline	Pro	P
Serine	Ser	S
Threonine	Thr	T
Tryptophan	Trp	W
Tyrosine	Tyr	Y
Valine	Val	V

Chapter 1

Introduction

Part of this introduction has been prepared for publication in The Springer Nature Singapore Pte Ltd. *Membrane Protein Complexes: Structure and Function,* Subcellular Biochemistry (Chapter 8 The SarcoEndoplasmic Reticulum Calcium ATPase and has been revised for incorporation in the present thesis.

1.1 Why Calcium?

Many crucial cell activities are communicated by calcium. Although calcium isn't the most prevalent ion in an organism, it serves as a major signaling ion when compared to the more abundant magnesium ion. Already present in single-celled organisms, the evolution to multicellular life gave it a globally significant role. Its special coordination chemistry, which allows binding by complex molecules even in the presence of significant excesses of other cations, such as magnesium, was likely a deciding factor. Thus, it is possible to retain its free concentration within cells at the extremely low levels required for its signaling function. Many different proteins have developed the ability to bind or transport calcium. They help to buffer it within cells, or regulate it temporally or spatially, but some proteins leverage calcium as a signaling molecule. While essential for the proper operation of cellular processes, if it is not carefully managed both temporally and spatially, it can result in a variety of serious cell dysfunctions and even cell death (1,2).

1.2 Calcium & Muscle Function

Numerous cellular activities depend on the transporters and channels that carry ions across membranes. Calcium has many signaling roles in the cell and is involved in processes ranging from cell growth and development to muscle function. These processes are made possible by the maintenance of a calcium gradient across membranes that is produced by transporters and channels (2).

The contraction/relaxation cycle of muscle, the tissue that permits our bodies to move and function and our hearts to beat, is one process in which calcium plays a crucial role. Different forms of muscle exist, including cardiac, skeletal, and vascular smooth

muscle; cardiac muscle being the important target of this work. Focusing in to the functional unit of the cardiomyocyte, cardiac muscle is made up of specialized contractile units grouped as longitudinal myofibrils to produce a pattern of aligned bands that include the contractile machinery (3). The sarcomere, which is made up of thick (myosin) and thin (actin) filaments, serves as the functional unit of the myofibril. The sliding filament theory is based on the interactions between these filaments (4). These myofibrils are surrounded by the sarcolemma, the cell membrane surrounding the cardiomyocyte, and invaginations of the sarcolemma form T-tubules which are critical for conducting the signal to trigger muscle contraction (Figure 1.1).

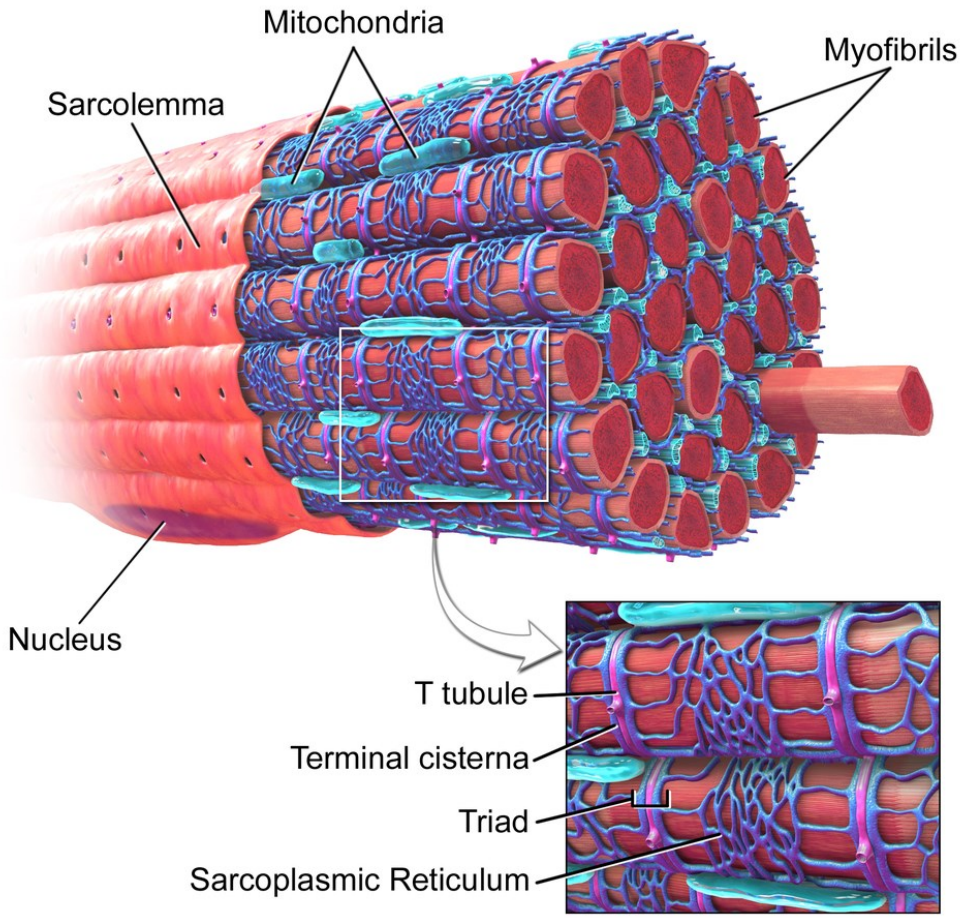

Figure 1.1. Schematic of skeletal muscle. Top: muscle fibre encapsulated by the sarcolemma. Bottom inlay: enlarged view displaying the sarcoplasmic reticulum (blue webbed structure) that surrounds the myofibrils. Image used under Creative Commons Attribution Unported License (5,6).

When muscle contraction is initiated, an action potential causes depolarization of the sarcolemma. This depolarization event is conducted to the cytoplasm via the T-tubule, an invagination of the sarcolemma which is in close proximity to the sarcoplasmic reticulum (SR) (Figure 1.1 & 1.2). A small amount of calcium enters the cell via the L-type calcium channel in the T-tubule. This entry of calcium near the SR triggers calcium release from the SR via the ryanodine receptor (7,8). This large efflux of calcium

from the SR results in a ten-fold increase in cytosolic calcium concentration, resulting in calcium-dependent activation of the contractile apparatus (Figure 1.2).

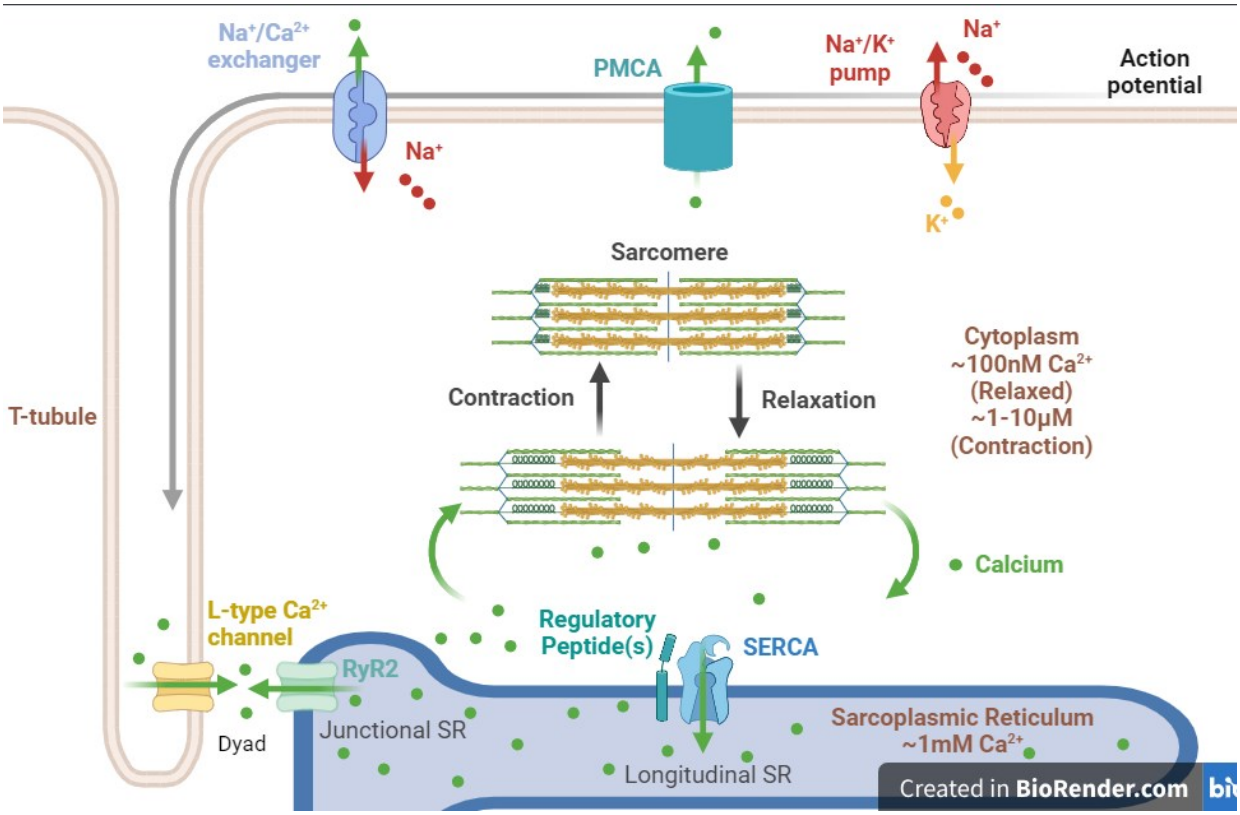

Figure 1.2. T-tubule structure. T-tubule structure displaying the key proteins involved in excitation-contraction (EC) coupling in the cardiomyocyte. Enlarged view of the t-tubule network (Figure 1.1) to illustrate positioning of EC coupling proteins. Na+ channels are opened, and the cell membrane depolarizes, thereby initiating EC coupling. This depolarization triggers the opening of voltage-gated L-type Ca^{2+}-channels (LTCCs) in the t-tubules, and subsequent Ca^{2+}-induced Ca^{2+} release from the SR through the opening of Ryanodine Receptors (RyRs). This process occurs at specialized junctions called dyads, where LTCCs and RyRs are in close proximity. After the released Ca^{2+} binds to the myofilaments to trigger contraction, Ca2+ is recycled into the SR by the sarco-endoplasmic reticulum ATPase (SERCA), and removed from the cell by the Na+-Ca2+ exchanger (NCX) and the plasma-membrane Ca^{2+} ATPase causing relaxation. Created with BioRender.com.

Once muscle contraction (systole) has taken place due to calcium-dependent activation of the contractile machinery, the calcium must be removed from the cytosol to achieve relaxation (diastole). Sarco(endo)plasmic reticulum calcium ATPase (SERCA) actively

pumps approximately 70% of the calcium back into the SR, while the remainder of the calcium is transported into the extracellular space by the plasma membrane calcium ATPase (PMCA) and the sodium calcium exchanger (NCX) (9). SERCA is reversibly regulated by small transmembrane peptide inhibitors, canonically phospholamban (PLN) and sarcolipin (SLN), although new regulators are being identified. The SR is the primary storage site for the calcium used to trigger muscle contraction, and SERCA determines the amount of calcium reserves in the SR lumen, thereby regulating the rate of relaxation and the strength of the subsequent contraction (10). It is this relationship that correlates SERCA function directly with the pumping force of the heart.

1.3 P-Type ATPases and SERCA

SERCA, a member of the P-type ATPase superfamily of active transporters, is principally responsible for moving cytosolic calcium into the SR lumen. P-type ATPases are a large family of evolutionarily related membrane proteins that are found in bacteria, archaea and eukaryotes, named due to their ability to catalyze auto-phosphorylation from ATP to power active transport (11). These integral membrane proteins are active transporters that pump a variety of ions and lipids across membranes, with SERCA being one of the most well-studied P-Type ATPases. SERCA is found in all eukaryotic cells where it is responsible for maintaining the low cytosolic calcium concentration by transporting calcium ions across the ER and SR membranes. For SERCA, ATP hydrolysis is coupled to the translocation of two calcium ions across the SR membrane against their concentration gradient. For every two calcium ions transported into the SR lumen, SERCA counter-transports two-to-three protons out of the SR lumen. Though, no proton

gradient is established because of this counter-transport as the SR is leaky to protons (12).

1.4 SERCA Gene Isoforms and Expression Patterns

Our understanding of the function of SERCA is attributed specifically to SERCA1a, the isoform readily isolated from rabbit fast-twitch skeletal muscle. The structure and function of SERCA1a is thought to be representative of the entire family of P-Type ATPases (13).

In vertebrates, there are three highly conserved genes that encode SERCA pumps (SERCA1-3 or ATP2A1-3) which give rise to multiple splice variants. These alternative splicing of transcripts occur mainly in the C-terminus of the protein, and result in at least twelve currently known isoforms (14,15) (Table 1.1).

Table 1.1. Tissue-specific expression of SERCA isoforms.

Isoform	Tissue
SERCA 1a	Adult fast-twitch skeletal muscle
SERCA 1b	Neonatal fast-twitch skeletal muscle
SERCA 2a, 2c	Cardiac and slow-twitch skeletal muscle
SERCA 2b	Ubiquitous. All tissues including skeletal, cardiac, and smooth muscle, as well as non-muscle
SERCA 2d	Skeletal Muscle
SERCA 3a-f	Non-muscle tissue, cardiomyocytes

These SERCA isoforms have tissue- and developmental-specificity, which is consistent with their varied functionalities. Two splice variants of the fast-twitch skeletal muscle seen in adult (SERCA1a; 994 residues) and fetal-neonatal (SERCA1b; 1001 residues) tissues are encoded by the SERCA1 gene. Only seven extra residues at the C-terminus

separate the functionally identical SERCA1a and SERCA1b isoforms from one another. The longer C-terminus of SERCA1b lacks a defined structure or function, however it is highly charged and might be involved in the growth of skeletal muscle (16). The short extension identified in SERCA1b may modify function during the transition from fetal to adult skeletal muscle throughout development.

The SERCA2 gene encodes both the cardiac 2a and 2c isoforms and the ubiquitous 2b isoform (17). All cell types express SERCA2b, but only cardiac muscle, slow-twitch skeletal muscle, and smooth muscle cells express SERCA2a. In humans, SERCA2a and SERCA2b encode proteins of 997 and 1042 amino acids, respectively. The addition of 45 amino acids at the C-terminus, providing SERCA2b an additional transmembrane helix that positions the C-terminus on the other side of the membrane in the SR lumen, distinguishes these two isoforms from one another. Among the SERCA isoforms, SERCA2b has the highest calcium affinity thanks to its lumenal tail and eleventh transmembrane helix (18). The SERCA2c isoform is expressed in cardiac muscle, and this isoform has a novel truncated C-terminus (19). Lastly, the SERCA2d isoform has been identified in skeletal muscle, although its implications are unknown (20).

The SERCA3 gene encodes the most splice variants with six isoforms (SERCA3 a-f). SERCA3 isoforms are expressed in non-muscle tissues, however it has also been found in cardiac muscle (20). SERCA3 is thought to modulate cytosolic calcium and ER calcium reserves differently than SERCA1 and SERCA2 via its fast action with low calcium affinity. The possible combinations of SERCA isoforms and unique expression patterns allow for distinct physiological features as a function of tissue type. The highly conserved nature of SERCA guides sensitivity of all isoforms to sub-nanomolar inhibition by the plant-derived sesquiterpene thapsigargin (21). In contrast, other P-type ATPases such as the sodium pump are relatively insensitive to inhibition by thapsigargin. It is

believed that the sequence differences between SERCA1, SERCA2, SERCA3, and their splice variants entail slight structural changes that result in subtle variances in the calcium affinities and turnover rates of the various isoforms. For example, although SERCA2b is a slower, higher-affinity calcium pump, SERCA3 isoforms are faster, lower-affinity calcium pumps. Changes in ER and SR calcium handling at the level of cell-specific functioning and development are explained by the minor structural variations present in the several SERCA isoforms. A unique splice variation and sequence divergence found in the ubiquitous SERCA2b isoform is the exception to this rule. In SERCA2b, an additional 11th transmembrane helix gives it a greater affinity for calcium and produces a lumenal C-terminus that could sense and react to the ER environment (22).

Comparing fast-twitch skeletal and cardiac muscle provides insight into the tissue specificity and functional implications of SERCA isoforms. Fast-twitch skeletal muscle contracts quickly and forcefully in response to voluntary impulse, and is the predominant source of sudden, powerful bursts of movement like kicking. In contrast, cardiac muscle contracts more slowly, with variable force over a wide dynamic range, and with continuous involuntary and rhythmic cadence. The primary SERCA isoform in fast twitch skeletal muscle is SERCA1a and the cardiac muscle isoform is SERCA2a. Prior work comparing SERCA1a and SERCA2a has shown that SERCA1a has a similar affinity for calcium to SERCA2a and a peak activity that is roughly twice that of SERCA2a (23). The density of SERCA1a is higher in skeletal muscle SR than SERCA2a is in cardiac muscle SR, lending itself well to purification for functional investigation. There are multiple factors that differentiate fast-twitch skeletal muscle from cardiac muscle, but these tissue-specific differences in SERCA allow skeletal muscle to achieve a faster rate

of calcium reuptake into the SR. Skeletal and cardiac myocytes contain multiple SERCA isoforms, likely leading to additional functional diversity as a function of cell type.

1.5 SERCA Structural Information

The transmembrane topology and tertiary structure of SERCA isoforms are projected to be conserved and similar. SERCA1a from rabbit skeletal muscle has become a canonical example for the P-type ATPase family due to the Toyoshima lab's publication of the first crystal structure of SERCA with bound calcium ions (24). SERCA has since become the target of multiple structural studies which have revealed a significant amount of SERCA's conformational changes throughout the calcium transport reaction cycle (Figure 1.3).

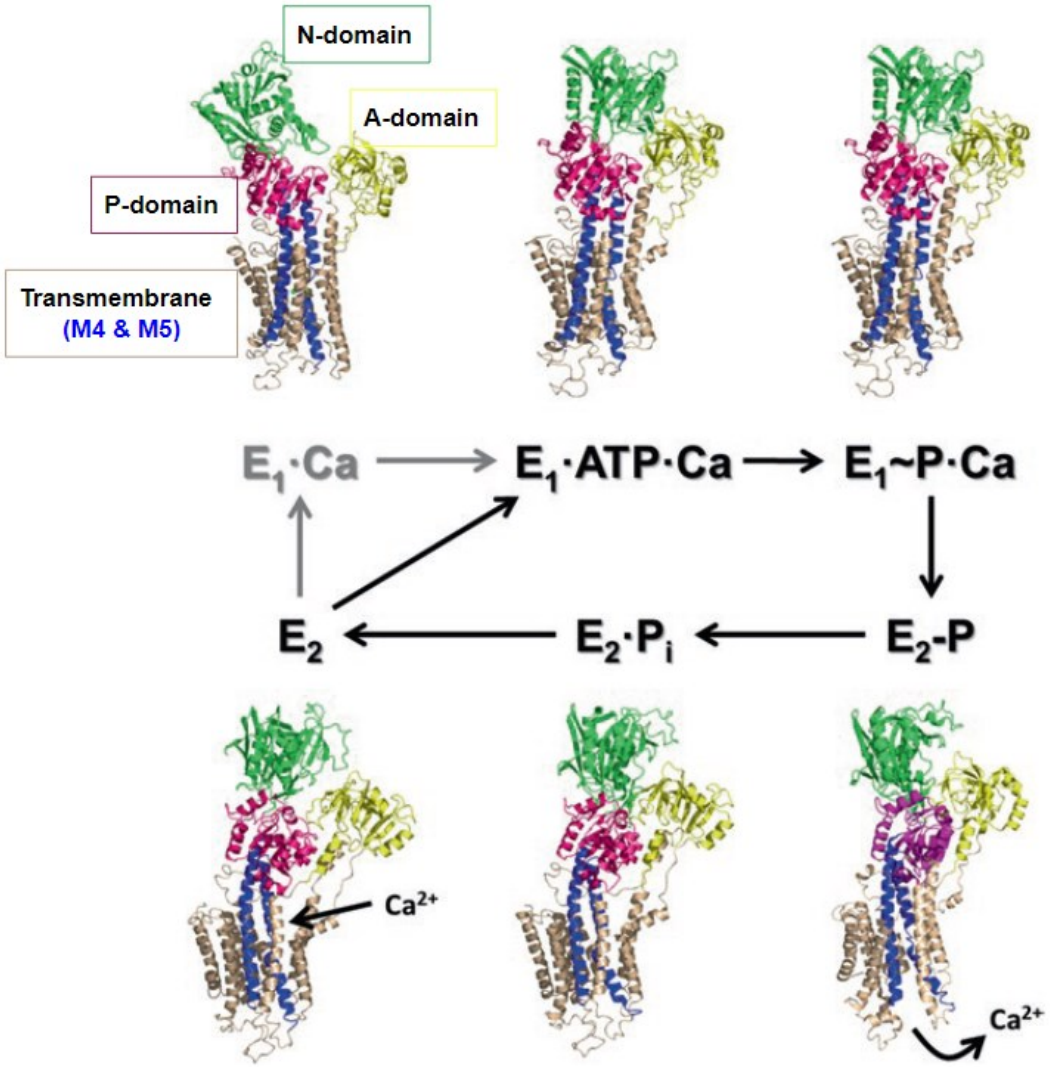

Figure 1.3. Structural intermediates of the SERCA calcium transport cycle with SERCA structures representing key intermediates in the calcium transport cycle. E2 – Ground state of the enzyme with 2-3 bound protons from the lumenal side of the SR membrane. E1·Ca – Release of 2-3 protons and binding of 2 calcium ions from the cytosolic side of the membrane. E1·ATP·Ca – ATP and calcium bound state with SERCA primed to initiate transport. E1~P·Ca – Phosphorylation of SERCA with the formation of an occluded calcium-bound state. E2-P – The conversion of an E1 to an E2 state following release of ADP and calcium to the SR lumen. E2·Pi –The formation of an occluded proton-bound state, followed by dephosphorylation and return to the E2 ground state. Under normal physiological conditions, SERCA likely transitions directly from E2 to E1·ATP·Ca. The structures are shown as a tan cartoon representation, with the A-domain in yellow, N-domain in green, P-domain in magenta. The transmembrane domain consists of ten transmembrane helices, withhelices M4 and M5 in blue.

All P-type ATPases contain 4 domains; the P-domain (phosphorylation), N-domain (nucleotide binding), A-domain (actuator), and M-domain (transmembrane helices). The P-domain is globular and has a central series of β-sheets flanked by helices that connect to nearby domains. As the name implies, this domain is the site of autophosphorylation. Given its significance in the P-type ATPase reaction mechanism, this domain—which is referred to as the catalytic core—contains the most sequence conservation of the domains. Reversible phosphorylation creates a temporary phosphoenzyme intermediate at a conserved Asp (Asp 351 in SERCA) residue. A Mg^{2+} cofactor is crucial for coordinating the enzyme and specifically balancing the charge repulsion between the negative Asp and phosphate group allowing the Asp residue to be phosphorylated. The N-domain extends from the P-domain, connected by a conserved link of anti-parallel strands. This domain contains a central β-strand and Lys residue. The A domain consists of two smaller components that connect to M1, M2, and M3. The A-domain has a dramatic range of motion through SERCA's conformational changes during the reaction cycle. Lastly, the M-domain spans the membrane and houses the ion binding sites (25).

SERCA is a 110 kDa protein consisting of ten transmembrane helices that coordinate to transport two calcium ions into the SR lumen and two-to-three protons for counter-transport into the cytoplasm. Although a proton gradient is not maintained by the SR membrane, SERCA actively transports and maintains a steep calcium concentration gradient in opposition to the high luminal concentration. The two calcium ions are coordinated by key residues in four of SERCA's ten transmembrane helices (M4, M5, M6, and M8). Partial helix unwinding of M4 in the middle of the membrane in concert with side chain and backbone carbonyl interactions provided by the four coordinating

helices form the two calcium binding sites. Two of the four transmembrane helices that coordinate calcium ions are particularly lengthy (M4 & M5; ~60Å) and reach the protein's cytoplasmic domain. SERCA's N, P, and A domains sit atop these transmembrane helices. With this domain architecture, SERCA uses the energy of ATP to move calcium ions across the membrane.

1.6 SERCA Mechanism of Calcium Transport

The generalized reaction scheme for P-Type ATPases can be described with the Post-Albers scheme, which involves the exchange (active transport) of two distinct metal ions across a membrane at the expense of ATP. The type and number of metal ions, or lipids, that are transported in each direction vary between different P-type ATPases. A central generalization of this scheme is that P-type ATPases switch between two major conformations, a high-affinity E1 state with ion binding sites facing one side of the membrane, and a lower-affinity E2 state with ion binding sites facing the other side of the membrane. E1 has high affinity and E2 has low affinity for the primary metal ion.

This applies to the calcium transport cycle of SERCA which displays a high affinity E1 and low affinity E2 state that are adopted during the reaction cycle (11,26) (Figure 1.3). SERCA transports calcium ions from the cytosolic side of the membrane, across the membrane, to the SR lumen side of the membrane while 2-3 protons are transported in the opposite direction (SR lumen to the cytosol). The original E1-E2 scheme states that to activate SERCA (5), two calcium ions must first bind (E1-Ca2). Next, ATP must be used to generate a phosphoenzyme intermediate (E1P). The conformational transition (E1P to E2P) that favours the release of calcium into the SR in exchange for lumenal protons is carried out using free energy from ATP, which is acquired during phosphoenzyme

synthesis. The final reaction step—hydrolytic cleavage of the phosphoenzyme intermediate, or dephosphorylation—returns the enzyme to the ground state and permits the start of a new transport cycle (13,27).

1.7 Regulatory Subunits of SERCA

PLN and SLN were the first transmembrane regulators of SERCA identified (28–30). PLN is a short single-pass 52 amino acid integral membrane protein found in cardiac and smooth muscle (31), while SLN is a homologous, and even shorter single-pass 31 amino acid integral membrane protein found in skeletal and atrial muscle (29). SERCA inhibition is the traditional term for the reversible one-to-one interaction that lowers SERCA's apparent calcium affinity in the conventional model of SERCA regulation by PLN and SLN (32). SERCA regulation by these peptides is maximal at low physiological calcium concentrations (~0.1μM cytosolic calcium) and is reversed at higher calcium concentrations (>1 μM) (Figure 1.4).

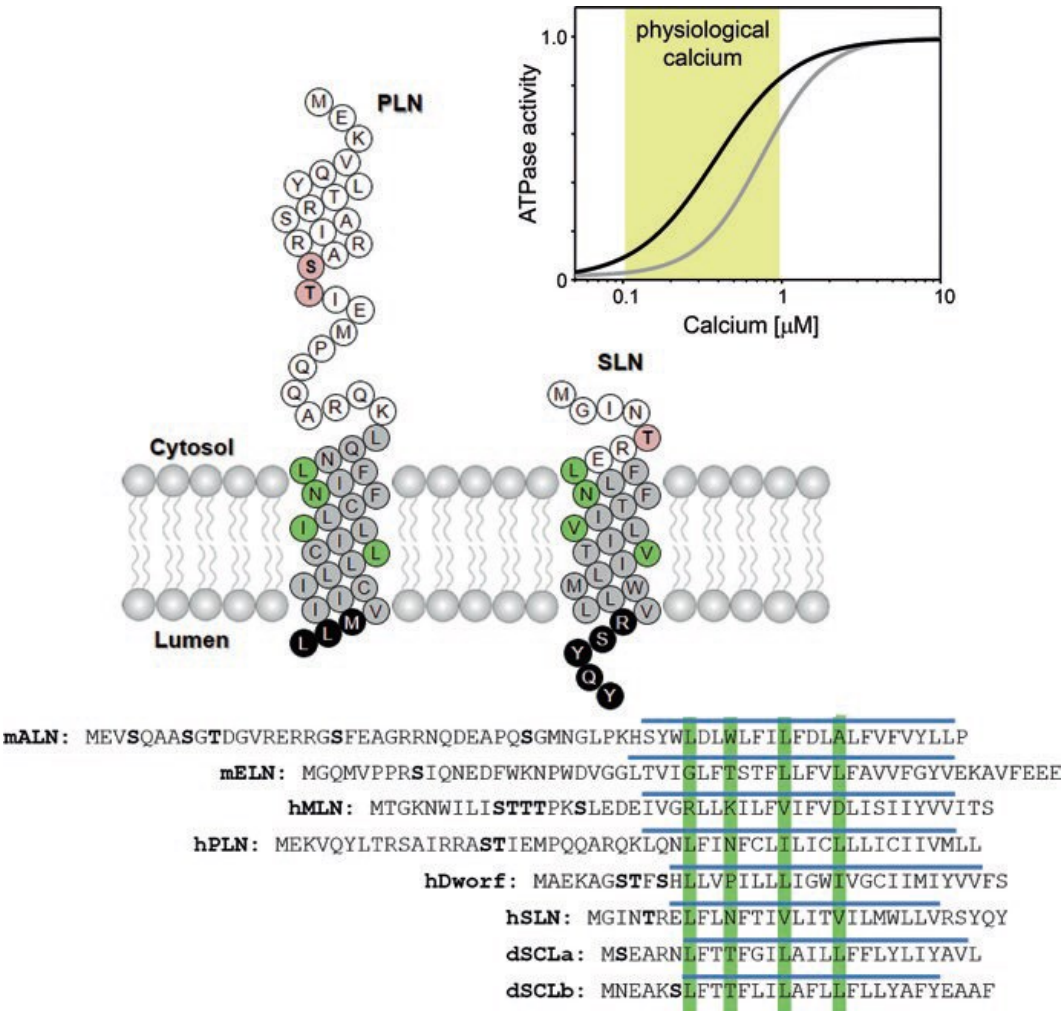

Figure 1.4. Primary structures and topology diagrams of SERCA regulatory peptides. Human phospholamban (PLN) and sarcolipin (SLN) are shown as topology diagrams with the cytosolic (white), transmembrane (grey) and lumenal (black) domains indicated. Residues in PLN and SLN transmembrane domains that are essential for functional regulation of SERCA are colored green. Inset is a representative curve for calcium-dependent SERCA ATPase activity in the absence (black line) and presence (grey line) of PLN. Lower: Sequence alignment of the reguling family of SERCA regulatory peptides. Mouse another-regulin (mALN), mouse endoregulin (mELN), human myoregulin (hMLN), human PLN (hPLN), human DWORF (hDWORF), human SLN (hSLN), and drosophila sarcolamban a and b isoforms (dSCLa & dSCLb). Alignment is based on the essential residues in PLN and SLN and maximum superposition of the transmembrane domains (blue bars).

This overly simplified view of SERCA regulation, however, has recently changed to incorporate newly discovered regulatory peptides and additional roles for PLN and SLN (33). The majority of these regulatory systems are restricted to the SR of skeletal and cardiac muscle (34). However, a universal regulatory mechanism in the ER is encoded in the SERCA2b isoform (17), and additional non-muscle regulators of SERCA have been found (REF=PMID 27923914).

1.8 Phospholamban (PLN)

PLN is a short single-pass 52 amino acid integral membrane protein recognized as a key regulator of cardiac contractility. PLN is observed at higher levels in the ventricular cardiac muscle and to a lower level in the smooth, atrial, and slow-twitch skeletal muscles. PLN's 52 residues can be divided into three domains; a soluble and dynamic cytoplasmic helix (residues 1-20), an unstructured linker region (residues 21-30), and a transmembrane helix that provides the majority of its SERCA inhibitory properties (residues 31-52). PLN was originally identified as a primary phosphorylation target of isolated cardiac SR membranes (28,35). Protein Kinase A (PKA) is a critical regulator of cardiac contractility, phosphorylating PLN in its cytosolic domain at Ser16. This phosphorylation of Ser16 mediated through β-adrenergic stimulation relieves the inhibitory effect of PLN on the function of SERCA. By this mechanism, PLN is a reversible and calcium-dependent inhibitor of SERCA that modulates cardiac contractility (36). PLN interacts directly with SERCA via a groove formed by M2, M6, and M9 of SERCA in the transmembrane domain. PLN inhibition of SERCA is not a simple binary on/off switch but rather a dynamic process dependent on (1) cytosolic calcium concentration, (2) phosphorylation state of PLN, and (3) the oligomeric state of PLN. First,

PLN binds when calcium is absent or at low (sub-micromolar) calcium concentrations, and this inhibition is reversed by micromolar calcium concentrations (37). Maximal SERCA inhibition is observed within the physiological window of cytosolic calcium concentration (~0.1-1.0 μM). Second, inhibition is relieved by phosphorylation of PLN, primarily by PKA via β-adrenergic signaling (38,39). Third, PLN is in dynamic equilibrium with its homopentamer form (40). The pentamer is described as an inactive storage reserve of PLN, although it is required for physiological function (41). The pentameric form of PLN has also been shown to interact with SERCA by our lab and others (42,43). The magnitude and permutations of these regulatory mechanisms provide dynamic modulation of SR calcium reserves and thereby cardiac contractility can be finely tuned in response to activity, stress, or disease.

Catecholamines act on the β-adrenergic pathway to activate PKA and phosphorylate several cardiac proteins, including PLN, which provides the primary mechanism for modulating SR calcium reserves (Figure 1.5).

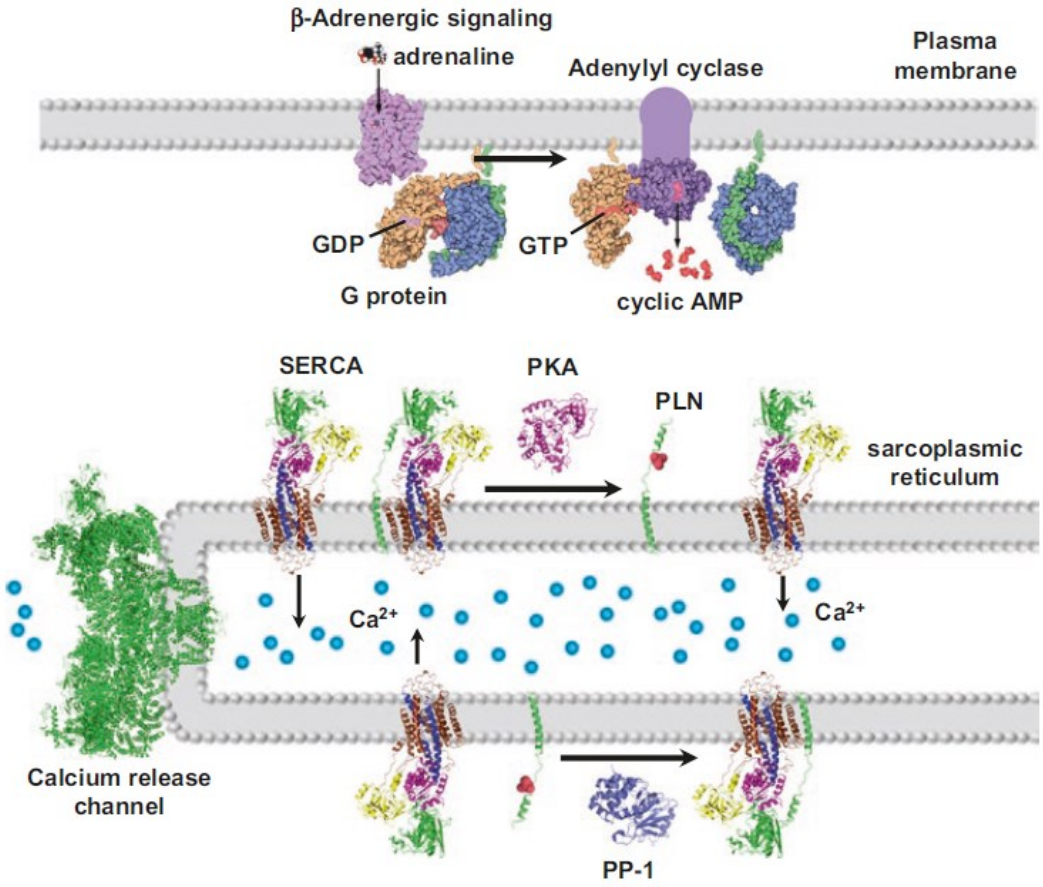

Figure 1.5. Schematic representation of SERCA-dependent calcium homeostasis in cardiac muscle. The β-adrenergic signaling pathway is activated by catecholamines, which in turn increases cyclic AMP levels via activation of a G-protein and adenylyl cyclase. The cyclic AMP binds to the regulatory subunit of protein kinase A (PKA), which activates the catalytic subunit. The catalytic subunit of PKA phosphorylates phospholamban (PLN) which relieves SERCA inhibition. A protein phosphatase (PP-1) can dephosphorylate PLN and restore SERCA inhibition (restoration of PLN function). SERCA recovers calcium into the lumen of the sarcoplasmic reticulum (SR) and triggers muscle relaxation. A comparatively large pool of SERCA and PLN molecules allow for dynamic modulation of cardiac muscle relaxation and SR calcium load for subsequent contractions. The adrenergic signaling illustrations are courtesy of David S. Goodsell and the RCSB PDB, Molecules of the Month (http://pdb101.rcsb.org/motm/58)

The inhibitory characteristics of PLN are reversed, and the apparent calcium affinity of SERCA is increased as a result of PKA's phosphorylation of PLN, resulting in a significant effect on cardiac contractility (44). Monomeric PLN inhibits SERCA and phosphorylation

of PLN is thought to cause dissociation of PLN from SERCA, shifting the dynamics of PLN toward its pentameric reserve form (32,38,40). PLN has two adjacent phosphorylation sites, it is phosphorylated by PKA at Ser16 (45) and at Thr17 by Ca^{2+}/calmodulin-dependent protein kinase II (39) and Akt (46). Phosphorylation at these sites separately or in combination is important for cardiac function (47). It is not well understood if these sites are phosphorylated independently and impart different effects on SERCA inhibition, or if they are phosphorylated concomitantly and have additive or synergistic effects on suppressing PLN's inhibition of SERCA. The delicate balance of PLN inhibition of SERCA are of clinical importance regarding cardiac disease. Disruptions to calcium flux as a result of PLN dysregulation lead to contractile dysfunction, hypertrophy, and dilated cardiomyopathy (48–53).

PLN inhibition is measured functionally as a direct effect on the apparent calcium affinity of SERCA. PLN inhibits the SERCA2a isoform in cardiac muscle, but PLN also inhibits SERCA1a and SERCA2b (54). The transmembrane domain of PLN encodes the majority of its inhibitory regulation of SERCA (~80% of inhibition (55)), while the linker region fine tunes the inhibitory interaction, and the N-terminal helix provides reversibility of inhibition via phosphorylation. The transmembrane domain of PLN contains key residues responsible for SERCA inhibition such as Leu31 and Asn34, in addition to key residues such as the Leu-Ile zipper motif which includes Leu37 and Ile40 responsible for homopentamer formation (38,56). The PLN pentamer has been described as an inactive storage form, but there has been no direct demonstration of the functional capabilities of oligomeric PLN on SERCA activity.

PLN's linker region (residues ~21-30) modulates the interaction of PLN's transmembrane domain with SERCA via charge repulsion. PLN residues Arg25 and Lys27 are in proximity to Arg324 and Lys328 of SERCA. This repulsive interaction is thought

to exert control over the positioning of the transmembrane domain of PLN in relation to the inhibitory groove formed by M2, M6, and M9 of SERCA. The linker region of PLN is also necessary in transmitting the reversal of inhibition from the N-terminal domain when phosphorylated at Ser16 or Thr17 to the transmembrane domain (residues ~31-52).

PKA recognizes Ser16 through the consensus sequence Arg13-Arg-Ala-Ser16 (36). Once phosphorylated, Ser16 may form salt bridges with Arg13 and/or Arg14, distorting the N-terminal helix of PLN and relieving SERCA inhibition (57). Phosphorylation changes the conformational dynamics of PLN's cytosolic domain, thereby altering the interaction with SERCA (58,59). PKA can phosphorylate PLN monomers bound to SERCA, poising PKA recognition of PLN as the first step in the reversal of SERCA inhibition. PKA has also been shown to target PLN monomers in the context of the PLN homopentamer (60,61) and to result in oligomerization of PLN into its pentameric form (40). The PKA consensus sequence spanning Arg13-Ser16 is essential. There are additional structural determinants important in PKA's recognition of PLN bound to SERCA such as Arg9 and Ser10, and PLN in the pentamer such as Arg9 (60).

The residues of PLN spanning from approximately Lys3 to Ile18 directly associate with the catalytic subunit of PKA. Upstream positively charged residues and downstream hydrophobic residues are preferred by PKA. Both Arg9 and Ile18 of PLN meet these requirements, though Ile18 has not received a lot of attention to date. Arg9 in PLN has been intensively investigated, and the results show that PKA prefers this residue, especially in the pentameric state. Arg9 of PLN packs against Glu203 and Asp241 in the peptide binding groove of PKA, and this has a strong influence on substrate recognition. PKA uses conformational selection to identify substrates (62), and the most efficient substrates are peptides in solution due to their conformational dynamics (63).

Phosphorylation is less efficient for monomeric, full-length PLN, and far less efficient for the PLN pentamer or the SERCA-PLN complex compared to a synthetic soluble peptide consisting only of the cytosolic domain. PLN's conformational dynamics are more constrained in the pentameric form, or when associated with SERCA. Arg9, Ser10, and Ile18 assist in PKA recognition of PLN in these conditions when PLN dynamics are more constrained. Arg9 is critical for PLN function and β-adrenergic signaling and human missense mutations of this residue such as Arg9-Cys and Arg9-Leu cause lethal, hereditary dilated cardiomyopathy. These mutations all but eliminate PLN function and create a kinetic trap for PKA, sequestering it from phosphorylating other cellular targets (50,60).

Equally important to phosphorylation of PLN by PKA is the dephosphorylation by Protein Phosphatase-1 (PP-1). Dephosphorylation of PLN reactivates function in the form of SERCA inhibition (64,65). Unfortunately, little is known about the consensus sequence determinants of PLN that dictate dephosphorylation dynamics. Which isoform of PP-1 dephosphorylates PLN in the myocardium is also still unknown. Although PP-2, PP-1α, and PP-1γ can dephosphorylate PLN in cardiomyocytes, PP-1β is the main isoform that associates with the SERCA-PLN complex (64). It is widely established that PP-1 activity significantly regulates SERCA-PLN function and cardiac contractility, regardless of which isoform is primarily responsible for dephosphorylating PLN in the human myocardium. The copy number of the SERCA and PLN molecules far exceeds that of the calcium release channel, which is another thing to keep in mind. As a result, compared to calcium release, calcium recovery comprises a sizable "pool" of SERCA pumps that can be differently and dynamically engaged or suppressed based on the demand for cardiac output.

1.9 Sarcolipin (SLN)

SLN has been the topic of significantly less published works relative to SERCA to date, likely due to its function mirroring that of PLN in skeletal muscle, and the human health implications being less obvious. Recent identification of distinct functions for SLN have rekindled interest in this important SERCA regulator. SLN is a helical 31 residue, single-pass integral membrane protein and serves as the principal regulator of SERCA in skeletal and atrial cardiac muscle. SLN is structurally and functionally homologous to PLN and is thought to regulate SERCA in a similar manner (29). SLN consists of a short cytoplasmic domain (residues ~1-7), a transmembrane α-helix (residues ~8-26), and a short, highly conserved lumenal tail (residues ~27-31). SLN interacts with SERCA in a groove formed by transmembrane helices M2, M6, and M9 much like PLN (Figure 1.6).

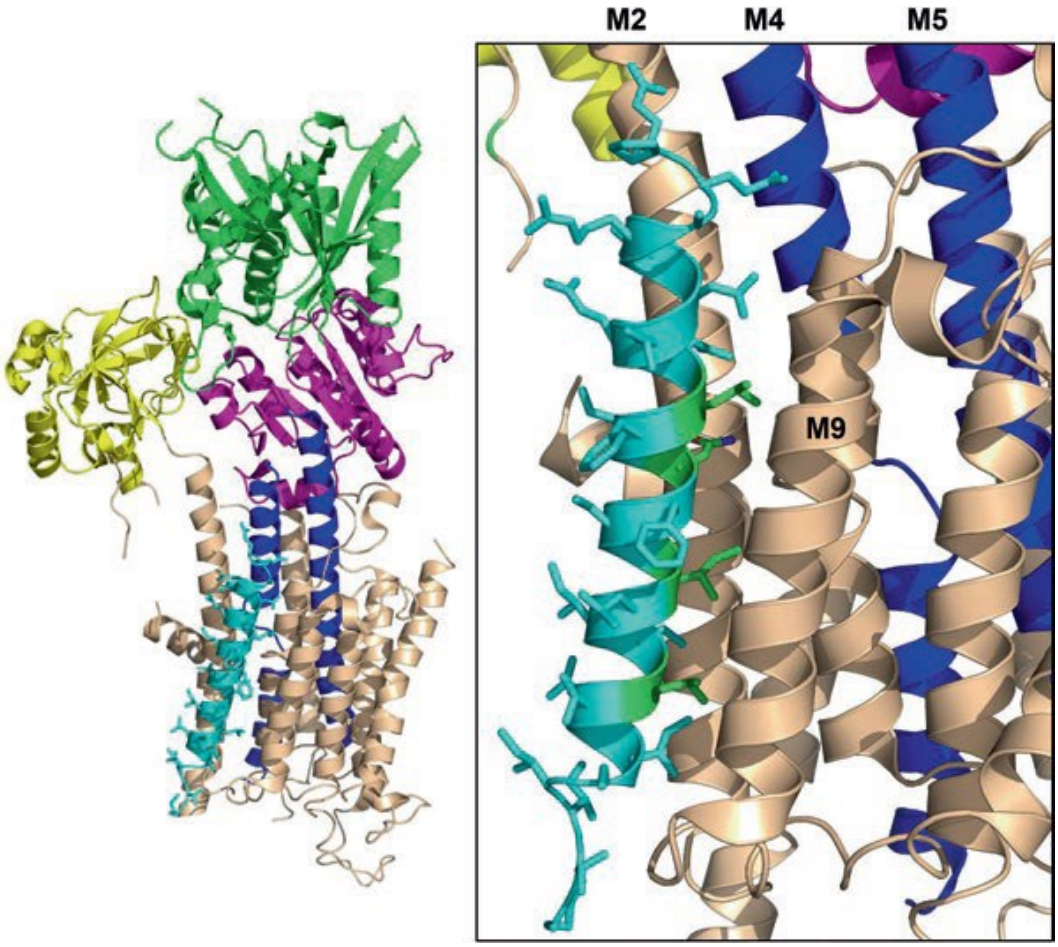

Figure 1.6. The structure of SERCA with phospholamban bound. PDB accession code 4Y3U is shown as a tan cartoon representation with the A-domain (yellow), N-domain (green), P-domain (magenta), and helices M4 and M5 (blue) indicated. PLN (cyan) lies in a groove between M2 and M6, and is shown with side chains. The four essential residues of PLN, Leu31, Asn34, Ile38, and Leu42 (green) interface with SERCA.

Crystal structures of the SERCA-SLN complex similarly display SLN binding SERCA in an E1-like state (66,67). Despite these similarities to PLN, SLN regulates SERCA differently. Unlike PLN, most of SLN's inhibitory function is encoded in its unique and highly conserved C-terminal RSYQY sequence (68). This C-terminal RSYQY sequence can be added to a generic transmembrane helix peptide, resulting in a SERCA inhibitor peptide. Lab-generated chimeras of PLN with this C-terminal RSYQY sequence added result in a

synergistic function in terms of inhibition of SERCA calcium affinity. The RSYQY sequence is helical and not in direct contact with SERCA in the SERCA-SLN crystal structures, suggesting that it functions to position SLN in the inhibitory groove of SERCA. The transmembrane helix may be positioned in relation to SERCA by the arginine and tyrosine residues, which may be located at the lipid bilayer's hydrocarbon core-water interface. It appears likely that the SERCA-SLN inhibitory complex involves interactions between the lumenal loops and calcium-exit channel of SERCA and the RSYQY lumenal tail of SLN.

SLN inhibitory function on SERCA is distinct from that of PLN. Both regulatory peptides decrease SERCA calcium affinity, but SLN decreases the maximal activity of SERCA (68,69) whereas the opposite effect has been observed with PLN increasing SERCA maximal activity at saturating calcium concentrations (55,70–72). The fact that SLN is a unique regulatory subunit of the SERCA calcium pump has led to the conclusion that SLN may also have a special physiological function in the control and maintenance of body temperature, a process known as thermogenesis (73–78). SLN has been suggested to increase the net balance of ATP consumption to calcium transport and encourages the cycling of SERCA without translocating calcium. The extra ATP hydrolysis helps to generate heat. Given that skeletal muscle should account for about 40% of total body mass, SERCA and SLN may play a role in muscle-based thermogenesis that is not accompanied by shivering (73). The prevalence of skeletal muscle and the function of SLN make it a possible contributor to metabolic demand and human illnesses like obesity, diabetes, and metabolic syndrome.

Relatively little is understood about the regulation of SLN. Regulation via phosphorylation similar to that of PLN may be expected, especially considering that SLN and PLN are both present in atrial muscle where they may form a super-inhibitory

complex with SERCA (79). SLN has a conserved threonine residue (Thr5) that appears to be a phosphorylation target of both calcium-calmodulin dependent protein kinase II (CaMKII) and serine/threonine kinase 16 (STK16). Thr5 has been identified as a critical residue and phosphomimetic mutations eliminate function (80). It is most likely that scaffolding proteins (AKAPs) will interact with the cytoplasmic domain of the SLN and form regulatory complexes. The cytoplasmic domain of SLN is the variable region however and the sequence is unique in humans. The N-terminal sequence in humans is MGINTRE compared to MERSTQE in mice and many other mammals. This variability may reflect the differing roles of SLN in various organisms and their individual thermogenic needs, in addition to skeletal and atrial muscle calcium handling and contractility.

1.10 Additional SERCA Regulators: The Regulins

The complexity of the three SERCA genes and two regulatory subunits may appear to be limited in breadth. However, the recent identification of several additional regulatory subunits of SERCA beyond PLN and SLN has significantly altered the environment of SERCA regulation. These recently discovered regulators of SERCA, dubbed the “regulins”, were initially hidden in what were labeled as long, non-coding RNA sequences. The breadth of regulins comprises of PLN, SLN, sarcolamban (SLB) in insect cardiac muscles (81), myoregulin (MLN) in skeletal muscle, endoregulin (ELN) in endothelial and epithelial tissues, the ubiquitous another-regulin (ALN) (33), and dwarf open reading frame (DWORF) in cardiac and skeletal muscle (34,82). DWORF is the only known endogenous regulatory peptide activator of SERCA; however, all other known SERCA regulators are inhibitors, in that they lower the apparent calcium affinity or maximal activity of SERCA. Each of these regulins has been shown to localize to the ER membrane and is co-expressed with the tissue-specific isoform of SERCA. Additionally, each regulator is

predicted to have α-helical structure in a single transmembrane domain. Structural studies combining techniques like NMR, CD spectroscopy, or co-crystallization with SERCA have yet to be done for these new regulins, providing a white space opportunity (33,82–84).

To date, studies exploring these new regulators have been conducted in-vivo using mouse models or whole-cell systems, and in chemically defined reconstituted membrane systems. While these peptides have been discovered and preliminary insights into their regulatory effect on SERCA have been explored, a full and detailed understanding of their structures, functions, regulatory dynamics, and physiological roles remain to be discovered.

1.11 Thesis Aims

Recent advances in genetic testing have revealed a large collection of rare genetic probable causes of idiopathic DCM, which is often found in families with a clinical history of the disease. Over 40 missense mutations have been identified to date in PLN and are recorded in databases such as ClinVar, COSMIC, & Ensembl. Most of these PLN mutations are categorized as variants of uncertain significance (VUS). PLN missense variants have appeared recently due to efforts to identify the genetic basis for familial cardiomyopathies. The overarching goal of this thesis is to investigate the properties of the SERCA-PLN regulatory axis, with an emphasis on hereditary missense variants found in PLN.

A variety of different missense variants have been studied (Chapters 2 & 4), ranging in the effected domain of this small regulatory peptide and the nature of the missense variant. Chapter 3 focuses on the possible modes of interaction between

SERCA and PLN and the effect of substrate preincubation conditions on PLN regulation of SERCA. As such, the work has been divided into three data chapters, each focusing on a distinct narrative of different PLN modes or PLN missense variants in SERCA regulation.

Chapter 2, the first data chapter, focuses on determining the regulatory role of the C-terminal residues of PLN on SERCA. This chapter aims to explore the role of PLN C-terminal residues in localization, oligomerization, and regulatory function.

The third chapter explores substrate preincubation condition effects of PLN on SERCA. Differences of inhibitory interactions established with SERCA and their distinct effects on SERCA's kinetic properties, and how the engaged mode persists throughout the SERCA transport cycle are investigated. These experiments aim to provide insights into the physiological role of PLN and its regulatory effect on SERCA transport activity.

The final section, Chapter 4, aims to assess two missense variants in PLN, an Ala15-Thr variant found in a 4-year-old female with a family history and clinical diagnosis of dilated cardiomyopathy and a Pro21-Thr variant found in a 60-year-old female with a family history and clinical diagnosis of dilated cardiomyopathy. Interestingly, both patients also harbored a Val896-Met variant in cardiac myosin binding protein. The PLN variants' effect on SERCA activity were characterized to assess defects in calcium homeostasis regulation and to classify these variants' probable significance and pathogenic potential. I aimed to characterize the potential for the variant in cardiac myosin binding protein to alter the structure of the protein and, the potential functional implications and interplay in the presence of dysregulated calcium regulation caused by PLN missense variants.

Chapter 1 References

1. Carafoli E, Krebs J. Why Calcium? How Calcium Became the Best Communicator. Journal of Biological Chemistry [Internet]. 2016 Sep;291(40):20849–57. Available from: http://www.jbc.org/content/291/40/20849.abstract

2. Crichton RR. Calcium – Cellular Signalling. Biological Inorganic Chemistry. 2012 Jan 1;215–28.

3. Ripa R, George T, Sattar Y. Physiology, Cardiac Muscle. StatPearls [Internet]. 2022 Jun 2 [cited 2022 Oct 29]; Available from: https://www.ncbi.nlm.nih.gov/books/NBK572070/

4. Thompson BR, Metzger JM. Cell biology of sarcomeric protein engineering: disease modeling and therapeutic potential. Anat Rec (Hoboken) [Internet]. 2014 [cited 2022 Oct 29];297(9):1663–9. Available from: https://pubmed.ncbi.nlm.nih.gov/25125179/

5. staff Blausen com, staff Blausen com. [[WikiJournal of Medicine/Medical gallery of Blausen Medical 2014|Medical gallery of Blausen Medical 2014]]. [[WikiJournal of Medicine|WikiJournal of Medicine]]. 2014;1(2).

6. Creative Commons Legal Code [Internet]. [cited 2023 Mar 11]. Available from: https://creativecommons.org/licenses/by/3.0/legalcode

7. Meissner G. Ryanodine receptor/Ca2+ release channels and their regulation by endogenous effectors. Annu Rev Physiol [Internet]. 1994 [cited 2022 Nov 4];56:485–508. Available from: https://pubmed.ncbi.nlm.nih.gov/7516645/

8. Franzini-Armstrong C, Protasi F, Ramesh V. Shape, size, and distribution of Ca(2+) release units and couplons in skeletal and cardiac muscles. Biophys J [Internet]. 1999 [cited 2022 Nov 4];77(3):1528–39. Available from: https://pubmed.ncbi.nlm.nih.gov/10465763/

9. Bers DM. Cardiac excitation-contraction coupling. Nature [Internet]. 2002 Jan 10 [cited 2022 Nov 4];415(6868):198–205. Available from: https://pubmed.ncbi.nlm.nih.gov/11805843/

10. Doroudgar S, Glembotski CC. New concepts of endoplasmic reticulum function in the heart: Programmed to conserve. J Mol Cell Cardiol [Internet]. 2013;55:85–91. Available from: http://www.sciencedirect.com/science/article/pii/S0022282812003744

11. Palmgren MG, Nissen P. P-Type ATPases. Annu Rev Biophys [Internet]. 2011 May;40(1):243–66. Available from: https://doi.org/10.1146/annurev.biophys.093008.131331

12. Toyoshima C. Ion pumping by calcium ATPase of sarcoplasmic reticulum. Adv Exp Med Biol [Internet]. 2007 [cited 2022 Nov 4];592:295–303. Available from: https://link.springer.com/chapter/10.1007/978-4-431-38453-3_25

13. Møller J v, Olesen C, Winther AML, Nissen P. The sarcoplasmic Ca2+-ATPase: design of a perfect chemi-osmotic pump. Q Rev Biophys [Internet]. 2010;43(4):501–66. Available from: https://www.cambridge.org/core/product/712917B2C432A2C19D12749FF667D772

14. Dally S, Corvazier E, Bredoux R, Bobe R, Enouf J. Multiple and diverse coexpression, location, and regulation of additional SERCA2 and SERCA3 isoforms in

nonfailing and failing human heart. J Mol Cell Cardiol [Internet]. 2010;48(4):633–44. Available from: http://www.sciencedirect.com/science/article/pii/S0022282809004878

15. Wuytack F, Raeymaekers L, Missiaen L. Molecular physiology of the SERCA and SPCA pumps. Cell Calcium [Internet]. 2002;32(5):279–305. Available from: http://www.sciencedirect.com/science/article/pii/S0143416002001847

16. Kósa M, Brinyiczki K, van Damme P, Goemans N, Hancsák K, Mendler L, et al. The neonatal sarcoplasmic reticulum Ca2+-ATPase gives a clue to development and pathology in human muscles. J Muscle Res Cell Motil [Internet]. 2015;36(2):195–203. Available from: https://doi.org/10.1007/s10974-014-9403-z

17. Vangheluwe P, Raeymaekers L, Dode L, Wuytack F. Modulating sarco(endo)plasmic reticulum Ca2+ ATPase 2 (SERCA2) activity: Cell biological implications. Cell Calcium [Internet]. 2005;38(3):291–302. Available from: http://www.sciencedirect.com/science/article/pii/S014341600500120X

18. Gorski P a., Trieber C a., Larivière E, Schuermans M, Wuytack F, Young HS, et al. Transmembrane helix 11 is a genuine regulator of the endoplasmic reticulum Ca2+ pump and acts as a functional parallel of β-subunit on α-Na+,K+-ATPase. Journal of Biological Chemistry. 2012;287(24):19876–85.

19. Gélébart P, Martin V, Enouf J, Papp B. Identification of a new SERCA2 splice variant regulated during monocytic differentiation. Biochem Biophys Res Commun [Internet]. 2003;303(2):676–84. Available from: http://www.sciencedirect.com/science/article/pii/S0006291X03004054

20. Chemaly ER, Bobe R, Adnot S, Hajjar RJ, Lipskaia L. Sarco (Endo) Plasmic Reticulum Calcium Atpases (SERCA) Isoforms in the Normal and Diseased Cardiac, Vascular and Skeletal Muscle. 2013;

21. Sagara Y, Fernandez-Belda F, de Meis L, Inesi G. Characterization of the inhibition of intracellular Ca2+ transport ATPases by thapsigargin. Journal of Biological Chemistry [Internet]. 1992 Jun;267(18):12606–13. Available from: http://www.jbc.org/content/267/18/12606.abstract

22. Vandecaetsbeek I, Trekels M, de Maeyer M, Ceulemans H, Lescrinier E, Raeymaekers L, et al. Structural basis for the high Ca2+ affinity of the ubiquitous SERCA2b Ca2+ pump. Proc Natl Acad Sci U S A. 2009;106(20102):18533–8.

23. Reddy LG, Jones LR, Pace RC, Stokes DL. Purified, Reconstituted Cardiac Ca2+-ATPase Is Regulated by Phospholamban but Not by Direct Phosphorylation with Ca2+/Calmodulin-dependent Protein Kinase. Journal of Biological Chemistry [Internet]. 1996 Jun;271(25):14964–70. Available from: http://www.jbc.org/content/271/25/14964.abstract

24. Toyoshima C, Nakasako M, Nomura H, Ogawa H. Crystal structure of the calcium pump of sarcoplasmic reticulum at 2.6 A resolution. Nature. 2000;405(M):647–55.

25. Kühlbrandt W. Biology, structure and mechanism of P-type ATPases. Nat Rev Mol Cell Biol. 2004;5(April):282–95.

26. Apell HJ. How do P-Type ATPases transport ions? [cited 2022 Nov 4]; Available from: www.elsevier.com/locate/bioelechem

27. Toyoshima C. How Ca2+-ATPase pumps ions across the sarcoplasmic reticulum membrane. Biochimica et Biophysica Acta (BBA) - Molecular Cell Research [Internet]. 2009;1793(6):941–6. Available from: http://www.sciencedirect.com/science/article/pii/S0167488908003558

28. Kirchberber MA, Tada M, Katz AM. Phospholamban: a regulatory protein of the cardiac sarcoplasmic reticulum. Recent Adv Stud Cardiac Struct Metab. 1975;5:103–15.

29. Odermatt a, Becker S, Khanna VK, Kurzydlowski K, Leisner E, Pette D, et al. Sarcolipin regulates the activity of SERCA1, the fast-twitch skeletal muscle sarcoplasmic reticulum Ca2+-ATPase. J Biol Chem. 1998;273(20):12360–9.

30. Wawrzynow A, Theibert JL, Murphy C, Jona I, Martonosi A, Collins JH. Sarcolipin, the “proteolipid” of skeletal muscle sarcoplasmic reticulum, is a unique, amphipathic, 31-residue peptide. Arch Biochem Biophys. 1992 Nov;298(2):620–3.

31. Simmerman HKB, Collins JH, Theibert JL, Wegener a. D, Jones LR. Sequence analysis of phospholamban. Identification of phosphorylation sites and two major structural domains. Journal of Biological Chemistry. 1986;261(28):13333–41.

32. Stokes DL. Keeping Calcium in its Place: Ca2+ ATPase and Phospholamban. Curr Opin Struct Biol. 1997;7:550–6.

33. Anderson DM, Makarewich CA, Anderson KM, Shelton JM, Bezprozvannaya S, Bassel-Duby R, et al. Widespread control of calcium signaling by a family of SERCA-inhibiting micropeptides. Sci Signal [Internet]. 2016 Dec;9(457):ra119 LP-ra119. Available from: http://stke.sciencemag.org/content/9/457/ra119.abstract

34. Rathod N, Bak JJ, Primeau JO, Fisher ME, Espinoza-fonseca LM, Lemieux MJ, et al. Nothing regular about the regulins: Distinct functional properties of SERCA transmembrane peptide regulatory subunits. Int J Mol Sci [Internet]. 2021 Aug 2 [cited 2023 Mar 11];22(16):22. Available from: /pmc/articles/PMC8396278/

35. KATZ AM. Discovery of Phospholamban: A Personal History. Ann N Y Acad Sci [Internet]. 1998 Sep;853(1):9–19. Available from: https://doi.org/10.1111/j.1749-6632.1998.tb08252.x

36. Simmerman HKB, Collins JH, Theibert JL, Wegener AD, Jones LR. Sequence analysis of phospholamban. Identification of phosphorylation sites and two major structural domains. Journal of Biological Chemistry. 1986 Oct 5;261(28):13333–41.

37. Asahi M, Mckenna E, Kurzydlowski K, Tada M, Maclennan DH. Physical Interactions between Phospholamban and Sarco (endo) plasmic Reticulum Ca 2 ⁺ - ATPases Are Dissociated by Elevated Ca 2 ⁺ , but Not by Phospholamban Phosphorylation , Vanadate , or Thapsigargin , and Are Enhanced by ATP *. 2000;275(20):15034–8.

38. Kimura Y, Kurzydlowski K, Tada M, MacLennan DH. Phospholamban Inhibitory Function Is Activated by Depolymerization. Journal of Biological Chemistry [Internet]. 1997 Jun;272(24):15061–4. Available from: http://www.jbc.org/content/272/24/15061.abstract

39. Tada M, Inui M, Yamada M, Kadoma M aki, Kuzuya T, Abe H, et al. Effects of phospholamban phosphorylation catalyzed by adenosine 3′:5′-monophosphate- and calmodulin-dependent protein kinases on calcium transport ATPase of cardiac

sarcoplasmic reticulum. J Mol Cell Cardiol [Internet]. 1983;15(5):335–46. Available from: http://www.sciencedirect.com/science/article/pii/0022282883913457

40. Cornea RL, Jones LR, Autry JM, Thomas DD. Mutation and Phosphorylation Change the Oligomeric Structure of Phospholamban in Lipid Bilayers. Biochemistry [Internet]. 1997 Mar;36(10):2960–7. Available from: https://doi.org/10.1021/bi961955q

41. Chu G, Li L, Sato Y, Harrer JM, Kadambi VJ, Hoit BD, et al. Pentameric assembly of phospholamban facilitates inhibition of cardiac function in vivo. Journal of Biological Chemistry. 1998;273(50):33674–80.

42. Glaves JP, Trieber C a., Ceholski DK, Stokes DL, Young HS. Phosphorylation and mutation of phospholamban alter physical interactions with the sarcoplasmic reticulum calcium pump. J Mol Biol [Internet]. 2011;405(3):707–23. Available from: http://dx.doi.org/10.1016/j.jmb.2010.11.014

43. Stokes DL, Pomfret AJ, Rice WJ, Glaves JP, Young HS. Interactions between Ca2+-ATPase and the pentameric form of phospholamban in two-dimensional co-crystals. Biophys J. 2006;90(June):4213–23.

44. Tada M, Kirchberger MA, Katz AM. Regulation of calcium transport in cardiac sarcoplasmic reticulum by cyclic AMP-dependent protein kinase. Recent Adv Stud Cardiac Struct Metab. 1976;9:225–39.

45. Tada M, Kirchberger MA, Repke DI, Katz AM. The Stimulation of Calcium Transport in Cardiac Sarcoplasmic Reticulum by Adenosine 3':5'-Monophosphate-dependent Protein Kinase. Journal of Biological Chemistry [Internet]. 1974

Oct;249(19):6174–80. Available from: http://www.jbc.org/content/249/19/6174.abstract

46. Catalucci D, Latronico MVG, Ceci M, Rusconi F, Young HS, Gallo P, et al. Akt Increases Sarcoplasmic Reticulum Ca2+ Cycling by Direct Phosphorylation of Phospholamban at Thr17. Journal of Biological Chemistry [Internet]. 2009 Oct;284(41):28180–7. Available from: http://www.jbc.org/content/284/41/28180.abstract

47. Bartel S, Vetter D, Schlegel WP, Wallukat G, Krause EG, Karczewski P. Phosphorylation of Phospholamban at Threonine-17 in the Absence and Presence of β -Adrenergic Stimulation in Neonatal Rat Cardiomyocytes. J Mol Cell Cardiol [Internet]. 2000;32(12):2173–85. Available from: http://www.sciencedirect.com/science/article/pii/S0022282800912434

48. Haghighi K, Kolokathis F, Pater L, Lynch RA, Asahi M, Gramolini AO, et al. Human phospholamban null results in lethal dilated cardiomyopathy revealing a critical difference between mouse and human. J Clin Invest [Internet]. 2003 Mar;111(6):869–76. Available from: https://doi.org/10.1172/JCI17892

49. Landstrom AP, Adekola BA, Bos JM, Ommen SR, Ackerman MJ. PLN-encoded phospholamban mutation in a large cohort of hypertrophic cardiomyopathy cases: Summary of the literature and implications for genetic testing. Am Heart J [Internet]. 2011;161(1):165–71. Available from: http://www.sciencedirect.com/science/article/pii/S0002870310006757

50. Schmitt JP, Kamisago M, Asahi M, Li GH, Ahmad F, Mende U, et al. Dilated cardiomyopathy and heart failure caused by a mutation in phospholamban. Science. 2003;299(February):1410–3.

51. P. SJ, Ferhaan A, Kristina L, Lutz H, Stefan S, Michio A, et al. Alterations of Phospholamban Function Can Exhibit Cardiotoxic Effects Independent of Excessive Sarcoplasmic Reticulum Ca2+-ATPase Inhibition. Circulation [Internet]. 2009 Jan;119(3):436–44. Available from: https://doi.org/10.1161/CIRCULATIONAHA.108.783506

52. DeWitt MM, MacLeod HM, Soliven B, McNally EM. Phospholamban R14 Deletion Results in Late-Onset, Mild, Hereditary Dilated Cardiomyopathy. J Am Coll Cardiol [Internet]. 2006;48(7):1396–8. Available from: http://www.sciencedirect.com/science/article/pii/S0735109706018377

53. Haghighi K, Kolokathis F, Gramolini AO, Waggoner JR, Pater L, Lynch RA, et al. A mutation in the human phospholamban gene, deleting arginine 14, results in lethal, hereditary cardiomyopathy. Proceedings of the National Academy of Sciences [Internet]. 2006 Jan;103(5):1388 LP – 1393. Available from: http://www.pnas.org/content/103/5/1388.abstract

54. Toyofuku T, Kurzydlowski K, Tada M, MacLennan DH. Amino acids Glu2 to Ile18 in the cytoplasmic domain of phospholamban are essential for functional association with the Ca(2+)-ATPase of sarcoplasmic reticulum. Journal of Biological Chemistry [Internet]. 1994 Jan;269(4):3088–94. Available from: http://www.jbc.org/content/269/4/3088.abstract

55. Trieber CA, Afara M, Young HS. Effects of Phospholamban Transmembrane Mutants on the Calcium Affinity, Maximal Activity, and Cooperativity of the Sarcoplasmic Reticulum Calcium Pump. Biochemistry [Internet]. 2009 Oct;48(39):9287–96. Available from: https://doi.org/10.1021/bi900852m

56. Autry JM, Jones LR. Functional Co-expression of the Canine Cardiac Ca2+Pump and Phospholamban in Spodoptera frugiperda (Sf21) Cells Reveals New Insights on ATPase Regulation. Journal of Biological Chemistry [Internet]. 1997 Jun;272(25):15872–80. Available from: http://www.jbc.org/content/272/25/15872.abstract

57. Sugita Y, Miyashita N, Yoda T, Ikeguchi M, Toyoshima C. Structural changes in the cytoplasmic domain of phospholamban by phosphorylation at Ser16: A molecular dynamics study. Biochemistry. 2006 Oct 3;45(39):11752–61.

58. Gustavsson M, Verardi R, Mullen DG, Mote KR, Traaseth NJ, Gopinath T, et al. Allosteric regulation of SERCA by phosphorylation-mediated conformational shift of phospholamban. Proc Natl Acad Sci U S A [Internet]. 2013;110(43):17338–43. Available from: http://www.pubmedcentral.nih.gov/articlerender.fcgi?artid=3808617&tool=pmcentrez&rendertype=abstract

59. Karim CB, Zhang Z, Howard EC, Torgersen KD, Thomas DD. Phosphorylation-dependent conformational switch in spin-labeled phospholamban bound to SERCA. J Mol Biol [Internet]. 2006 May;358(4):1032–40. Available from: http://www.sciencedirect.com/science/article/pii/S0022283606002506

60. Ceholski DK, Trieber C a., Holmes CFB, Young HS. Lethal, hereditary mutants of phospholamban elude phosphorylation by protein kinase A. Journal of Biological Chemistry. 2012;287:26596–605.

61. Wittmann T, Lohse MJ, Schmitt JP. Phospholamban pentamers attenuate PKA-dependent phosphorylation of monomers. J Mol Cell Cardiol [Internet]. 2015 Jan;80C:90–7. Available from: http://www.sciencedirect.com/science/article/pii/S0022282814004325

62. Masterson LR, Cheng C, Yu T, Tonelli M, Kornev A, Taylor SS, et al. Dynamics connect substrate recognition to catalysis in protein kinase A. Nat Chem Biol [Internet]. 2010 Oct;6:821. Available from: https://doi.org/10.1038/nchembio.452

63. Kemp BE, Bylund DB, Huang TS, Krebs EG. Substrate specificity of the cyclic AMP-dependent protein kinase. Proc Natl Acad Sci U S A [Internet]. 1975 Sep;72(9):3448–52. Available from: https://www.ncbi.nlm.nih.gov/pubmed/1059131

64. MACDOUGALL LK, JONES LR, COHEN P. Identification of the major protein phosphatases in mammalian cardiac muscle which dephosphorylate phospholamban. Eur J Biochem [Internet]. 1991 Mar;196(3):725–34. Available from: https://doi.org/10.1111/j.1432-1033.1991.tb15871.x

65. Steenaart NAE, Ganim JR, Di Salvo J, Kranias EG. The phospholamban phosphatase associated with cardiac sarcoplasmic reticulum is a type 1 enzyme. Arch Biochem Biophys [Internet]. 1992;293(1):17–24. Available from: http://www.sciencedirect.com/science/article/pii/0003986192903595

66. Winther AML, Bublitz M, Karlsen JL, Møller J V, Hansen JB, Nissen P, et al. The sarcolipin-bound calcium pump stabilizes calcium sites exposed to the cytoplasm. Nature [Internet]. 2013;495(7440):265–9. Available from: http://www.ncbi.nlm.nih.gov/pubmed/23455424

67. Toyoshima C, Iwasawa S, Ogawa H, Hirata A, Tsueda J, Inesi G. Crystal structures of the calcium pump and sarcolipin in the Mg2+-bound E1 state. Nature [Internet]. 2013 Mar;495:260. Available from: https://doi.org/10.1038/nature11899

68. Gorski PA, Glaves JP, Vangheluwe P, Young HS. Sarco(endo)plasmic Reticulum Calcium ATPase (SERCA) Inhibition by Sarcolipin Is Encoded in Its Luminal Tail. Journal of Biological Chemistry [Internet]. 2013 Mar;288(12):8456–67. Available from: http://www.jbc.org/content/288/12/8456.abstract

69. Sahoo SK, Shaikh S a., Sopariwala DH, Bal NC, Periasamy M. Sarcolipin protein interaction with Sarco(endo)plasmic reticulum CA 2+ ATPase (SERCA) Is distinct from phospholamban protein,and only sarcolipin can promote uncoupling of the serca pump. Journal of Biological Chemistry. 2013;288:6881–9.

70. Reddy LG, Cornea RL, Winters DL, McKenna E, Thomas DD. Defining the Molecular Components of Calcium Transport Regulation in a Reconstituted Membrane System. Biochemistry [Internet]. 2003 Apr;42(15):4585–92. Available from: https://doi.org/10.1021/bi026995a

71. Ceholski DK, Trieber C a., Young HS. Hydrophobic imbalance in the cytoplasmic domain of phospholamban is a determinant for lethal dilated cardiomyopathy. Journal of Biological Chemistry. 2012;287(20):16521–9.

72. Trieber CA, Douglas JL, Afara M, Young HS. The Effects of Mutation on the Regulatory Properties of Phospholamban in Co-Reconstituted Membranes†. Biochemistry [Internet]. 2005 Mar;44(9):3289–97. Available from: http://dx.doi.org/10.1021/bi047878d

73. Bal NC, Maurya SK, Sopariwala DH, Sahoo SK, Gupta SC, Shaikh S a, et al. Sarcolipin is a newly identified regulator of muscle-based thermogenesis in mammals. Nat Med [Internet]. 2012;18(10):1575–9. Available from: http://dx.doi.org/10.1038/nm.2897

74. Pant M, Bal NC, Periasamy M. Sarcolipin: A Key Thermogenic and Metabolic Regulator in Skeletal Muscle. Trends in Endocrinology and Metabolism. 2016.

75. Campbell KL, Dicke AA. Sarcolipin Makes Heat, but Is It Adaptive Thermogenesis? Front Physiol [Internet]. 2018 Jun;9:714. Available from: https://www.ncbi.nlm.nih.gov/pubmed/29962960

76. Bal NC, Sahoo SK, Maurya SK, Periasamy M. The Role of Sarcolipin in Muscle Non-shivering Thermogenesis [Internet]. Vol. 9, Frontiers in Physiology. 2018. p. 1217. Available from: https://www.frontiersin.org/article/10.3389/fphys.2018.01217

77. Gamu D, Bombardier E, Smith IC, Fajardo VA, Tupling AR. Sarcolipin Provides a Novel Muscle-Based Mechanism for Adaptive Thermogenesis. Exerc Sport Sci Rev. 2014;42(3):136–42.

78. Bal NC, Maurya SK, Sopariwala DH, Sahoo SK, Gupta SC, Shaikh S a, et al. Sarcolipin is a newly identified regulator of muscle-based thermogenesis in mammals. Nat Med [Internet]. 2012;18(10):1575–9. Available from: http://dx.doi.org/10.1038/nm.2897

79. MacLennan DH, Asahi M, Tupling AR. The regulation of SERCA-type pumps by phospholamban and sarcolipin. Ann N Y Acad Sci. 2003 Apr;986:472–80.

80. Bhupathy P, Babu GJ, Ito M, Periasamy M. Threonine-5 at the N-terminus can modulate sarcolipin function in cardiac myocytes. J Mol Cell Cardiol [Internet]. 2009;47(5):723–9. Available from: http://dx.doi.org/10.1016/j.yjmcc.2009.07.014

81. Magny EG, Pueyo JI, Pearl FMG, Cespedes M a., Niven JE, Bishop S a., et al. Conserved Regulation of Cardiac Calcium Uptake by Peptides Encoded in Small Open Reading Frames. Science (1979) [Internet]. 2013;341:1116–20. Available from: http://www.sciencemag.org/cgi/doi/10.1126/science.1238802

82. Nelson BR, Catherine A. Makarewich Benjamin R. Winders Constantine D. Troupes Fenfen Wu DMA, Reese AL, McAnally JR, Chen X, Kavalali ET, et al. A peptide encoded by a transcript annotated as long noncoding RNA enhances SERCA activity in muscle. Science (1979). 2016;351(6270).

83. Anderson DM, Anderson KM, Bassel-duby R, Olson EN, Mcanally JR, Kasaragod P, et al. A Micropeptide Encoded by a Putative Long Noncoding RNA Regulates Muscle Performance Article A Micropeptide Encoded by a Putative Long Noncoding RNA Regulates Muscle Performance. Cell [Internet]. 2015;160:1–12. Available from: http://dx.doi.org/10.1016/j.cell.2015.01.009

84. Magny EG, Pueyo JI, Pearl FMG, Cespedes MA, Niven JE, Bishop SA, et al. Conserved regulation of cardiac calcium uptake by peptides encoded in small open reading frames. Science [Internet]. 2013 [cited 2023 Mar 11];341(6150):1116–20. Available from: https://pubmed.ncbi.nlm.nih.gov/23970561/

Chapter 2

Phospholamban C-Terminal Residues are Critical Determinants of the Structure and Function of the Calcium ATPase Regulatory Complex

This research was originally published in The Journal of Biological Chemistry and has been revised for incorporation in the present thesis.

Abrol N, Smolin N, Armanious G, Ceholski DK, Trieber CA, Young HS, Robia SL. Phospholamban C-Terminal Residues are Critical Determinants of the Structure and Function of the Calcium ATPase Regulatory Complex. *Journal of Biological Chemistry. 2014*;289:25855-66.

© the American Society for Biochemistry and Molecular Biology.

Acknowledgements: Dr. C. Trieber purified SERCA, reconstituted & quantitated individual alanine PLN mutants, and provided guidance throughout experimentation. Abrol N, Smolin N and Robia SL performed FRET Experiments.

2.1 Abstract

To determine the structural and regulatory role of the C-terminal residues of PLN in the membranes of living cells, fluorescent protein tags were fused to PLN and SERCA. PLN-SERCA FRET information was corroborated with steady state activity measurements of SERCA reconstituted in the presence of PLN alanine substitution mutants or C-terminal truncation mutants. Alterations of the PLN pentamer and the SERCA-PLN regulatory complex conformation were observed as significant changes in FRET signal. Particularly, a PLN Val49-Ala substitution had large effects on PLN pentamer structure and SERCA-PLN regulatory complex conformation. A decrease in PLN oligomerization affinity, an increase in SERCA binding affinity of V49A-PLN, and a gain of inhibitory capacity through steady state calcium-dependent ATPase activity were quantified. Truncation of only a few C-terminal residues resulted in significant loss of PLN membrane anchoring and mislocalization from the sarcoplasmic reticulum to the cytoplasm and nucleus in the membrane of living cells. Inhibitory activity of purified co-reconstituted PLN truncation mutants was also progressively blunted. A decrease in PLN oligomerization affinity resulted from C-terminal truncations was monitored by loss of PLN-PLN FRET. A similar decrease in SERCA binding affinity and loss of inhibitory capacity was quantified for truncated PLN. In light of a decreased SERCA-PLN binding affinity, Val49-truncation of PLN increased intermolecular FRET by conformational changes in PLN reducing the distance between fluorophores by approximately 11Å. This chapter and corresponding published article highlight the critical importance and far-reaching effects that PLN C-terminal residues have on subcellular localization, oligomerization, and regulatory function of PLN.

2.2 Introduction

Heart failure is a leading cause of morbidity and mortality, affecting an estimated 26 million people worldwide and up to 6 million people in the United States alone (1). Dilated cardiomyopathy (DCM) and hypertrophic cardiomyopathy (HCM) are the two most common primary phenotypes of idiopathic cardiomyopathy (2,3). DCM and HCM are frequently associated with mutations in genes encoding cardiac calcium-handling proteins, including phospholamban (PLN) (2–19). PLN is a homopentameric integral sarcoplasmic reticulum membrane protein, with the pentamer canonically thought to be an inactive storage form of PLN. Deoligomerization of PLN into active monomers allows for reversible inhibition of SERCA (20–23) directly regulating intracellular Ca^{2+} kinetics and cardiac contractility (24–29). PLN architecture consists of a helix-loop-helix tertiary structure, beginning with the N-terminal cytosolic domain (residues 1–18), a flexible linker domain (residues 19–23), and the C-terminal transmembrane domain (residues 24–52) (Figure 2.1) (30,31).

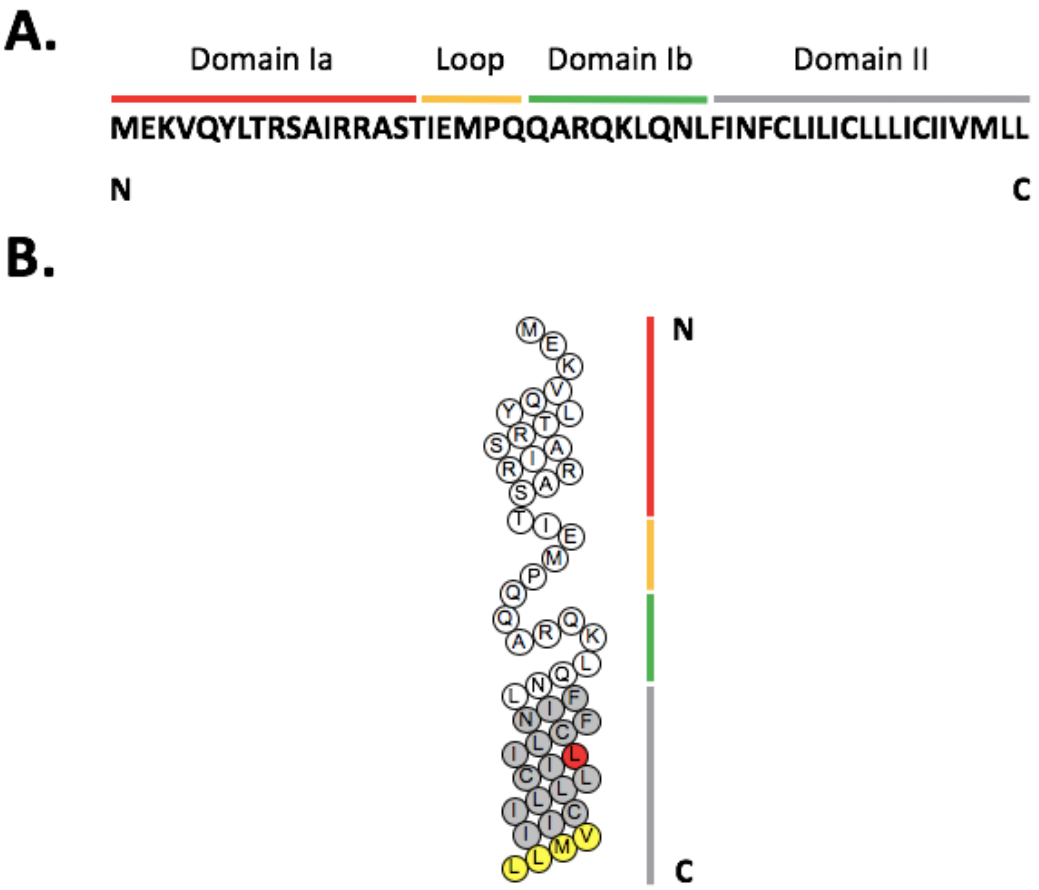

Figure 2.1 Schematic representation of C-terminal mutants of PLB. A, The amino acid sequence of WT PLN showing the N-terminal cytosolic domain Ia (residues 1–16), flexible linker (residues 17–22), domain Ib (residues 23–30), and the C-terminal transmembrane domain II (residues 31–52). Cer or YFP was fused to the N terminus for FRET assays, no tag was present for steady-state functional assessment. B, Schematic of the PLN monomer highlighting the mutation sites. Human mutation site Leu-39-truncation marked in red, C-terminal residues manipulated in this chapter shown in yellow. The thickness of the lipid bilayer is ~40 Å.

The C-terminal transmembrane domain is highly conserved across species (21) and is responsible for SERCA regulation (32) as well as PLN oligomerization through its Leu/Ile zipper (33,34). Substitution of a stop codon for Leu-39 (Leu-39-truncation) because of a naturally occurring human PLN missense mutation results in a loss of PLN protein, mistargeted subcellular targeting and dysregulation of cardiomyocyte calcium flux. The

resulting dysregulation of SR calcium handling has been shown to result in HCM in heterozygous individuals, and DCM resulting in heart failure and premature death in homozygous mutation carriers (15,16,18). The Young lab has shown previously that truncation of the C-terminus of PLN by Leu39-truncation mutation disrupted PLN oligomerization and SERCA binding (35). This body of work investigated the role of C-terminal residues of PLN in conferring subcellular localization, membrane anchoring, PLN oligomerization, and SERCA regulation. Evident structural and functional consequences resulted from mutating or truncating C-terminal transmembrane domain residues, and revealed an unanticipated capacity to influence the quaternary structure conformation of the SERCA-PLN regulatory complex.

2.3 Results

2.3.1 Individual Alanine Mutation

To investigate the role of C-terminal residues in determining the inhibitory potency of PLN, SERCA was reconstituted with WT or with C-terminal Ala substitutions or truncations of PLN. Previous Ala scanning substitution of individual residues in this region spanning Val^{49}-Met-Leu-Leu^{52} revealed very little change in inhibitory potency for the Leu52-Ala or Met50-Ala mutants and a gain of inhibitory function for the Leu51Ala and Val49-Ala mutants (36). This gain of inhibitory function effect of the individual Ala substitutions is visible in **Figure 2.2** as an increase in K_{Ca} (decrease of apparent calcium affinity) for the Leu51-Ala and Val49-Ala mutants compared with WT PLN.

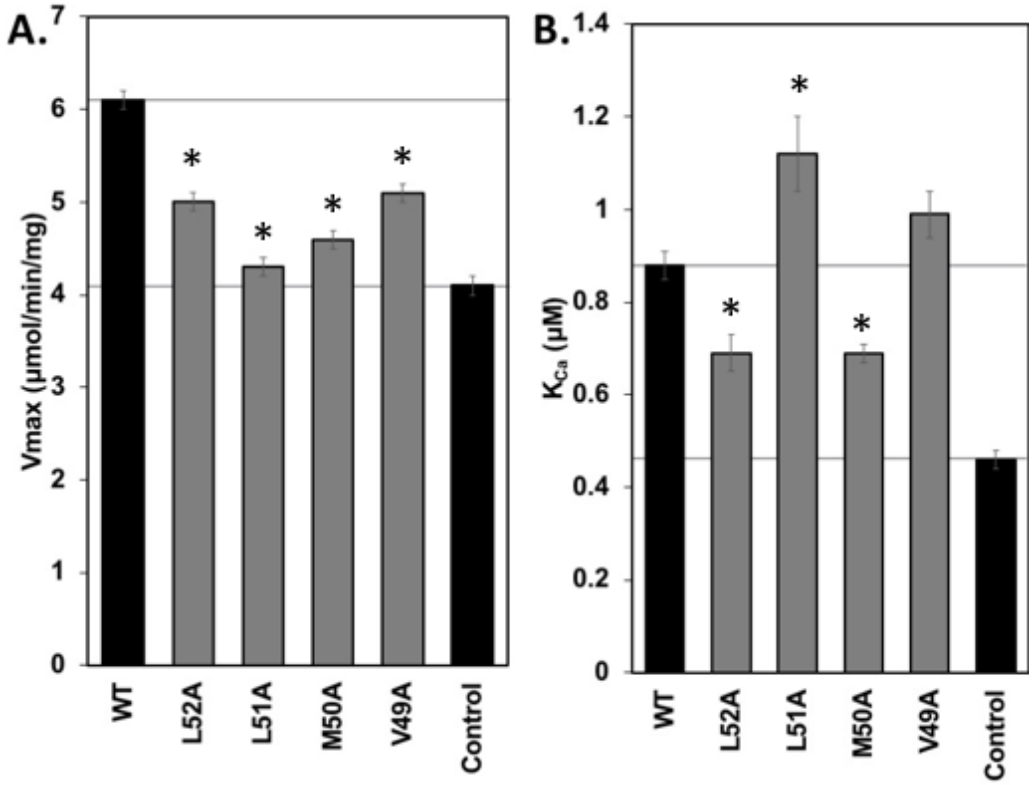

Figure 2.2 C-Terminal PLN Alanine Substitutions. A, Impact of C-terminal PLN alanine substitutions on SERCA Ca2+ Affinity. Calcium-dependent ATPase activity assays of SERCA co-reconstituted with WT and mutants of PLN were performed. The horizontal line at the bottom represents KCa of SERCA reconstituted alone, and the horizontal line at the top represents KCa of SERCA co-reconstituted with WT-PLN. Error bars represent S.E.M. B, Impact of C-terminal PLN alanine substitutions on SERCA Ca2+-dependent maximal activity. Calcium-dependent ATPase activity assays of SERCA co-reconstituted with WT and mutants of PLN were performed. The horizontal line at the bottom represents maximal activity of SERCA reconstituted alone, and the horizontal line at the top represents maximal activity of SERCA co-reconstituted with WT-PLN. Error bars represent S.E.M. *, $p < 0.05$, minimum 4 independent measurements.

2.3.2 Multiple Alanine Mutations

Multiple Ala mutations in this C-terminal region did not correlate with an additive effect of the individual Ala mutations. Mutation of the last two residues (Leu-52-Ala, Leu-51-Ala) resulted in a slight loss of inhibitory function where a wild-type like level of

inhibition might be expected. Mutation of the last three residues (Leu-52-Ala, Leu-51-Ala, Met-50-Leu) resulted in wild-type like inhibition of SERCA where a slight loss of inhibitory function might be expected (Figure 2.3.).

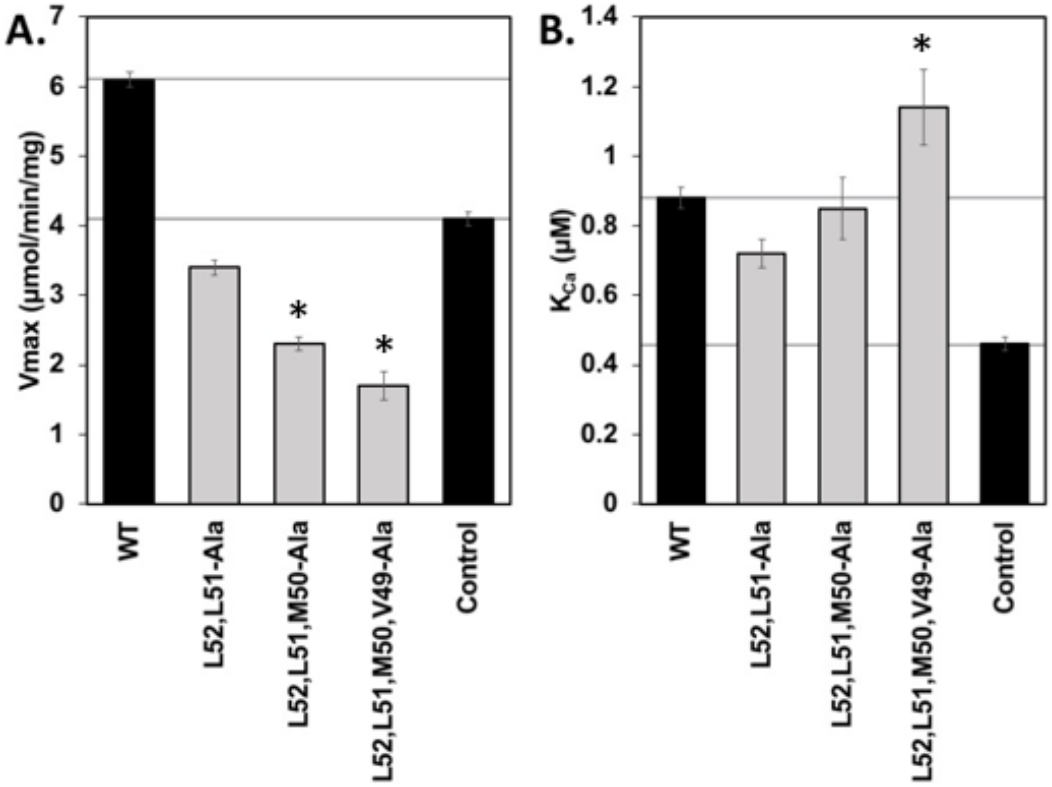

Figure 2.3 C-Terminal PLN Alanine Substitutions. A, Impact of C-terminal PLN alanine substitutions on SERCA Ca2+ Affinity. Calcium-dependent ATPase activity assays of SERCA co-reconstituted with WT and mutants of PLN were performed. The horizontal line at the bottom represents KCa of SERCA reconstituted alone, and the horizontal line at the top represents KCa of SERCA co-reconstituted with WT-PLN. Error bars represent S.E.M. B, Impact of C-terminal PLN alanine substitutions on SERCA Ca2+-dependent maximal activity. Calcium-dependent ATPase activity assays of SERCA co-reconstituted with WT and mutants of PLN were performed. The horizontal line at the bottom represents maximal activity of SERCA reconstituted alone, and the horizontal line at the top represents maximal activity of SERCA co-reconstituted with WT-PLN. Error bars represent S.E.M. *, $p < 0.05$, minimum 4 independent measurements.

Interestingly, there appeared to be a trend towards a gain of function at Val49 for both individual and multiple alanine substitutions.

2.3.3 Sequential Truncation of the PLN C-Terminus

In contrast, deletion of these same residues, which shortens the C-terminal PLN TM helix, resulted in a loss of function. Deletion of only 1 C-terminal residue, Leu^{52}, yielded 50% of the inhibitory potency of wild-type PLN akin to Leu-52-Ala mutation. Subsequent deletions resulted in a complete loss of PLN inhibitory function. Deletion of the last 2 or 3 residues decreased PLN inhibitory capacity to the extent that the observed K_{Ca} values were no longer significantly different from that of SERCA alone (Fig. 2.4 & Table 2.1).

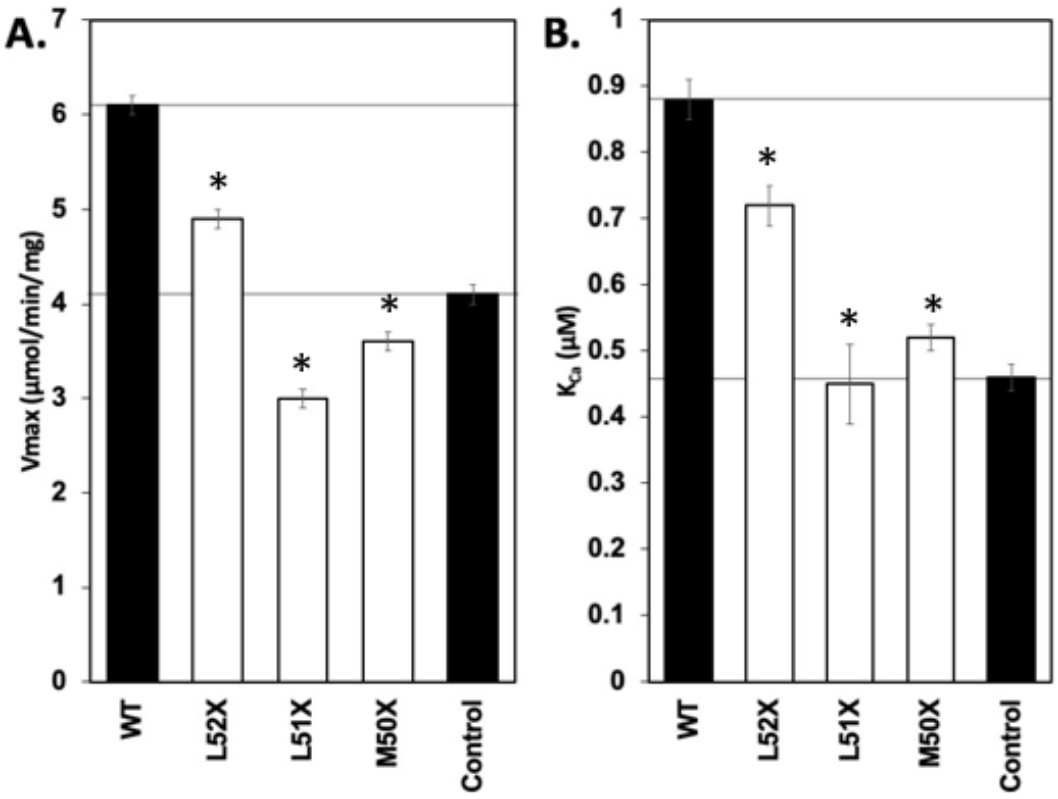

Figure 2.4 Impact of C-terminal PLN sequential truncation on SERCA activity. A, Impact of C-terminal PLN sequential truncation on SERCA Ca2+ affinity. Calcium-dependent ATPase activity assays of SERCA co-reconstituted with WT and mutants of PLN were performed. The horizontal line at the bottom represents KCa of SERCA reconstituted alone, and the horizontal line at the top represents KCa of SERCA co-reconstituted with WT-PLN. Error bars represent S.E.M. **B**, Impact of C-terminal PLN sequential truncations on SERCA Ca2+-dependent maximal activity. Calcium-dependent ATPase activity assays of SERCA co-reconstituted with WT and mutants of PLN were performed. The horizontal line at the bottom represents maximal activity of SERCA reconstituted alone, and the horizontal line at the top represents maximal activity of SERCA co-reconstituted with WT-PLN. Error bars represent S.E.M. *, $p < 0.05$, minimum 4 independent measurements.

Table 2.1 Summary of kinetic parameters of calcium-dependent ATPase activity of SERCA co-reconstituted with WT and mutant constructs of PLN. effect of C-terminal alanine substitutions and truncation mutations on K_{Ca} and V_{max}. Error is S.E.M. *, $p < 0.05$, minimum 4 independent measurements.

	K_{Ca} (μM)	*Vmax* (μmol/min/mg)
SERCA	0.46 ± 0.02	4.1 ± 0.1
WT-PLN	0.88 ± 0.03	4.7 ± 0.2
Individual alanine substitutions		
Leu52-Ala	0.69 ± 0.04	5.0 ± 0.1
Leu51-Ala	1.12 ± 0.08*	4.3 ± 0.1
Met50-Ala	0.69 ± 0.02*	4.6 ± 0.1
Val49-Ala	0.99 ± 0.05	5.1 ± 0.1
Multiple alanine substitutions		
Leu51-Ala/Leu52-Ala	0.72 ± 0.04*	3.4 ± 0.1
Met50-Ala/Leu51-Ala/Leu52-Ala	0.85 ± 0.09	2.3 ± 0.1
Val49-Ala/Met50-Ala/Leu51-Ala/Leu52-Ala	1.14 ± 0.03*	1.7 ± 0.2
Sequential truncation mutations		
Leu52-Truncation (L52X)	0.72 ± 0.03*	4.9 ± 0.1
Leu51-Truncation (L51X)	0.45 ± 0.06*	3.0 ± 0.1
Met50-Truncation (M50X)	0.52 ± 0.02*	3.6 ± 0.1

The truncation data indicate that the C-terminal residues of PLN are highly important determinants for exerting SERCA inhibition and that small deletions have the capacity to negate the entirety of PLN's inhibitory effect.

2.4 Discussion

Alanine substitution has been a common mutagenesis strategy for understanding how residues of PLN influence the functional regulation of SERCA ATPase activity (32,36,37). This method effectively removes the side chain of the individual residues in PLN, providing information on the impact they exert on SERCA. The single residue Arg14 deletion (9–11) and the multiple residue Leu39 truncation (15,16,18) are two of the most common human PLN mutations which have been linked to heart failure. Because such a relatively large portion of the C-terminus of PLN is missing in this latter truncation variant (14 of 52 residues), we strove to understand the comparative effects of C-terminal mutations and truncations. Dramatic effects were observed in PLN function with only moderate mutations relative to the Leu39-stop human PLN mutation. Only the last four C-terminal residues of PLN were manipulated (Val49-Met-Leu-Leu52) due to the elimination of PLN function observed with the loss of so few residues. In steady-state measurements of SERCA ATPase activity in the absence and presence of PLN, individual and multiple Ala substitutions revealed a propensity towards a gain of function at Val49 of PLN (Fig. 2.2). This gain of function was unexpected, and it contrasted sharply with the detrimental effects of truncating the last few residues. Truncation of 1 residue

severely reduced PLN function by approximately 50%, and truncation of two or more residues completely eliminated PLN function.

To investigate the role of C-terminal residues (Fig 2.2) in determining the inhibitory characteristics of PLN we reconstituted SERCA with WT or with C-terminal Ala substitutions or truncations of PLN. Previous Ala substitution of individual residues in the region of Val^{49}-Met-Leu-Leu^{52} did not reveal large changes in inhibitory efficacy for the L52A or M50A mutants, but resulted in a gain of function for the Leu51-Ala and Val49-Ala mutants (36). The resulting gain-of-function effect of the individual Ala substitutions Leu51-Ala and Val49-Ala is visible in Fig. 2.2 as an increase in K_{Ca} for Leu51-Ala and Val49-Ala compared with SERCA in the presence of WT-PLN. Multiple Ala mutations of 3 or 4 residues in this C-terminal region also maintained PLN inhibitory function with a gain-of-function effect for Ala substitution of all four residues (38–41). Taken together, Leu52 is an important residue which accounted for approximately 50% of PLN's inhibitory capacity. Interestingly, there appeared to be a trend towards a gain of function at Val^{49} for both individual and multiple alanine substitutions. An atypical result of multiple alanine mutation was the reduction in SERCA V_{max} with 3 or more residues mutated to alanine, again with a maximal effect occurring with all four C-terminal residues including Val49-Ala. This increased inhibitory effect was demonstrated in parallel with a K_{Ca} decrease below that of SERCA in the presence of WT-PLN. In contrast, shortening the PLN TM domain helix by deleting these same residues resulted in a complete loss of function. Deletion of only one C-terminal residue, Leu^{52}, from the full-length protein yielded 50% of the inhibitory potency of wild-type PLN, while further deletions abolished all PLN function. Deletion of the last two-to-three residues decreased PLN inhibitory potency to the extent that observed K_{Ca} values were not significantly different from that of SERCA alone (Fig 2.4 and Table 2.1). Together, the

data indicate that these four C-terminal residues of PLN are critical determinants for tuning SERCA inhibition. A surprising amount of control over the nature of the PLN-SERCA interaction is dictated by these residues and even small deletions or substitutions either significantly decrease or increase the inhibitory effect of PLN.

In an attempt to assess the function of C-terminal residues in the context of the inhibitory capacity exerted through the PLN transmembrane domain, SERCA was co-reconstituted in the presence of synthetic transmembrane domain PLN peptides. We observed complete lack of inhibitory activity when only two residues were deleted (Figure 2.4). Although the cytosolic domain itself does not contribute to the majority of PLN's inhibitory activity, a minimum requirement is likely present to aid in docking PLN to SERCA in a functionally active conformation. Identifying such a potential minimum requirement for the cytosolic domain of PLN was not the aim for this study.

The collective observations of this published study, including the FRET assays completed by our collaborators (credit: Robia Lab) (42), are summarized in the schematic model in Fig. 2.6. Reversible equilibria are indicated by black arrows and effects of PLN mutations are highlighted by red arrows. C-terminal deletions decreased PLN-PLN binding (Fig. 9B, i) without altering pentamer structure. Alanine substitutions resulted in a mix of increased or decreased PLN pentamer FRETmax supporting a structural change (Fig. 2.6) that altered the distance between FRET pairs. Key FRET experiments conducted by our collaborators, the Robia lab, supported our functional studies of SERCA inhibition (42). Only one C-terminal residue of PLB has to be deleted in order to increase FRETmax by 1.2-fold, which changes the distance from 61.9Å to 58.9 Å. ((42), Table 2.2) The distance between the donor and acceptor fluorophores was reduced by 11.3Å after truncating four C-terminal residues (V49X), which boosted FRETmax by more

than twofold (Table 2.2). Similarly, the donor-acceptor distance decreased by 3.3Å because of certain Ala substitutions, with V49A showing a 23% increase in FRETmax. The misregistration of PLN in the inhibitory cleft due to substitutions and deletions is one explanation for the observed structural alteration (Fig. 2.6, A and B, iii). The observed rise in FRET from a donor fluorophore on the SERCA N terminus could be explained by a shift in the position of the TM domain allowing cytoplasmic domain relocation. Val49 seems to have a key role in determining how the TM helix is registered in the bilayer, influencing the placement of the TM domain and the farther-reaching PLN cytoplasmic domain, which is located on the opposite side of the bilayer and more than 40Å away.

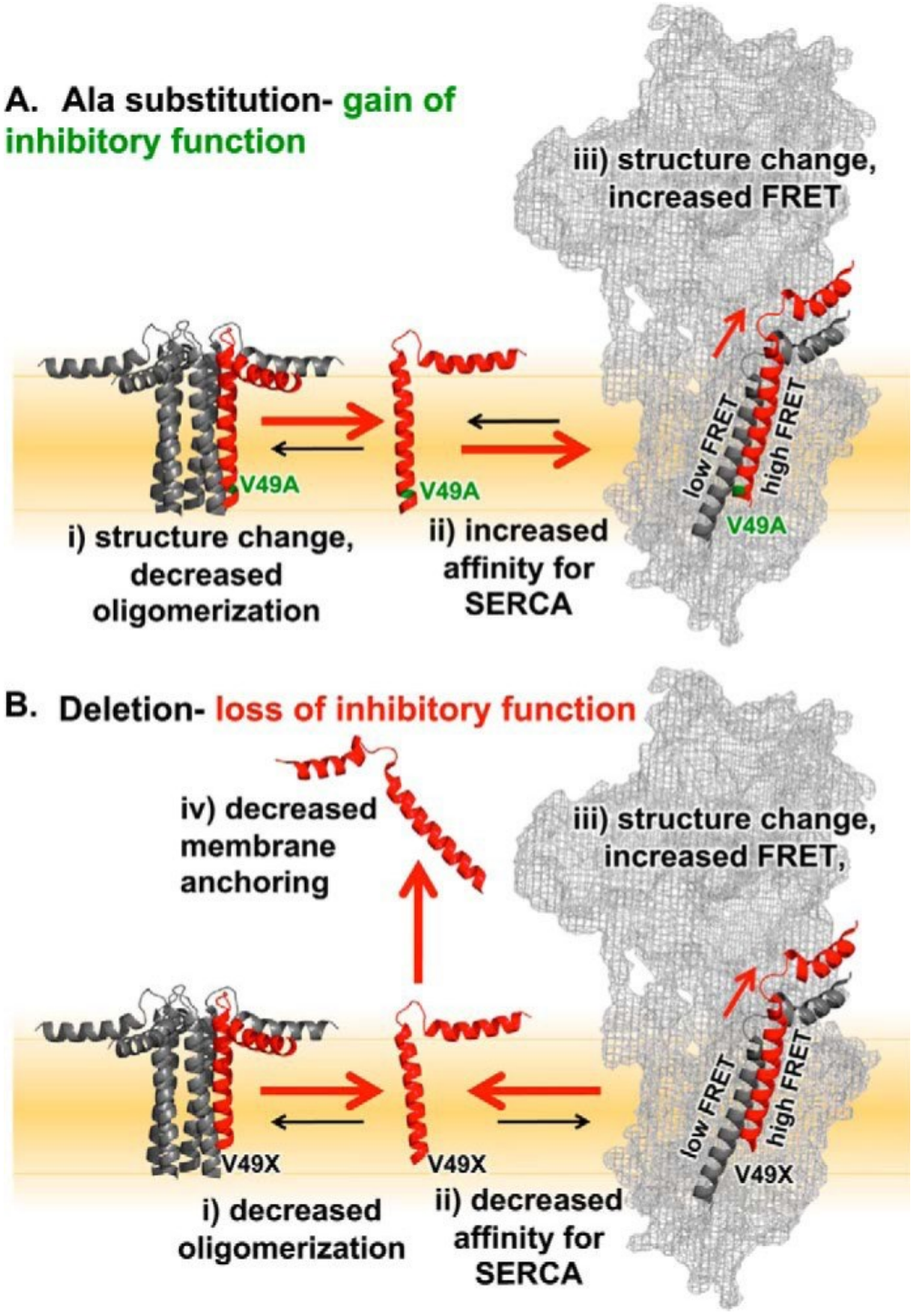

Figure 2.5 Proposed model for the effect of PLB C-terminal substitution and deletion mutations on membrane localization, oligomerization, and interaction with SERCA. The WT PLN monomers and SERCA are shown in gray, and the alanine substitution (V49A) or the deletion mutant (V49X) PLN monomers are highlighted in red. Reversible equilibria are indicated by black arrows, and effects of mutations are

highlighted with red arrows. **A,** we propose that C-terminal PLN alanine substitution mutations result in altered pentamer structure and decreased oligomerization affinity (i), increased SERCA-PLN binding affinity (ii), and altered quaternary conformation of the SERCA-PLN regulatory complex (iii). B, in addition, C-terminal deletions of PLN result in decreased oligomerization affinity (i), decreased SERCA-PLB binding affinity (ii), altered quaternary conformation of the SERCA-PLB regulatory complex (iii), and decreased membrane anchoring (iv).

Taken from Abrol N, Smolin N, Armanious G, Ceholski DK, Trieber CA, Young HS, Robia SL. Phospholamban C-Terminal Residues are Critical Determinants of the Structure and Function of the Calcium ATPase Regulatory Complex. Journal of Biological Chemistry. 2014;289:25855-66.

It is possible that C-terminal substitutions disrupt PLN topology or perturb the structural equilibrium of PLN akin to a transition between ordered and disordered states, explaining the difference in observed FRETmax (43,44). The largest increases in FRETmax were observed for Leu51-Ala and Val49-Ala PLN, correlating with the increased inhibitory effect of these mutants. It is interesting that these C-terminal mutations impact N-terminal FRET probe positioning relative to SERCA over such a long distance of over 40Å through PLN.

Quantitating the affinity of PLN for SERCA is made difficult by the pentameric quaternary structure of the regulatory peptide and cellular localization. The results in this study allow for the clear qualitative interpretation of Alanine substitution mutations increasing the affinity for SERCA, while deletion mutations exert a decreased affinity for SERCA. This is exemplified by the increase in SERCA binding by Leu51-Ala and Val49-Ala mutants and the contrasting reduction in SERCA binding with sequential C-terminal residue truncation, with a precipitous drop seen with Val49 truncation. In agreement with our steady-state functional studies, Leu51-Ala increased FRETmax by 14.9% while Val49-Ala mutation resulted in a 23% increase in FRETmax ((42) Table 2.2). In agreement with our steady-state functional studies, deletion of one C-terminal residue of PLN

decreased FRETmax 1.2-fold. It is possible that the structural changes altered the nature of the transmembrane inhibitory interaction between SERCA and PLN. This was observed by the change in FRET probe pair signal because of the substitutions and truncations made (Fig. 2.6). The evidence suggests a specific importance for Val49 in establishing the positioning and nature of the interaction with SERCA. Furthermore, the evidence gathered highlights the role of Val49 in the positioning of the transmembrane domain and distant effects on the cytoplasmic domain on the other side of the lipid bilayer.

As may be expected in addition to the functional effects of C-terminal residues, membrane anchoring of PLN is an important function of the residues investigated (Fig 2.6). Only C-terminal truncations decreased PLN membrane retention as measured by the cellular localization of FRET probes (Fig 2.6, (42)). C-terminal truncation resulted in a mislocalization of PLN to the cytoplasm where it is presumed to no longer exert an inhibitory effect on SERCA. The importance of the C-terminal region of PLN for subcellular trafficking has been demonstrated in experiments that increased the length of the transmembrane domain of PLN by appending four leucine residues to the C terminus which resulted in mistargeting to the plasma membrane (39). Similarly, the five residue C-terminal Arg-Ser-Tyr-Gln-Tyr sequence of the related SERCA regulator sarcolipin was shown to mediate its retention in the ER (40) in addition to its inhibitory potency (41). The results from our collaborators (Robia Lab) display a similar role for the PLN C-terminal residues in the cellular localization of the peptide. The structural conformation and functional capabilities of the SERCA-PLN regulatory complex, the PLN pentamer conformation and dynamics, and membrane anchoring, are critical capabilities of the luminal residues of the PLN C-terminus despite the many hydrophobic residues of the transmembrane domain. The intolerance of small deletions to the structure and function of PLN and the SERCA-PLN regulatory complex is noteworthy. Truncation of a

single C-terminal residue from the 22-amino acid transmembrane domain of PLN impacted the cellular localization of the regulatory peptide, the PLN pentamer, and PLN-SERCA inhibitory interactions. PLN localization was not improved by coexpression of SERCA in this study or previous reports, despite an improvement in the localization of sarcolipin truncation mutants having been seen prior (39,40,45).

There is a dramatic difference between the substitution and deletion mutants in their divergent effects on PLN inhibitory behaviour. The data suggests the loss-of-function observed in the truncation mutants may be a consequence of some combination of decreased membrane anchoring and a reduction in SERCA binding (Fig. 2.6). To the contrary, the presumed misalignment of the PLN transmembrane domain in the SERCA regulatory site may result in an interaction which holds no inhibitory value. It has been shown that PLN and SERCA can interact in a non-inhibitory complex following PLN phosphorylation (46), or in the presence of micromolar Ca^{2+} concentrations (47–49). The relief of inhibition seen at micromolar Ca^{2+} concentrations and from PLN phosphorylation alters the structure of the SERCA-PLN regulatory complex with a limited effect on SERCA-PLN affinity (46–48,50). The structural change resulting from either Val49-Ala or Leu51-Ala produces a sizable gain in inhibitory function, opposite to truncation mutants or physiological regulation (Fig. 2.2 and Table 2.1). More recent crystallographic evidence places Val49 of PLN in close proximity to Val89 in M2 of SERCA, adding mechanistic detail to the potential steric clash that may be experienced by longer chain amino acids at the residue 49 position in PLN (51). Our data is in alignment with this more recent functional and crystallographic information, supporting the hypothesis that replacement of PLN Val49 with smaller residues will eliminate this steric hindrance and allow for a higher affinity and closer heterodimer interaction, netting an increase in inhibitory potency and efficacy (26,51,52). Truncation of Val49

did not, however, result in a similar gain-of-function result. The PLN-SERCA inhibitory interaction was decreased with truncation and was susceptible to loss of inhibitory function with the removal of a minimal number of residues.

Taken together, C-terminal residues of PLN are critical determinants of the structure and function of the SERCA regulatory complex. We have demonstrated the impact of C-terminal PLN residues on SERCA-PLN and PLN-PLN interactions. Both truncations and Ala substitutions of these C-terminal PLN residues increased SERCA-PLN FRET but had divergent effects on SERCA. The mechanistic details concerning the ability of alterations in C-terminal residues to transmit such a strong effect to the cytoplasmic domain of PLN remains unclear, and a potential target for later structural studies.

2.5 Future Directions

It has been demonstrated that much of the inhibitory capacity of SLN is encoded in its unique C-terminal Arg-Ser-Tyr-Gln-Tyr motif (62) . An interesting parallel may be drawn to the completely dissimilar four C-terminal PLN residues Val49-Met-Leu-Leu52, with both Val49-Ala and Leu51-Ala mutation resulting in an increased inhibitory effect. An avenue of investigation we did not pursue was to assess the inhibitory potency of the double alanine Val49-Ala/Leu51-Ala PLN mutant and whether these residues could impart a combinatorial super-inhibitory effect. I would predict that this would result in both a suppressed SERCA Vmax akin to Val-49-Ala alone and combinatorial effect of a K_{Ca} increased significantly above that of Leu51-Ala or Val49-Ala PLN alone.

A dramatic effect on PLN cytoplasmic domain positioning was seen as a result of C-terminal residue truncation or mutation. If possible, a high-SERCA affinity PLN variant

with either one to four C-terminal residue truncation or alanine substitution PLN mutant would be a high value target for co-crystallization studies. Structural information regarding the positioning of PLN in the inhibitory site of SERCA may answer the questions of whether PLN retains a WT-like positioning relative to SERCA, in accordance with the Val49 steric hindrance theory. Such an experiment may also rationalize how a repositioning of the cytoplasmic domain is achieved, whether by a change in PLN secondary structure, or a translocation of PLN in the inhibitory site of SERCA.

An interesting avenue of investigation to glean information on the interplay of the positioning of the cytosolic domain of PLN and the translocation of the transmembrane domain could be followed up on as a result of this study. The PLN cytosolic domain has been previously shown to exert an effect on SERCA Vmax (46) and a rearrangement of PLN relative to SERCA was seen with sequential truncation mutations, individual and multiple alanine mutations of the C-terminus. In these instances, an effect on SERCA Vmax was also observed. Sequential truncation and multiple alanine mutation saw the most pronounced effect as demonstrated by the reduction in SERCA Vmax beyond what was seen from SERCA reconstituted in the presence of individual alanine mutations and SERCA alone. The severity of the impact of C-terminal residue mutation or truncation is further highlighted by the complete inversion of the effect PLN has on SERCA Vmax seen in both cases of C-terminal truncation and multiple alanine substitution. This mutual decrease in Vmax is especially interesting given the completely divergent effect of multiple alanine mutation (decreased calcium affinity beyond the capacity of WT PLN) and C-terminal truncation (loss of inhibitory capacity).

2.6 Materials and Methods

2.6.1 Quantification of PLB/SERCA Function

SERCA and PLB were co-reconstituted as described previously (53). SERCA1a was purified from rabbit skeletal muscle sarcoplasmic reticulum using affinity chromatography (54,55), and recombinant PLB was purified from Escherichia coli using a two-step method (53). The purified proteoliposomes yielded a final molar ratio of 1:4.5:120 SERCA:PLB:lipids. The SERCA and PLB concentrations were determined by quantitative SDS-PAGE, and lipid concentration was determined by phosphate assay (56,57). Ca2+-dependent ATPase activities of SERCA co-reconstituted with PLB were determined using a coupled enzyme assay as described previously (58). All co-reconstituted PLB Ala and truncation mutants were compared with a negative control (SERCA alone) and a positive control (SERCA with wild-type PLB). A minimum of three independent reconstitutions and activity assays were performed for each mutant, and the ATPase activity was measured over a range of Ca2+ concentrations (0.1–10 μm). The Ca2+ concentration at half-maximal activity (KCa) and the maximal activity (Vmax) were calculated based on non-linear least square fitting of the activity data to the Hill equation using Sigma Plot (SPSS Inc., Chicago, IL).

2.6.2. Statistical Analysis

All experiments were independently repeated three or four times for each sample. Errors are reported as standard error, and statistical significance was evaluated where $p < 0.05$ was considered significant. The comparison of KCa and Vmax was carried out using one-way analysis of variance (between subjects) followed by the Holm-Sidak test for pairwise comparisons.

Chapter 2 References

1. Roger VL. The Heart Failure Epidemic. International Journal of Environmental Research and Public Health 2010, Vol 7, Pages 1807-1830 [Internet]. 2010 Apr 19 [cited 2022 Oct 5];7(4):1807–30. Available from: https://www.mdpi.com/1660-4601/7/4/1807/htm

2. Towbin JA, Bowles NE. Molecular diagnosis of myocardial disease. Expert Rev Mol Diagn [Internet]. 2002 Nov [cited 2022 Oct 5];2(6):587–602. Available from: https://pubmed.ncbi.nlm.nih.gov/12465455/

3. Kimura A. Molecular etiology and pathogenesis of hereditary cardiomyopathy. Circ J [Internet]. 2008 [cited 2022 Oct 5];72 Suppl A(SUPPL. A). Available from: https://pubmed.ncbi.nlm.nih.gov/18772524/

4. te Rijdt WP, van der Klooster ZJ, Hoorntje ET, Jongbloed JDH, van der Zwaag PA, Asselbergs FW, et al. Phospholamban immunostaining is a highly sensitive and specific method for diagnosing phospholamban p.Arg14del cardiomyopathy. Cardiovasc Pathol [Internet]. 2017 Sep 1 [cited 2022 Oct 5];30:23–6. Available from: https://pubmed.ncbi.nlm.nih.gov/28759816/

5. te Rijdt WP, van Tintelen JP, Vink A, van der Wal AC, de Boer RA, van den Berg MP, et al. Phospholamban p.Arg14del cardiomyopathy is characterized by phospholamban aggregates, aggresomes, and autophagic degradation. Histopathology [Internet]. 2016 Oct 1 [cited 2022 Oct 5];69(4):542–50. Available from: https://pubmed.ncbi.nlm.nih.gov/26970417/

6. te Rijdt WP, ten Sande JN, Gorter TM, van der Zwaag PA, van Rijsingen IA, Boekholdt SM, et al. Myocardial fibrosis as an early feature in phospholamban p.Arg14del mutation carriers: phenotypic insights from cardiovascular magnetic resonance imaging. Eur Heart J Cardiovasc Imaging [Internet]. 2019 Jan 1 [cited 2022 Oct 5];20(1):92–100. Available from: https://pubmed.ncbi.nlm.nih.gov/29635323/

7. van Rijsingen IAW, van der Zwaag PA, Groeneweg JA, Nannenberg EA, Jongbloed JDH, Zwinderman AH, et al. Outcome in phospholamban R14del carriers: results of a large multicentre cohort study. Circ Cardiovasc Genet [Internet]. 2014 Aug 1 [cited 2022 Oct 5];7(4):455–65. Available from: https://pubmed.ncbi.nlm.nih.gov/24909667/

8. van der Zwaag PA, van Rijsingen IAW, Asimaki A, Jongbloed JDH, van Veldhuisen DJ, Wiesfeld ACP, et al. Phospholamban R14del mutation in patients diagnosed with dilated cardiomyopathy or arrhythmogenic right ventricular cardiomyopathy: evidence supporting the concept of arrhythmogenic cardiomyopathy. Eur J Heart Fail [Internet]. 2012 Nov [cited 2022 Sep 30];14(11):1199–207. Available from: https://pubmed.ncbi.nlm.nih.gov/22820313/

9. Posch MG, Perrot A, Geier C, Boldt LH, Schmidt G, Lehmkuhl HB, et al. Genetic deletion of arginine 14 in phospholamban causes dilated cardiomyopathy with attenuated electrocardiographic R amplitudes. Heart Rhythm [Internet]. 2009 Jan 18 [cited 2022 Oct 2];6(4):480–6. Available from: http://europepmc.org/article/MED/19324307

10. DeWitt MM, MacLeod HM, Soliven B, McNally EM. Phospholamban R14 Deletion Results in Late-Onset, Mild, Hereditary Dilated Cardiomyopathy. J Am Coll Cardiol

[Internet]. 2006;48(7):1396–8. Available from: http://www.sciencedirect.com/science/article/pii/S0735109706018377

11. Haghighi K, Kolokathis F, Gramolini AO, Waggoner JR, Pater L, Lynch RA, et al. A mutation in the human phospholamban gene, deleting arginine 14, results in lethal, hereditary cardiomyopathy. Proceedings of the National Academy of Sciences [Internet]. 2006 Jan;103(5):1388 LP – 1393. Available from: http://www.pnas.org/content/103/5/1388.abstract

12. Ha KN, Mastersona LR, Hou Z, Verardi R, Walsh N, Veglia G, et al. Lethal Arg9Cys phospholamban mutation hinders Ca2+-ATPase regulation and phosphorylation by protein kinase A. Proc Natl Acad Sci U S A [Internet]. 2011 Feb 15 [cited 2022 Oct 5];108(7):2735–40. Available from: https://www.pnas.org/doi/abs/10.1073/pnas.1013987108

13. Schmitt JP, Kamisago M, Asahi M, Li GH, Ahmad F, Mende U, et al. Dilated cardiomyopathy and heart failure caused by a mutation in phospholamban. Science. 2003;299(February):1410–3.

14. Pugh TJ, Kelly MA, Gowrisankar S, Hynes E, Seidman MA, Baxter SM, et al. The landscape of genetic variation in dilated cardiomyopathy as surveyed by clinical DNA sequencing. Genetics in Medicine. 2014;16(8):601–8.

15. Landstrom AP, Adekola BA, Bos JM, Ommen SR, Ackerman MJ. PLN-encoded phospholamban mutation in a large cohort of hypertrophic cardiomyopathy cases: Summary of the literature and implications for genetic testing. Am Heart J [Internet].

2011;161(1):165–71. Available from: http://www.sciencedirect.com/science/article/pii/S0002870310006757

16. Chiu C, Tebo M, Ingles J, Yeates L, Arthur JW, Lind JM, et al. Genetic screening of calcium regulation genes in familial hypertrophic cardiomyopathy. J Mol Cell Cardiol. 2007 Sep 1;43(3):337–43.

17. Mollanoori H, Naderi N, Amin A, Hassani B, Shahraki H, Teimourian S. A novel human T17N-phospholamban variation in idiopathic dilated cardiomyopathy. Gene Rep [Internet]. 2018;12(June):122–7. Available from: https://doi.org/10.1016/j.genrep.2018.06.014

18. Haghighi K, Kolokathis F, Pater L, Lynch RA, Asahi M, Gramolini AO, et al. Human phospholamban null results in lethal dilated cardiomyopathy revealing a critical difference between mouse and human. J Clin Invest [Internet]. 2003 Mar;111(6):869–76. Available from: https://doi.org/10.1172/JCI17892

19. Medeiros A, Biagi DG, Sobreira TJP, de Oliveira PSL, Negrão CE, Mansur AJ, et al. Mutations in the human phospholamban gene in patients with heart failure. Am Heart J [Internet]. 2011;162(6):1088-1095.e1. Available from: http://dx.doi.org/10.1016/j.ahj.2011.07.028

20. Kimura Y, Kurzydlowski K, Tada M, MacLennan DH. Phospholamban Inhibitory Function Is Activated by Depolymerization. Journal of Biological Chemistry [Internet]. 1997 Jun;272(24):15061–4. Available from: http://www.jbc.org/content/272/24/15061.abstract

21. Simmerman HKB, Jones LR. Phospholamban: Protein structure, mechanism of action, and role in cardiac function. Physiol Rev [Internet]. 1998 [cited 2022 Oct 1];78(4):921–47. Available from: https://journals.physiology.org/doi/10.1152/physrev.1998.78.4.921

22. Robia SL, Campbell KS, Kelly EM, Hou Z, Winters DL, Thomas DD. Förster Transfer Recovery Reveals That Phospholamban Exchanges Slowly From Pentamers but Rapidly From the SERCA Regulatory Complex. Circ Res [Internet]. 2007 Nov;101(11):1123–9. Available from: https://www.ahajournals.org/doi/10.1161/CIRCRESAHA.107.159947

23. Karim CB, Stamm JD, Karim J, Jones LR, Thomas DD. Cysteine Reactivity and Oligomeric Structures of Phospholamban and Its Mutants†. Biochemistry [Internet]. 1998 Sep 1 [cited 2022 Oct 5];37(35):12074–81. Available from: https://pubs.acs.org/doi/abs/10.1021/bi980642n

24. Zvaritch E, Backx PH, Jirik F, Kimura Y, de Leon S, Schmidt AG, et al. The transgenic expression of highly inhibitory monomeric forms of phospholamban in mouse heart impairs cardiac contractility. J Biol Chem [Internet]. 2000 May 19 [cited 2022 Oct 5];275(20):14985–91. Available from: https://pubmed.ncbi.nlm.nih.gov/10809743/

25. Bluhm WF, Kranias EG, Dillmann WH, Meyer M. Phospholamban: A major determinant of the cardiac force-frequency relationship. Am J Physiol Heart Circ Physiol [Internet]. 2000 [cited 2022 Oct 10];278(1 47-1). Available from: https://journals.physiology.org/doi/10.1152/ajpheart.2000.278.1.H249

26. Haghighi K, Schmidt AG, Hoit BD, Brittsan AG, Yatani A, Lester JW, et al. Superinhibition of sarcoplasmic reticulum function by phospholamban induces cardiac

contractile failure. J Biol Chem [Internet]. 2001 Jun 29 [cited 2022 Oct 10];276(26):24145–52. Available from: https://pubmed.ncbi.nlm.nih.gov/11328820/

27. MacLennan DH, Kranias EG. Phospholamban: a crucial regulator of cardiac contractility. Nat Rev Mol Cell Biol [Internet]. 2003 Jul;4(7):566–77. Available from: http://www.nature.com/articles/nrm1151

28. Kranias EG, Hajjar RJ. Modulation of cardiac contractility by the phopholamban/SERCA2a regulatome. Circ Res. 2012;110(12):1646–60.

29. Park WJ, Oh JG. SERCA2a: a prime target for modulation of cardiac contractility during heart failure. BMB Rep [Internet]. 2013 [cited 2022 Oct 10];46(5):237–43. Available from: https://pubmed.ncbi.nlm.nih.gov/23710633/

30. Zamoon J, Mascioni A, Thomas DD, Veglia G. NMR Solution Structure and Topological Orientation of Monomeric Phospholamban in Dodecylphosphocholine Micelles. Biophys J [Internet]. 2003 Oct 1 [cited 2022 Oct 10];85(4):2589. Available from: /pmc/articles/PMC1303482/

31. Verardi R, Shi L, Traaseth NJ, Walsh N, Veglia G. Structural topology of phospholamban pentamer in lipid bilayers by a hybrid solution and solid-state NMR method. Proc Natl Acad Sci U S A [Internet]. 2011 May 31 [cited 2022 Oct 1];108(22):9101–6. Available from: https://www.pnas.org/doi/abs/10.1073/pnas.1016535108

32. Kimura Y, Kurzydlowski K, Tada M, MacLennan DH. Phospholamban regulates the Ca2+-ATPase through intramembrane interactions. J Biol Chem [Internet]. 1996 [cited

2022 Oct 10];271(36):21726–31. Available from: https://pubmed.ncbi.nlm.nih.gov/8702967/

33. Simmerman HKB, Kobayashi YM, Autry JM, Jones LR. A leucine zipper stabilizes the pentameric membrane domain of phospholamban and forms a coiled-coil pore structure. Journal of Biological Chemistry. 1996;271(10):5941–6.

34. Fujii J, Maruyama K, Tada M, MacLennan DH. Expression and Site-specific Mutagenesis of Phospholamban: Studies of Residues Involved in Phosphorylation and Pentamer Formation. Journal of Biological Chemistry. 1989 Aug 5;264(22):12950–5.

35. Kelly EM, Hou Z, Bossuyt J, Bers DM, Robia SL. Phospholamban oligomerization, quaternary structure, and sarco(endo)plasmic reticulum calcium ATPase binding measured by fluorescence resonance energy transfer in living cells. Journal of Biological Chemistry. 2008;283:12202–11.

36. Trieber CA, Afara M, Young HS. Effects of Phospholamban Transmembrane Mutants on the Calcium Affinity, Maximal Activity, and Cooperativity of the Sarcoplasmic Reticulum Calcium Pump. Biochemistry [Internet]. 2009 Oct;48(39):9287–96. Available from: https://doi.org/10.1021/bi900852m

37. Ceholski DK, Trieber C a., Young HS. Hydrophobic imbalance in the cytoplasmic domain of phospholamban is a determinant for lethal dilated cardiomyopathy. Journal of Biological Chemistry. 2012;287(20):16521–9.

38. Hou Z, Kelly EM, Robia SL. Phosphomimetic Mutations Increase Phospholamban Oligomerization and Alter the Structure of Its Regulatory Complex. Journal of Biological

Chemistry [Internet]. 2008 Oct;283(43):28996–9003. Available from: http://www.jbc.org/lookup/doi/10.1074/jbc.M804782200

39. Butler J, Lee AG, Wilson DI, Spalluto C, Hanley NA, East JM. Phospholamban and sarcolipin are maintained in the endoplasmic reticulum by retrieval from the ER-Golgi intermediate compartment. Cardiovasc Res [Internet]. 2007 Apr 1 [cited 2022 Oct 10];74(1):114–23. Available from: https://pubmed.ncbi.nlm.nih.gov/17307155/

40. Gramolini AO, Kislinger T, Asahi M, Li W, Emili A, MacLennan DH. Sarcolipin retention in the endoplasmic reticulum depends on its C-terminal RSYQY sequence and its interaction with sarco(endo)plasmic Ca(2+)-ATPases. Proc Natl Acad Sci U S A [Internet]. 2004 Nov 30 [cited 2022 Oct 10];101(48):16807–12. Available from: https://pubmed.ncbi.nlm.nih.gov/15556994/

41. Gorski PA, Glaves JP, Vangheluwe P, Young HS. Sarco(endo)plasmic Reticulum Calcium ATPase (SERCA) Inhibition by Sarcolipin Is Encoded in Its Luminal Tail. Journal of Biological Chemistry [Internet]. 2013 Mar;288(12):8456–67. Available from: http://www.jbc.org/content/288/12/8456.abstract

42. Abrol N, Smolin N, Armanious G, Ceholski DK, Trieber CA, Young HS, et al. Phospholamban C-terminal Residues Are Critical Determinants of the Structure and Function of the Calcium ATPase Regulatory Complex. J Biol Chem [Internet]. 2014 Sep 9 [cited 2022 Oct 12];289(37):25855. Available from: /pmc/articles/PMC4162186/

43. Karim CB, Zhang Z, Howard EC, Torgersen KD, Thomas DD. Phosphorylation-dependent conformational switch in spin-labeled phospholamban bound to SERCA. J

Mol Biol [Internet]. 2006 May;358(4):1032–40. Available from: http://www.sciencedirect.com/science/article/pii/S0022283606002506

44. Traaseth NJ, Thomas DD, Veglia G. Effects of Ser16 phosphorylation on the allosteric transitions of phospholamban/Ca(2+)-ATPase complex. J Mol Biol [Internet]. 2006 May 12 [cited 2022 Oct 12];358(4):1041–50. Available from: https://pubmed.ncbi.nlm.nih.gov/16564056/

45. Stenoien DL, Knyushko T v., Londono MP, Opresko LK, Mayer MU, Brady ST, et al. Cellular trafficking of phospholamban and formation of functional sarcoplasmic reticulum during myocyte differentiation. Am J Physiol Cell Physiol [Internet]. 2007 Jun [cited 2022 Oct 12];292(6). Available from: https://pubmed.ncbi.nlm.nih.gov/17287364/

46. Pallikkuth S, Blackwell DJ, Hu Z, Hou Z, Zieman DT, Svensson B, et al. Phosphorylated phospholamban stabilizes a compact conformation of the cardiac calcium-ATPase. Biophys J [Internet]. 2013;105(8):1812–21. Available from: http://dx.doi.org/10.1016/j.bpj.2013.08.045

47. Bidwell P, Blackwell DJ, Hou Z, Zima A v, Robia SL. Phospholamban Binds with Differential Affinity to Calcium Pump Conformers. Journal of Biological Chemistry [Internet]. 2011 Oct;286(40):35044–50. Available from: http://www.jbc.org/content/286/40/35044.abstract

48. Mueller B, Karim CB, Negrashov I v, Kutchai H, Thomas DD. Direct Detection of Phospholamban and Sarcoplasmic Reticulum Ca-ATPase Interaction in Membranes Using Fluorescence Resonance Energy Transfer. Biochemistry [Internet]. 2004 Jul;43(27):8754–65. Available from: https://doi.org/10.1021/bi049732k

49. Li J, Bigelow DJ, Squier TC. Conformational Changes within the Cytosolic Portion of Phospholamban upon Release of Ca-ATPase Inhibition. Biochemistry [Internet]. 2004 Apr;43(13):3870–9. Available from: https://doi.org/10.1021/bi036183u

50. Li J, Bigelow DJ, Squier TC. Conformational Changes within the Cytosolic Portion of Phospholamban upon Release of Ca-ATPase Inhibition†. Biochemistry [Internet]. 2004 Apr 6 [cited 2022 Oct 12];43(13):3870–9. Available from: https://pubs.acs.org/doi/abs/10.1021/bi036183u

51. Akin BL, Hurley TD, Chen Z, Jones LR. The structural basis for phospholamban inhibition of the calcium pump in sarcoplasmic reticulum. Journal of Biological Chemistry. 2013;288(42):30181–91.

52. Chen Z, Akin BL, Stokes DL, Jones LR. Cross-linking of C-terminal residues of phospholamban to the Ca 2+ pump of cardiac sarcoplasmic reticulum to probe spatial and functional interactions within the transmembrane domain. Journal of Biological Chemistry. 2006;281(20):14163–72.

53. Trieber CA, Douglas JL, Afara M, Young HS. The Effects of Mutation on the Regulatory Properties of Phospholamban in Co-Reconstituted Membranes†. Biochemistry [Internet]. 2005 Mar;44(9):3289–97. Available from: http://dx.doi.org/10.1021/bi047878d

54. Eletr S, Inesi G. Phospholipid orientation in sarcoplasmic membranes: spin-label ESR and proton MNR studies. Biochim Biophys Acta. 1972 Sep;282(1):174–9.

55. Stokes DL, Green NM. Three-dimensional crystals of CaATPase from sarcoplasmic reticulum. Symmetry and molecular packing. Biophys J. 1990;57(January):1–14.

56. Young HS, Jones LR, Stokes DL. Locating phospholamban in co-crystals with Ca(2+)-ATPase by cryoelectron microscopy. Biophys J. 2001;81(May):884–94.

57. Young HS, Rigaud JL, Lacapère JJ, Reddy LG, Stokes DL. How to make tubular crystals by reconstitution of detergent-solubilized Ca2(+)-ATPase. Biophys J [Internet]. 1997;72(6):2545–58. Available from: http://www.sciencedirect.com/science/article/pii/S0006349597788982

58. Warren GB, Toon P a, Birdsall NJ, Lee a G, Metcalfe JC. Reconstitution of a calcium pump using defined membrane components. Proc Natl Acad Sci U S A. 1974;71(3):622–6.

Chapter 3

Conformational memory in the association of the transmembrane protein phospholamban with the sarcoplasmic reticulum calcium pump SERCA

This research was originally published in The Journal of Biological Chemistry and has been revised for incorporation in the present thesis.

Serena Smeazzetto, Gareth P Armanious, Maria Rosa Moncelli, Jessi J Bak, M Joanne Lemieux, Howard S Young, Francesco Tadini-Buoninsegni. Conformational memory in the association of the transmembrane protein phospholamban with the sarcoplasmic reticulum calcium pump SERCA. *Journal of Biological Chemistry. 2017*; 292(52):21330-21339.

© the American Society for Biochemistry and Molecular Biology.

Acknowledgements: Jessi J Bak purified SERCA, reconstituted & quantitated individual PLN reconstitutions and assisted in steady-state substrate-jump experiments and optimization of steady-state assay methodology. Serena Smeazzetto, Maria Rosa Moncelli, Francesco Tadini-Buoninsegni performed solid-supported membrane (SSM) pre-steady-state substrate jump experiments. Special thank you to Dr. Paul Lapointe, Rebecca Mercier, and Annemarie Wolmarans for technical assistance.

3.1 Abstract

By pumping calcium ions from the cytoplasm into the sarcoplasmic reticulum, the sarcoplasmic reticulum Ca2+-ATPase SERCA aids in muscle relaxation. SERCA activity is regulated by a variety of small transmembrane peptides, most notably by phospholamban in cardiac muscle. However, the exact mechanism of how phospholamban regulates SERCA is not fully understood. In this study, we evaluated the effects of phospholamban on calcium transport and ATP hydrolysis by SERCA under conditions that mimic sarcoplasmic reticulum membranes. A collaborating lab performed pre-steady-state current measurements with proteoliposomes containing SERCA and phospholamban or sarcolipin adsorbed to a solid-supported membrane and activated by substrate concentration jumps (1). These important pre-steady-state calcium current measurements supported and aligned with the steady-state SERCA ATPase activity presented herein. Our collaborators observed that phospholamban altered ATP-dependent calcium translocation by SERCA within the first transport cycle, using pre-steady-state charge (calcium) translocation measurements. Our steady-state ATPase activity assays under varying substrate conditions (various calcium and/or ATP concentrations) promoted particular conformational states of SERCA. We found that the effect of phospholamban on SERCA depends on substrate preincubation conditions. Our findings also showed that different conformations of SERCA can engage with phospholamban to produce inhibitory interactions, each of which has a unique impact on the kinetics of SERCA. We identified various ways that SERCA and phospholamban interact, and we saw that once a given mode of association was established, it persisted throughout the SERCA transport cycle and subsequent turnover events. These findings support conformational memory in the connection between SERCA and

phospholamban, shedding light on phospholamban's physiological function and its control over SERCA transport activity.

3.2 Introduction

The sarcoplasmic reticulum (SR) Ca^{2+}-ATPase (SERCA) plays a central role in muscle relaxation by a well-described transport of calcium from the cytosol into the lumen of the SR (2–5). The original E1-E2 scheme states that to activate SERCA (5), two calcium ions must first bind (E1-Ca2). Next, ATP must be used to generate a phosphoenzyme intermediate (E1P). The conformational transition (E1P to E2P) that favours the release of calcium into the SR in exchange for luminal protons is carried out using the free energy from ATP and the formation of high-energy (E1P) and low-energy (E2P) phosphoenzyme intermediates. The final reaction step—hydrolytic cleavage of the phosphoenzyme intermediate, or dephosphorylation—returns the enzyme to the ground state and permits the start of a new transport cycle (2,4).

Phospholamban (PLN; 52 amino acids) and sarcolipin (SLN; 31 amino acids), two homologous transmembrane peptides, control SERCA transport activity in muscle cells. While SLN expression predominates in skeletal muscle and controls SERCA1a, PLN is predominantly expressed in cardiac muscle and controls SERCA2a. According to cross-linking studies (6), molecular modelling (7), NMR (8,9), and X-ray crystallography (10–12), PLN and SLN interact with SERCA in a groove formed by transmembrane helices M2, M6, and M9. When PLN is phosphorylated by protein kinase A (13) or calcium-calmodulin-dependent protein kinase II, the inhibitory impact that PLN has on SERCA is reversed (14).

The oligomeric state of PLN in addition to the cytosolic calcium concentration and phosphorylation status of PLN, are crucial for SERCA regulation. An equilibrium of PLN monomers and pentamers is present in the membrane and both are necessary for healthy heart function (15). The primary inhibitor, the PLN monomer, interacts physically with SERCA and modifies its apparent affinity for calcium. Although the PLN pentamer has been labelled as an inactive storage form, experimental data indicates that it also interacts with SERCA (16). There is evidence that PLN remains associated with SERCA and can adopt multiple conformational states in the SERCA-PLN complex, despite the conventional model for PLN control of SERCA involving the reversible attachment of a monomer under calcium-free conditions (16–19).

Our collaborators performed pre-steady-state current measurements on a solid-supported membrane (SSM) to assess the effects of PLN and SLN on ATP-dependent calcium translocation by SERCA. The pre-steady-state charge transfer during the initial SERCA turnover events (1) were compared to our steady-state assessments (20,21) of the ATPase activity presented in this chapter. Different substrate conditions encouraged specific conformational states of SERCA from which catalytic turnover might be started. When we compared steady-state ATPase activity with our collaborator's pre-steady-state charge translocation, we discovered that the effect of PLN on SERCA activity depended on the initial conditions. Contrary to earlier assumptions, we conclude that PLN can interact with at least two conformations of SERCA, each of which has a unique impact on SERCA's maximum activity, apparent calcium affinity, and cooperative calcium binding. Furthermore, a specific SERCA-PLN inhibitory association persisted after it was created even when SERCA was continuously turning over. The SERCA-PLN regulatory complex's "conformational memory" (22) sheds light on the functional applicability of the published crystal structures of SERCA bound to PLN (12).

3.3 Results

3.3.1 Steady-state ATPase activity

An essential reference point for the pre-steady-state measurements was the determination of the SERCA proteoliposomes' rates of ATP hydrolysis in the presence and absence of PLN (20,21,23). The following conditions (Table 3.1) were applied to proteoliposomes containing SERCA alone or SERCA and PLN (Figure 3.1). Condition I, “simultaneous calcium–ATP jumps” reaction initiation by the simultaneous addition of calcium and ATP; Condition II, “ATP jumps” reaction initiation by the addition of ATP; and Condition III, “calcium jumps” reaction initiation by the addition of calcium (0.1-10 μM). Based on our observations, we decided to include Condition IV with reaction initiation using physiological, resting-state substrate concentrations (4mM ATP and 60 nM calcium).

Table 3.1. Kinetic parameters for SERCA and SERCA–PLN proteoliposomes derived from pre-steady-state charge movement and steady-state ATPase activity measurements. Statistical significance was evaluated based on a threshold p value ($p < 0.05$). Note: Pre-steady-state charge movement is our collaborator's work shown in yellow column. (a) Statistically significant compared with SERCA in the absence of PLN under the same conditions, (b) Statistically significant compared with SERCA in the presence of PLN for condition I, minimum 4 independent measurements.

Starting conditions	Kinetic parameters	Steady-state ATPase activity	Pre-steady state charge movement
(i) Calcium & ATP jump		pre-incubate in the absence of substrates; start reaction with 4 mM ATP and 0.1-10 μM free Ca^{2+}	simultaneous addition of 100 μM ATP 0.1-10 μM free Ca^{2+}
SERCA	K_{Ca}	0.39 ± 0.03	0.49 ± 0.03
	V_{max}	4.3 ± 0.1	
	n_H	1.5 ± 0.2	1.6 ± 0.1
SERCA+PLN	K_{Ca}	0.89 ± 0.04[a]	0.79 ± 0.09[a]
	V_{max}	5.9 ± 0.2[a]	
	n_H	2.0 ± 0.1[a]	1.8 ± 0.3
(ii) ATP jump		pre-incubate with 0.1-10 μM free Ca^{2+}; start reaction with 4 mM ATP	pre-incubate with 0.1-10 μM free Ca^{2+} start reaction with 100 μM ATP
SERCA	K_{Ca}	0.26 ± 0.01	0.38 ± 0.04
	V_{max}	2.9 ± 0.1	
	n_H	1.2 ± 0.2	1.7 ± 0.2
SERCA+PLN	K_{Ca}	0.82 ± 0.01[a]	0.70 ± 0.06[a]
	V_{max}	3.9 ± 0.1[a,b]	
	n_H	1.4 ± 0.2[b]	1.4 ± 0.1
(iii) Calcium jump		pre-incubate with 4 mM ATP; start reaction with 0.1-10 μM free Ca^{2+}	pre-incubate with 100 μM ATP start reaction with 0.1-10 μM free Ca^{2+}
SERCA	K_{Ca}	0.35 ± 0.03	0.40 ± 0.01
	V_{max}	3.9 ± 0.1	
	n_H	1.9 ± 0.3	1.4 ± 0.1
SERCA+PLN	K_{Ca}	0.84 ± 0.01[a]	1.15 ± 0.21[a,b]
	V_{max}	5.1 ± 0.2[a]	
	n_H	1.3 ± 0.2[a,b]	1.1 ± 0.1[a,b]
(iv) Physiological conditions		pre-incubate with 0.06 μM free Ca^{2+} and 4 mM ATP; start reaction with 0.1-10 μM free Ca^{2+}	These experiments could not be performed because of low signal-to-noise ratios at low calcium concentrations.
SERCA	K_{Ca}	0.36 ± 0.01	
	V_{max}	3.5 ± 0.3	
	n_H	1.6 ± 0.2	
SERCA+PLN	K_{Ca}	0.65 ± 0.03[a,b]	
	V_{max}	2.8 ± 0.1[a,b]	
	n_H	3.0 ± 0.4[a,b]	

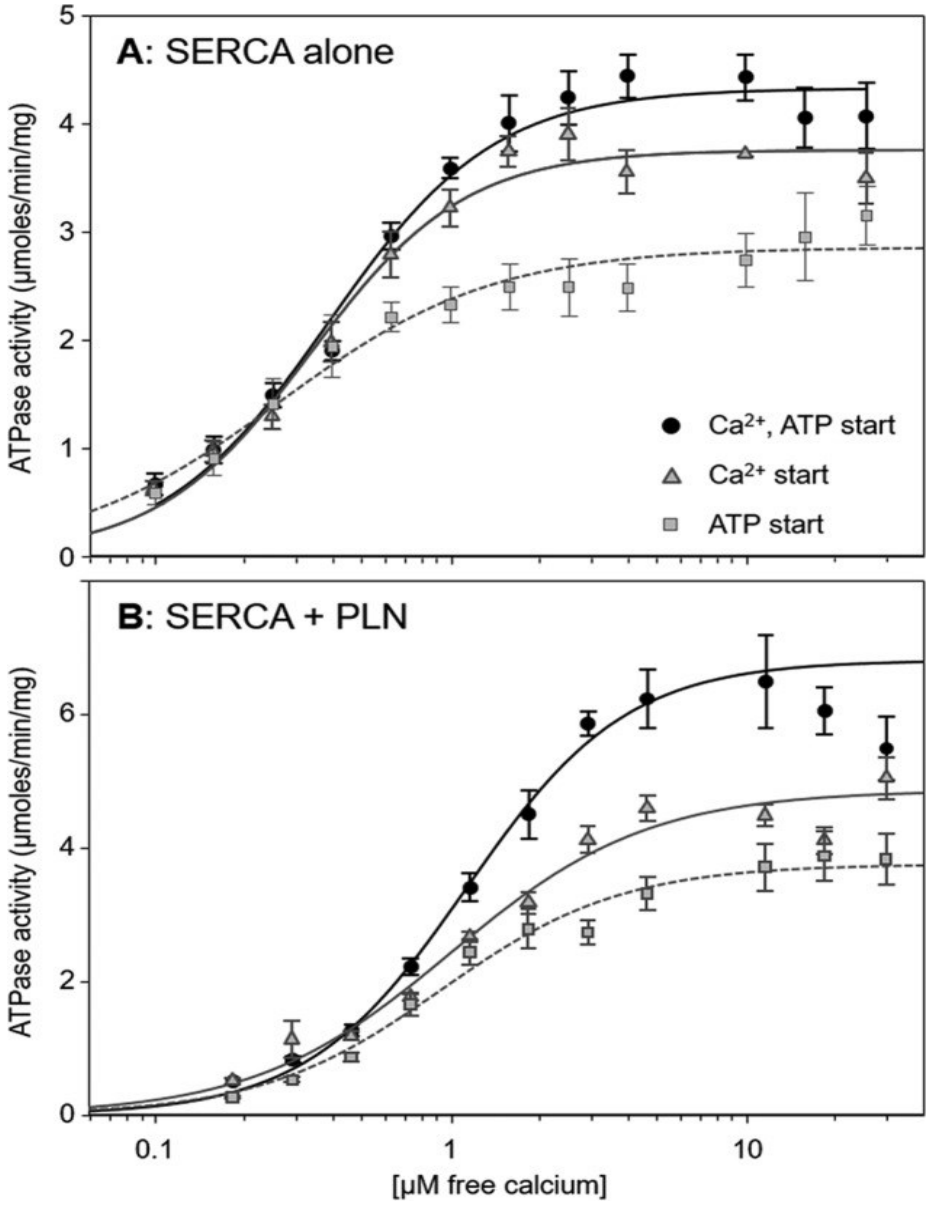

Figure 3.1. ATPase activity as a function of Ca2+ concentration for proteoliposomes under different starting conditions. A, proteoliposomes containing SERCA alone. B, proteoliposomes containing SERCA and PLN. SERCA ATPase activity was initiated by the simultaneous addition of calcium and ATP (circles; black line), addition of calcium (preincubation with ATP; triangles; gray line), or addition of ATP (preincubation with calcium; squares; gray dashed line). The lines represent curve fitting of the experimental data using the Hill equation (kinetic parameters can be found in Table 1. Each data point is the mean ± S.E. ($n \geq 4$). Error bars represent S.E. of at least four independent measurements.

The conventional way of starting the steady-state reaction, simultaneous addition of calcium and ATP, gave baseline values for the apparent calcium affinity, peak activity, and cooperativity of SERCA in SERCA proteoliposomes. This condition can also be considered as the pre-incubation of SERCA in the absence of substrates. The findings obtained (Table 3.1) were in close alignment with the previously published values (20,21,23). The ATPase activity (Figure 3.1) and the kinetic parameters calculated by fitting to the Hill equation were affected by changing the starting conditions. The highest apparent calcium affinity was observed when SERCA was preincubated with calcium (ATP jump), and calcium affinity varied slightly as a function of starting conditions (KCa ranged from 0.26 to 0.39 μM; $p < 0.01$). The cooperativity for calcium binding also varied (average Hill coefficient nH of 1.6), such that when SERCA was preincubated with calcium, the cooperativity was lower (ATP jump; nH of 1.2). The maximal activity of SERCA also changed depending on the initial conditions, and this had an indirect relationship with the impact on SERCA's apparent calcium affinity (highest Vmax was observed with the lowest calcium affinity). ATP jump produced the highest affinity and lowest maximal activity, whereas simultaneous calcium–ATP jump had the lowest affinity and highest maximal activity.

We typically observe effects of PLN on the apparent calcium affinity (2-fold decrease), maximal activity (1.4-fold increase), and cooperativity (1.3-fold increase) of SERCA by initiating ATPase activity by SERCA-PLN proteoliposomes with the simultaneous addition of calcium and ATP (condition I in Table 3.1) (20,21,23). The capacity of PLN to change the apparent calcium affinity of SERCA was only marginally affected by changing these initial circumstances (K_{Ca} varied from 0.82 to 0.89 μM calcium; $p < 0.01$). When SERCA was preincubated with calcium (ATP jump; K_{Ca} of 0.82 μM), there

was a similar trend toward increased affinity even though the alterations were small. Similar to what was seen with SERCA proteoliposomes, starting conditions had a substantial impact on the maximal activity. Simultaneous calcium–ATP starting condition had the lowest affinity and highest maximal activity, while the ATP starting condition resulted in the highest affinity and lowest maximal activity. The cooperativity for calcium binding had the largest change (nH ranged from 1.3 to 2.0; $p < 0.04$). When SERCA was preincubated with either calcium or ATP, cooperativity was lost. A similar pattern was seen for steady-state ATPase activity (continuous SERCA turnover) and in our collaborator's pre-steady-state charge displacement (single SERCA turnover) (1). In conclusion, PLN inhibition only increased the cooperativity for calcium binding when SERCA was preincubated without both substrates.

3.3.2 Mimicking physiological conditions

We investigated additional physiological substrate concentrations (starting Condition IV in Table 3.1) since SERCA inhibition by PLN was starting condition-dependent. At rest, SERCA experiences low cytosolic calcium (<0.1 μM) and high ATP (1–10 mM) substrate concentrations. In these experiments, we preincubated SERCA and SERCA–PLN proteoliposomes with 60 nM calcium and 4 mM ATP and followed this by a calcium jump in which the addition of calcium was used to achieve various concentrations (0.1–10 μM; Figure 3.2). In sum, the SERCA proteoliposomes reacted similarly to other beginning conditions with comparable kinetic characteristics (Table 3.1). A marked increase in cooperativity for calcium binding to SERCA was seen in the SERCA-PLN proteoliposomes. In fact, the nH value of 3.0 marks the biggest change in cooperativity observed with our SERCA-PLN proteoliposome preparation (20,21,23). In

conclusion, PLN inhibition increased the cooperativity for calcium binding when SERCA was preincubated in the presence or absence of both substrates, but not in the presence of either individual substrate (calcium or ATP).

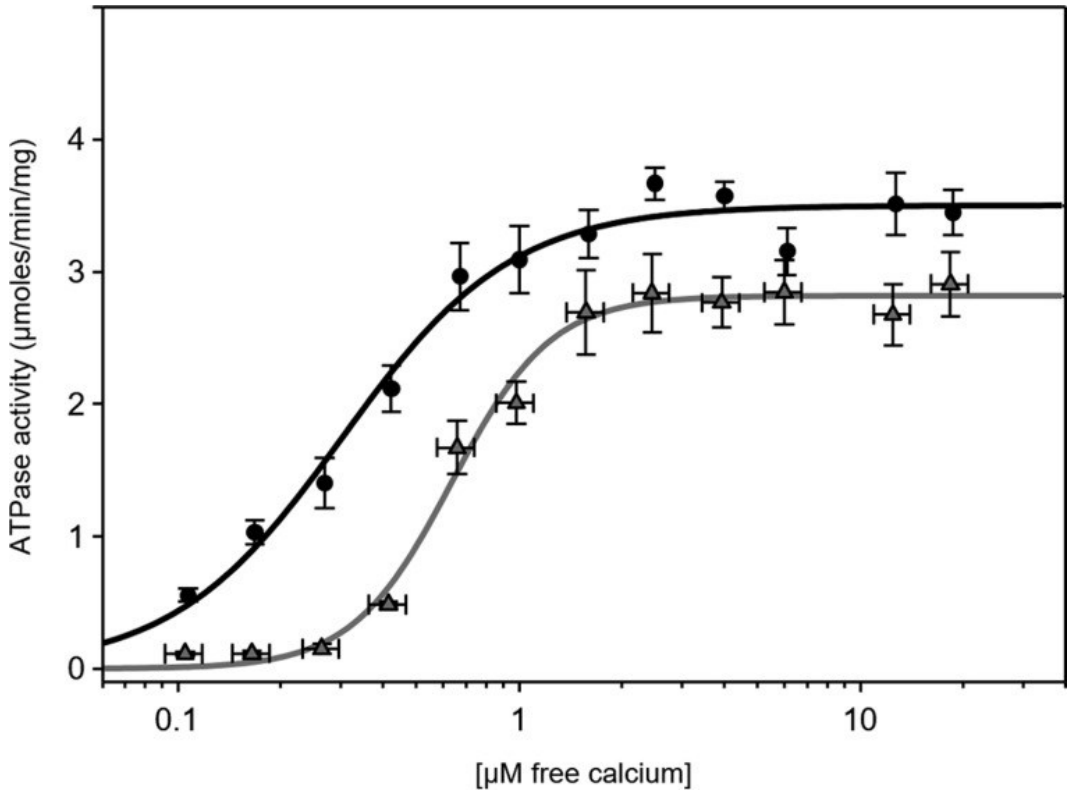

Figure 3.2. ATPase activity as a function of Ca2+ concentration for SERCA (circles) and SERCA + PLN (triangles) proteoliposomes. To mimic physiological resting-state conditions, the proteoliposomes were preincubated with 0.06 μM calcium and 4 mM ATP. SERCA ATPase activity was initiated by the addition of the remaining calcium required to achieve 0.1–10 μM free calcium. The lines represent curve fitting of the experimental data using the Hill equation (kinetic parameters can be found in Table 1). Each data point is the mean ± S.E. ($n \geq 4$). *Error bars* represent S.E. of at least four independent measurements.

3.4 Discussion

The pre-steady-state calcium translocation across the proteoliposome membrane during the initial SERCA transport cycle is reflected in the SERCA-dependent current transients that were completed by our collaborators. The conditions tested place SERCA

in distinct conformational states prior to the start of the SERCA transport cycle. These same conditions were tested in steady-state measurements of SERCA ATPase activity where calcium-dependent ATP hydrolysis by SERCA remained constant over time. In general, there was good agreement between the kinetic parameters for our collaborator's pre-steady-state charge transport and our steady-state ATPase activity measurements (Table 3.1). However, the K_{Ca} values for SERCA in the presence of PLN under calcium jump conditions (Condition III, Table 3.1), were noticeably different between the two approaches. This discrepancy may be due to limitations of the experimental assays and potential incomplete coupling between calcium transport and ATP hydrolysis by SERCA (2 calcium:1 ATP expected stoichiometry) under single turnover and continuous turnover conditions.

Conformational memory in the SERCA–PLN regulatory complex

Specific conformational states of SERCA are promoted by the substrate conditions chosen, from which catalytic turnover and calcium transport can start (Figure 3.3). Preincubation of SERCA in the absence of substrates promotes the E2 state (24), preincubation of SERCA with calcium promotes the E1 calcium-bound state (25), and preincubation of SERCA with ATP promotes an E2 ATP-bound state (26). The calcium-free E2 SERCA conformational state is traditionally associated with PLN inhibition (7,8), however, SERCA-SLN complex crystal structures (10,11) have revealed a new calcium-free, magnesium-bound E1-like state. Although magnesium is lacking, the structure of the SERCA-PLN complex is very comparable to an E1-like state (12). To think about the mechanism of PLN inhibition, molecular models of the SERCA-PLN complex based on the calcium-free E2 state are helpful. Transmembrane helices M2, M6, and M9 of SERCA form a groove where PLN binds when calcium is absent. Since calcium binding causes this

groove formed by M2, M6, and M9 of SERCA to close, PLN changes the apparent calcium affinity of SERCA by preventing groove closure, calcium binding, and the E2-E1 transition. The kinetic arguments that PLN modifies the activation energy for a gradual conformational shift brought about by calcium binding to SERCA are supported by this model (Ref=PMID 8349590). This has an effect on both the cooperativity and apparent calcium affinity.

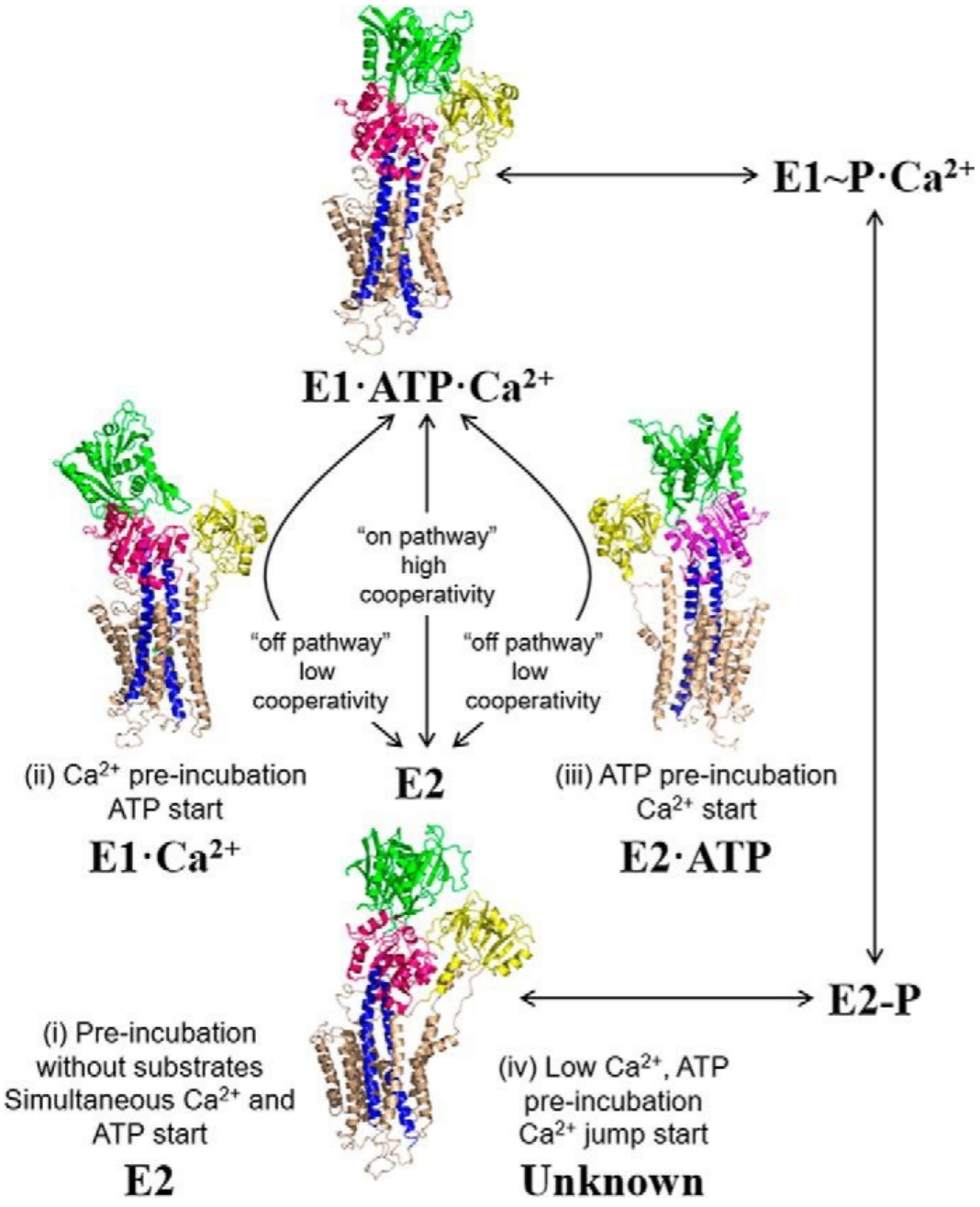

Figure 3.3. The SERCA transport cycle with structural states relevant to the present study. The preincubation and starting conditions used herein are indicated with corresponding structures of SERCA. Shown are the calcium-free E2 state (Protein Data Bank code 1IWO), an E1-like state promoted by calcium (Protein Data Bank code 1SU4), an E2-like state promoted by ATP (Protein Data Bank code 4H1W), and a catalytically active E1-ATP-Ca^{2+} state (Protein Data Bank code 1T5S). For condition iv with low calcium and high ATP concentrations, PLN inhibition appears to follow the on-pathway E2 to E1 transition; however, the structural state of SERCA under these conditions is unknown.

PLN did inhibit SERCA under the various starting conditions, but the kinetics of inhibition were dependent on how SERCA was poised prior to the start of transport (Table 3.1, Figures 1-3). The most significant change was observed in the cooperativity for calcium binding as indicated by the large change in Hill coefficients across the different preincubation conditions (Table 3.1). PLN strongly increased the cooperativity of calcium binding in the absence of substrates or under physiological substrate conditions (low calcium and high ATP). The theoretical limit for the Hill coefficient is 2 due to one SERCA molecule actively transporting 2 Ca^{2+} ions per cycle, however, we observed a value of 3 (nH of 3.0). One possible explanation for this nH of 3.0 is the interaction of multiple SERCA molecules, in a substrate- and PLN-dependent coupling (27). These conditions encourage an "on-pathway" reaction trajectory from the E2 calcium-free state to the E1-ATP-Ca2+ state of SERCA such that PLN produces a highly cooperative transition between the calcium-free and calcium-bound states (Figure 3.3). The absence of substrate favors SERCA's E2 state, which undergoes a significant multidomain conformational shift to transform into the catalytically active E1-ATP-Ca2+ state (24). A probable explanation for the rise in cooperativity is the stabilization of the SERCA E2 state by PLN: PLN reduces the likelihood of binding the first calcium ion but increases the likelihood of binding the second calcium ion once the first ion is bound. Additionally, at more physiological substrate conditions (low calcium and high ATP), the highest cooperativity was seen. However, it is unknown what conformational state SERCA might be in under these latter circumstances.

The opposite trend was observed when SERCA was preincubated with either calcium or ATP alone, there was decreased cooperativity for calcium binding. This observation persisted in our collaborator’s pre-steady-state charge displacement

(Condition I versus Condition III; nH decreased from 1.8 to 1.1; $p < 0.025$) and our steady-state ATPase activity (Condition I versus Condition III; nH decreased from 2.0 to 1.3; $p < 0.04$). This begs the question of why is there reduced cooperativity when SERCA is preincubated with either ATP or calcium in the presence of PLN? Because only a single substrate (ATP or Ca^{2+}) is present, these conditions are described as an "off-pathway" reaction trajectory from the E2 calcium-free state to the catalytically active E1-ATP-Ca2+ state of SERCA. Calcium promotes the E1 calcium-bound state in a concentration-dependent manner. Despite the fact that this provides a rationale for the decreased cooperativity, PLN can still change SERCA's apparent calcium affinity. On the other hand, ATP alone supports an E2 ATP-bound state, but the decreased cooperativity suggests that SERCA adopts a conformation more suited to calcium binding. The unique E1-like state that was discovered in the crystal structures of the SERCA-SLN (10,11) and SERCA-PLN (12) complexes is suggestive of these traits. The calcium-binding sites have formed and are accessible to the cytoplasm in this state. Since the conformational change that promotes cooperativity and creates the calcium-binding sites has already taken place, PLN stabilisation of this E1-like state provides a plausible explanation for the lowered cooperativity for calcium binding to SERCA. The calcium sites are kept in an E1-like condition by magnesium ions in the crystal structures of the SERCA-SLN complex (10,11). This potentially explains the decrease in the apparent calcium affinity of SERCA and the inhibition of PLN because magnesium ions must be displaced before calcium can bind. This is consistent with our collaborator's observation of the effects of the higher magnesium concentration (5 mM) on pre-steady-state charge displacement by SERCA–PLN proteoliposomes (1).

Overall, our findings are consistent with the idea that PLN can create an inhibitory interaction with a variety of SERCA conformational states, at the very least an E2 state

that is calcium-free and one that is closer to an E1 state. We postulate that the classic complex represented by molecular modelling (7,8) represents the calcium-free inhibitory state, while the more recent crystal structures reflect the E1-like inhibitory state (10–12). These PLN interaction modes last during numerous SERCA transport cycles after they have been established. When SERCA activity is initiated from the absence of substrates, PLN establishes and retains the ability to interact with the E2 state of SERCA through multiple turnover events with an effect on both K_{Ca} and nH. On the other hand, if SERCA is preincubated with either ATP or calcium, PLN establishes and retains the ability to interact with an E1-like state of SERCA through multiple turnover events exerting an effect only on K_{Ca}. More crucially, under these circumstances, PLN does not seem to access the E2 state of SERCA.

SERCA performs the intricate processes of ATP hydrolysis and active calcium transport, and this process involves flexibility and spontaneous conformational fluctuations throughout transitions from one conformational state to the next. Transition from one conformational state to the next is driven by the availability of substrates and the suppression of backward transitions. By changing the transition between the E2 and E1 conformational states, which results in a reduction in SERCA's calcium affinity, PLN controls SERCA. Our data are consistent with the concept of conformational memory (22) in the SERCA–PLN regulatory complex, where particular interactions persist throughout multiple turnover events. Depending on the substrate conditions, the SERCA-PLN complex can form several structural states that are maintained throughout SERCA's catalytic cycle and conformational cycling (Figure 3.3). Put simply, SERCA and PLN interact in a variety of ways, and once a given mode of interaction is established, it persists through several turnover events and the SERCA calcium transport cycle.

3.5 Future Directions

Performing co-reconstitutions with SERCA in the presence of wild-type SLN or wild-type PLN to perform steady-state ATPase activity assays would provide additional insights to the possibilities of off trajectory pathways. One curiosity is if SLN can facilitate similar functional intermolecular interaction between SERCA molecules, thus impacting cooperativity of calcium binding under similar starting conditions as observed with PLN. Additionally, co-reconstitutions of SERCA in the presence of phospho-PLN or phospho-SLN could be explored to assess the implications across the SERCA regulatory axis.

3.6 Materials and Methods

3.6.1 Co-reconstitution of SERCA and recombinant PLN or SLN

Human PLN and SLN were expressed and purified as described (28). Peptides were confirmed by DNA sequencing (TAGC Sequencing, University of Alberta) and MALDI-TOF mass spectrometry (Alberta Proteomics and Mass Spectrometry Facility, University of Alberta). SERCA1a was purified from rabbit skeletal muscle SR (29,30) and co-reconstituted with PLN and SLN as described (23,31). The purified proteoliposomes yielded a final molar ratio of 1 SERCA:4.5 PLN (or SLN):~120 lipids. For the calculation of specific activity, the SERCA, PLN, and SLN concentrations were determined by quantitative SDS-PAGE (32).

3.6.2 ATPase activity assays

Calcium-dependent ATPase activities of the co-reconstituted proteoliposomes were measured by a coupled enzyme assay (33). The coupled enzyme assay reagents

were of the highest purity available (Sigma-Aldrich). The proteoliposomes contained SERCA alone or SERCA in the presence of PLN. A minimum of three independent reconstitutions and activity assays were performed for each set of proteoliposomes, and the calcium-dependent ATPase activity was measured over a wide range of calcium concentrations (0.1–10 μm). The assay was adapted to a 96-well format utilizing a BioTek Synergy 4 hybrid microplate reader (340-nm wavelength; 150-μl volume; 10–20 nm SERCA/well; 30 ˚C; data points collected every 39 s for 1 h). The reactions were initiated by (i) the simultaneous addition of calcium and ATP (preincubation of the proteoliposomes without calcium or ATP), (ii) the addition of ATP (preincubation of the proteoliposomes with calcium), or (iii) the addition of calcium (preincubation of the proteoliposomes with ATP). The KCa, Vmax, and nH were calculated based on non-linear least-squares fitting of the activity data to the Hill equation using Sigma Plot software (SPSS Inc., Chicago, IL). Errors were calculated as the standard error of the mean for a minimum of three independent measurements. Comparison of KCa, Vmax, and nH parameters was carried out using analysis of variance (between-subjects, one-way) followed by the Holm-Sidak test for pairwise comparisons (Sigma Plot).

Chapter 3 References

1. Smeazzetto S, Armanious GP, Moncelli MR, Bak JJ, Lemieux MJ, Young HS, et al. Conformational memory in the association of the transmembrane protein phospholamban with the sarcoplasmic reticulum calcium pump SERCA. Journal of Biological Chemistry. 2017;292(52):21330–9.

2. Toyoshima C. How Ca2+-ATPase pumps ions across the sarcoplasmic reticulum membrane. Biochimica et Biophysica Acta (BBA) - Molecular Cell Research [Internet].

2009;1793(6):941–6. Available from: http://www.sciencedirect.com/science/article/pii/S0167488908003558

3. Toyoshima C, Cornelius F. New crystal structures of PII-type ATPases: excitement continues. Curr Opin Struct Biol [Internet]. 2013 Aug [cited 2022 Oct 17];23(4):507–14. Available from: https://pubmed.ncbi.nlm.nih.gov/23871101/

4. Møller J v, Olesen C, Winther AML, Nissen P. The sarcoplasmic Ca2+-ATPase: design of a perfect chemi-osmotic pump. Q Rev Biophys [Internet]. 2010;43(4):501–66. Available from: https://www.cambridge.org/core/product/712917B2C432A2C19D12749FF667D772

5. de Meis L, Vianna AL. Energy interconversion by the Ca2+-dependent ATPase of the sarcoplasmic reticulum. Annu Rev Biochem. 1979;48:275–92.

6. Jones LR, Cornea RL, Chen Z. Close proximity between residue 30 of phospholamban and cysteine 318 of the cardiac Ca2+ pump revealed by intermolecular thiol cross-linking. Journal of Biological Chemistry. 2002;277:28319–29.

7. Toyoshima C, Asahi M, Sugita Y, Khanna R, Tsuda T, MacLennan DH. Modeling of the inhibitory interaction of phospholamban with the Ca2+ ATPase. Proc Natl Acad Sci U S A. 2003;100:467–72.

8. Seidel K, Andronesi OC, Krebs J, Griesinger C, Young HS, Becker S, et al. Structural Characterization of Ca2+-ATPase-Bound Phospholamban in Lipid Bilayers by Solid-State Nuclear Magnetic Resonance (NMR) Spectroscopy,. Biochemistry [Internet]. 2008 Apr;47(15):4369–76. Available from: https://doi.org/10.1021/bi7024194

9. Gustavsson M, Traaseth NJ, Veglia G. ACTIVATING AND DEACTIVATING ROLES OF LIPID BILAYERS ON THE CA2+-ATPASE/PHOSPHOLAMBAN COMPLEX. Biochemistry [Internet]. 2011 Nov 11 [cited 2022 Oct 21];50(47):10367. Available from: /pmc/articles/PMC3487395/

10. Winther AML, Bublitz M, Karlsen JL, Møller J V, Hansen JB, Nissen P, et al. The sarcolipin-bound calcium pump stabilizes calcium sites exposed to the cytoplasm. Nature [Internet]. 2013;495(7440):265–9. Available from: http://www.ncbi.nlm.nih.gov/pubmed/23455424

11. Toyoshima C, Iwasawa S, Ogawa H, Hirata A, Tsueda J, Inesi G. Crystal structures of the calcium pump and sarcolipin in the Mg2+-bound E1 state. Nature [Internet]. 2013 Mar;495:260. Available from: https://doi.org/10.1038/nature11899

12. Akin BL, Hurley TD, Chen Z, Jones LR. The structural basis for phospholamban inhibition of the calcium pump in sarcoplasmic reticulum. Journal of Biological Chemistry. 2013;288(42):30181–91.

13. Tada M, Kirchberger MA, Katz AM. Regulation of calcium transport in cardiac sarcoplasmic reticulum by cyclic AMP-dependent protein kinase. Recent Adv Stud Cardiac Struct Metab. 1976;9:225–39.

14. Bilezikjian LM, Kranias EG, Potter JD, Schwartz A. Studies on phosphorylation of canine cardiac sarcoplasmic reticulum by calmodulin-dependent protein kinase. Circ Res [Internet]. 1981 [cited 2022 Oct 21];49(6):1356–62. Available from: https://pubmed.ncbi.nlm.nih.gov/6273007/

15. Chu G, Li L, Sato Y, Harrer JM, Kadambi VJ, Hoit BD, et al. Pentameric assembly of phospholamban facilitates inhibition of cardiac function in vivo. Journal of Biological Chemistry. 1998;273(50):33674–80.

16. Glaves JP, Trieber C a., Ceholski DK, Stokes DL, Young HS. Phosphorylation and mutation of phospholamban alter physical interactions with the sarcoplasmic reticulum calcium pump. J Mol Biol [Internet]. 2011;405(3):707–23. Available from: http://dx.doi.org/10.1016/j.jmb.2010.11.014

17. Bidwell P, Blackwell DJ, Hou Z, Zima A v, Robia SL. Phospholamban Binds with Differential Affinity to Calcium Pump Conformers. Journal of Biological Chemistry [Internet]. 2011 Oct;286(40):35044–50. Available from: http://www.jbc.org/content/286/40/35044.abstract

18. Li J, James ZM, Dong X, Karim CB, Thomas DD. Structural and Functional Dynamics of an Integral Membrane Protein Complex Modulated by Lipid Headgroup Charge. J Mol Biol [Internet]. 2012 May 5 [cited 2022 Oct 21];418(5):379. Available from: /pmc/articles/PMC3327772/

19. Gustavsson M, Verardi R, Mullen DG, Mote KR, Traaseth NJ, Gopinath T, et al. Allosteric regulation of SERCA by phosphorylation-mediated conformational shift of phospholamban. Proc Natl Acad Sci U S A [Internet]. 2013;110(43):17338–43. Available from: http://www.pubmedcentral.nih.gov/articlerender.fcgi?artid=3808617&tool=pmcentrez&rendertype=abstract

20. Trieber CA, Afara M, Young HS. Effects of Phospholamban Transmembrane Mutants on the Calcium Affinity, Maximal Activity, and Cooperativity of the Sarcoplasmic Reticulum Calcium Pump. Biochemistry [Internet]. 2009 Oct;48(39):9287–96. Available from: https://doi.org/10.1021/bi900852m

21. Ceholski DK, Trieber C a., Young HS. Hydrophobic imbalance in the cytoplasmic domain of phospholamban is a determinant for lethal dilated cardiomyopathy. Journal of Biological Chemistry. 2012;287(20):16521–9.

22. Schörner M, Beyer SR, Southall J, Cogdell RJ, Köhler J. Conformational Memory of a Protein Revealed by Single-Molecule Spectroscopy. Journal of Physical Chemistry B. 2015;119(44):13964–70.

23. Trieber CA, Douglas JL, Afara M, Young HS. The Effects of Mutation on the Regulatory Properties of Phospholamban in Co-Reconstituted Membranes†. Biochemistry [Internet]. 2005 Mar;44(9):3289–97. Available from: http://dx.doi.org/10.1021/bi047878d

24. Toyoshima C, Nomura H. Structural changes in the calcium pump accompanying the dissociation of calcium. Nature. 2002 Aug;418(6898):605–11.

25. Toyoshima C, Nakasako M, Nomura H, Ogawa H. Crystal structure of the calcium pump of sarcoplasmic reticulum at 2.6 A resolution. Nature. 2000;405(M):647–55.

26. Toyoshima C, Yonekura SI, Tsueda J, Iwasawa S. Trinitrophenyl derivatives bind differently from parent adenine nucleotides to Ca2+-ATPase in the absence of Ca2+. Proc Natl Acad Sci U S A [Internet]. 2011/01/14. 2011 Feb;108(5):1833–8. Available from: https://www.ncbi.nlm.nih.gov/pubmed/21239683

27. Blackwell DJ, Zak TJ, Robia SL. Cardiac Calcium ATPase Dimerization Measured by Cross-Linking and Fluorescence Energy Transfer. Biophys J [Internet]. 2016;111(6):1192–202. Available from: http://www.sciencedirect.com/science/article/pii/S0006349516306622

28. Douglas JL, Trieber C a., Afara M, Young HS. Rapid, high-yield expression and purification of Ca2+-ATPase regulatory proteins for high-resolution structural studies. Protein Expr Purif [Internet]. 2005 Mar;40(1):118–25. Available from: http://www.sciencedirect.com/science/article/pii/S1046592804004036

29. Eletr S, Inesi G. Phospholipid orientation in sarcoplasmic membranes: spin-label ESR and proton MNR studies. Biochim Biophys Acta. 1972 Sep;282(1):174–9.

30. Stokes DL, Green NM. Three-dimensional crystals of CaATPase from sarcoplasmic reticulum. Symmetry and molecular packing. Biophys J. 1990;57(January):1–14.

31. Gorski PA, Glaves JP, Vangheluwe P, Young HS. Sarco(endo)plasmic Reticulum Calcium ATPase (SERCA) Inhibition by Sarcolipin Is Encoded in Its Luminal Tail. Journal of Biological Chemistry [Internet]. 2013 Mar;288(12):8456–67. Available from: http://www.jbc.org/content/288/12/8456.abstract

32. Young HS, Jones LR, Stokes DL. Locating phospholamban in co-crystals with Ca(2+)-ATPase by cryoelectron microscopy. Biophys J. 2001;81(May):884–94.

33. Warren GB, Toon P a, Birdsall NJ, Lee a G, Metcalfe JC. Reconstitution of a calcium pump using defined membrane components. Proc Natl Acad Sci U S A. 1974;71(3):622–6.

Chapter 4

Human Phospholamban Mutations – N-Terminus

This research has been prepared for publication in Biochimica et Biophysica Acta – Molecular Cell Research and has been revised for incorporation in the present thesis.

Acknowledgements: Authors on the submitted manuscript are as follows: Gareth P. Armanious, M. Joanne Lemieux, L. Michel Espinoza-Fonseca,
and Howard S. Young L. Michel Espinoza-Fonseca conducted molecular dynamics simulations of cMyBPC3, Sara Amidian piloted initial MD simulation feasibility studies (data not shown). Dr. Charles Holmes and Phuwadet (Ply) Pasarj consulted on phosphorylation and phosphatase assay design. Dr. Larry Fliegel & Dr. Charles Holmes provided Canadian Nuclear Safety Commission Certified lab space & materials for radioactive label incorporation assays.

4-1. Introduction

The ability of PLN to regulate SERCA activity in response to β-adrenergic signaling is essential for normal cardiac contractility. Altered calcium reuptake into the SR by SERCA and aberrant regulation by PLN is a known fundamental feature of human heart failure (1). The cytoplasmic domain of PLN is the regulatory region responsible for reversing SERCA inhibition depending on the phosphorylation state of PLN, while the transmembrane domain is considered to be the inhibitory region responsible for interacting with and altering SERCA's apparent calcium affinity. Residues in the cytoplasmic domain of PLN are essential for this functional regulation of SERCA, by the phosphorylation sites Ser16 and Thr17. Ser16 is the target of β-adrenergic signaling and protein kinase A (PKA), while Thr17 is the target of calcium/calmodulin-dependent protein kinase II (CaMKII). Impairments in the β-adrenergic signaling process and regulation of SERCA can lead to dilated cardiomyopathy (DCM), and in some cases hypertrophic cardiomyopathy (HCM) and arrhythmogenic right ventricular cardiomyopathy (AVRC) (2). Certain mutations in the cytosolic region of PLN are associated with DCM (3), such as both well studied Arg9-Cys missense mutation and an Arg14-deletion mutation associated with DCM and ARVC (2,4). These two known PLN mutations disrupt PLN regulation by phosphorylation, resulting in dysregulated cardiac calcium transients and heart failure.

Recent advances in genetic testing have revealed a large collection of rare genetic probable causes of idiopathic DCM, which is often found in families with a clinical history of the disease. Over 40 missense mutations have been identified to date in PLN and are recorded in databases such as ClinVar, COSMIC, & Ensembl. Most of these PLN mutations are categorized as variants of uncertain significance (VUS). PLN missense

variants have appeared recently due to efforts to identify the genetic basis for familial cardiomyopathies, such as the Ala15-Thr variant identified in a 4-year-old female with a family history and clinical diagnosis of DCM, and a Pro21-Thr variant identified in a 60-year-old female with a family history and clinical diagnosis of DCM (5). Interestingly, both patients also harbored a Val896-Met missense mutation in cardiac myosin binding protein C (MyBPC3). The mutation is in the C7 module of MyBPC3, a fibronectin-like domain involved in anchoring to the thick filament. This mutation has been identified previously in genetic screening of HCM patients, although it is currently classified as benign due to a lack of clear disease association (6).

This body of work investigates the disease potential of the Ala15-Thr and Pro21-Thr PLN mutants, and the potential role of the Val896-Met MyBPC3 mutant as a genetic modifier. A series of mutants in the cytosolic region of PLN (Figure 4.1), including Ala15-Thr and Pro21-Thr, were assessed for their ability to inhibit SERCA activity, their ability to be phosphorylated at Ser16 by PKA and dephosphorylated by protein phosphatase 1 (PP1), and their helical characteristics were compared to wild-type PLN. Our results reveal deficits in SERCA inhibition by PLN, as well as abnormalities in phosphorylation and dephosphorylation of PLN.

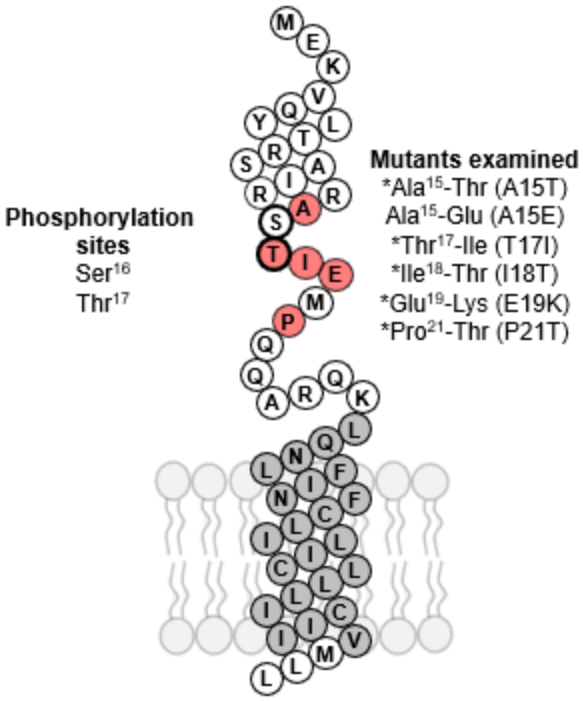

Figure 4.1: Topology diagram of phospholamban (PLN). The transmembrane domain is coloured grey. Phosphorylated residues Ser16 and Thr17 are outlined. The mutant forms of PLN in the present study are indicated with the asterisks denoting mutations found in heart failure patients.

To assess the association of the Val896-Met mutant of MyBPC3 as a potential modifier of these defects in PLN, molecular dynamics simulations were employed to evaluate the structural stability of the mutant compared to the wild-type C7 domain and C6-C7 tandem domains. We propose that the PLN variants cause dysregulation of cellular calcium homeostasis, while the altered structure and dynamics of the MyBPC3 variant worsens the disease outcome.

4.2 Results

The goal of the present study was to identify the relationship between PLN mutations in the region of residues Ala-15 to Pro-21 and the mechanistic regulation of

SERCA that may underlie the development of DCM. Despite complete alanine scanning mutagenesis of PLN being completed previously, the highly conserved nature of PLN provides opportunity for discovery of the key residue requirements for PLN function (7–9). Human mutations in PLN provide an alternative mutagenesis approach to determine the residue characteristics required to maintain PLN structure and function of the SERCA regulatory complex.

4.2.2 PLN Variant Effect on SERCA Inhibition

To assess the functional implication of human mutations in PLN on calcium transport, SERCA was reconstituted into membrane vesicles (proteoliposomes) in the presence and absence of human PLN variants under conditions that mimic native SR membrane (10–12). Functional characterization of the proteoliposomes was assessed by the measurement and comparison of calcium-dependent ATPase activity of SERCA in the presence of wild-type or mutant PLN, where SERCA in the absence of PLN served as a negative control and SERCA in the presence of wild-type PLN served as a positive control (**Figures 4.2** & **Table 4.1**).

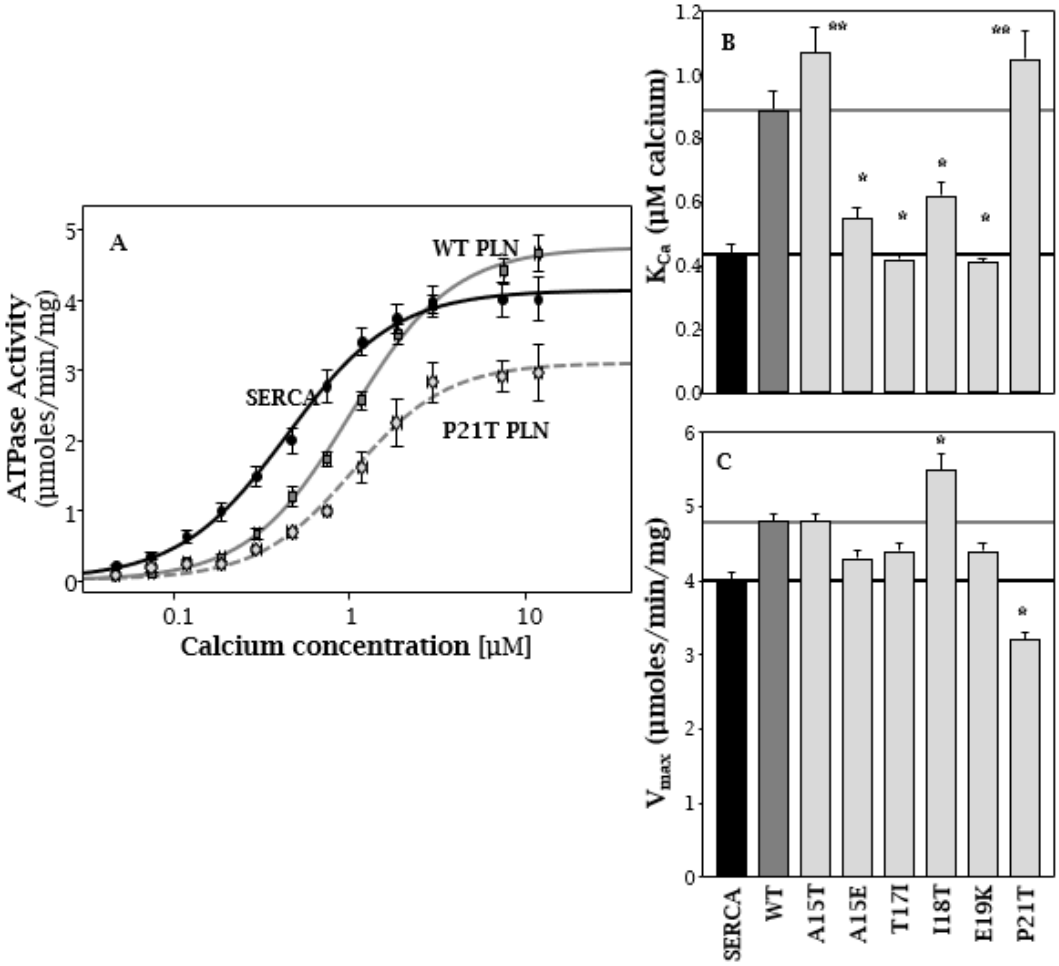

Figure 4.2 ATPase activity of co-reconstituted proteoliposomes. (A) ATPase activity of co-reconstituted proteoliposomes containing SERCA in the absence (black line) and presence of wild-type PLN (gray line) or Pro21-Thr (P21T) PLN (dashed gray line). Data points represent a minimum of three independent reconstitutions and a minimum of six ATPase activity assays (mean ± SEM). From these data, the calcium concentration at half-maximal activity (KCa) and the maximal activity (Vmax) were calculated based on non-linear least-squares fitting of the activity data to the Hill equation. **(B)** and **(C)** The effects of PLN mutants on the apparent calcium affinity (KCa) and maximal activity (Vmax) of SERCA. The blacks line indicates the KCa and Vmax values for SERCA alone. The dark grey line indicates the KCa and Vmax values for SERCA in the presence of wild-type PLN. Asterisks (*) indicate $p < 0.01$ and double asterisks (**) indicate $p < 0.05$ compared to SERCA in the presence of wild-type PLN.

Table 4.1: Kinetic parameters for SERCA ATPase activity in the absence and presence of wild-type and mutant forms of PLN. The calcium concentration to achieve half-maximal activity (K_{Ca}) and the maximal activity (V_{max}) of SERCA were calculated based on non-linear least-squares fitting of the ATPase activity data to the Hill equation. Asterisk (*) indicates $p < 0.01$ compared to SERCA in the presence of wild-type PLN.

PLN variant	K_{Ca} [μM calcium]	V_{max} (μmol/min/mg)
SERCA	0.44 ± 0.04	4.0 ± 0.1
Wild-type (WT)	0.88 ± 0.06	4.8 ± 0.1
Ala^{15}-Thr (A15T)	1.07 ± 0.08*	4.8 ± 0.1
Ala^{15}-Glu (A15E)	0.55 ± 0.03*	4.3 ± 0.1
Thr^{17}-Ile (T17I)	0.42 ± 0.02*	4.4 ± 0.1
Ile^{18}-Thr (I18T)	0.62 ± 0.04*	5.5 ± 0.2*
Glu^{19}-Lys (E19K)	0.40 ± 0.01*	4.4 ± 0.1
Pro^{21}-Thr (P21T)	1.05 ± 0.08*	3.2 ± 0.1*

The first variant examined was the Ala^{15}-Thr mutation found in a 4-year-old female with a family history and clinical diagnosis of DCM (5). Interestingly, Ala15 has been neglected in previous studies as a target for manipulation despite virtually every other residue in the peptide being probed for functional importance (10,13). This Ala15-Thr mutation exerts similar inhibition of SERCA calcium affinity to WT PLN (Figure 4.2 & Table 4.1) (K_{Ca} value of 1.07 ± 0.08 μM Ca^{2+}), compared to SERCA in the absence and presence of wild-type PLN (K_{Ca} values of 0.44 ± 0.04 and 0.88 ± 0.06 μM Ca^{2+}, respectively). As this Ala15-Thr mutation is located within the PKA recognition motif, we assessed the importance of this residue in tuning PLN functional properties. Introduction of a charged glutamate residue in place of Ala15 would be possible via SNP of the native human PLN

genetic sequence, and this more extreme substitution was assessed and found to lack inhibition of SERCA calcium affinity like phospho-PLN (K_{Ca} and V_{max} values for the A15E mutant were 0.55 ± 0.03 μM Ca^{2+} and 4.3 ± 0.1 μmole/min/mg, respectively) (Figure 4.2 & Table 4.1). These parameters are similar to what is observed upon PKA-mediated phosphorylation of PLN (10,14), suggesting that Ala^{15}-Glu may be a phosphomimetic mutant of PLN.

Three additional missense variants in this region of PLN, Thr^{17}-Ile, Ile^{18}-Thr, and Glu^{19}-Lys, appeared in the COSMIC database (15), with the Ile^{18}-Thr mutation also appearing in clinical databases Ensembl (16) and ClinVar (17) with reported inheritance conditions of DCM and HCM. These residues are of interest due to the importance Thr17 in PLN signaling and phosphorylation, as PLN is phosphorylated by both PKA at Ser16 and CaMKII at Thry17 to relieve the inhibitory effect of PLN on SERCA, while hydrophobic residues such as Ile^{18} can influence PLN function and phosphorylation by PKA. Thr17 phosphorylation by CaMKII has also been reported following exercise. Substitution of Thr17 for Ile is expected to have an effect on PLN phosphorylation and this is further investigated later in the chapter. With respect to its impact on maintaining regulation of SERCA, Thr17-Ile exhibits a loss-of-function phenotype (Figure 4.2 & Table 4.1) in contrast to past Thr17-Ala mutation having little effect on PLN inhibition of SERCA (10).

Previous mutagenesis studies of this Ile18 residue have indicated a loss of inhibitory activity of the peptide when replaced by a positively charged arginine (Ile18-Arg), but little effect with Ile18-Ala substitution (13). The present results are in alignment with prior literature finding that residues Glu2 to Ile18 are essential for the functional association with SERCA, we observed Ile18 mutation resulted in loss of the inhibitory effect of PLN on SERCA activity (Figure 4.2, Table 4.1). The K_{Ca} values for SERCA in the

presence of the variants were comparable to SERCA alone (0.42 ± 0.02 μM Ca^{2+} for Thr17-Ile, 0.62 ± 0.04 μM Ca^{2+} for Ile18-Thr, and 0.40 ± 0.01 μM Ca^{2+} for Glu19-Lys; compared to 0.44 ± 0.04 μM Ca^{2+} for SERCA alone). The Ile^{18}-Thr mutant also slightly increased the maximal activity of SERCA compared to SERCA in the presence of wild-type PLN (V_{max} values of 5.5 ± 0.1 versus 4.8 ± 0.1 μmole/min/mg, respectively). We have previously observed that alanine substitutions in this region further increase the maximal activity of SERCA compared to wild-type PLN (e.g. alanine substitution of Arg^{13}, Arg^{14} & Ser^{16} all exhibited further increases in V_{max} (10)). We can now add Ile^{18}-Thr, but not Thr^{17}-Ile PLN variants to this list of residues that can further activate SERCA.

A charge reversal mutation Glu19-Lys was reported in the COSMIC database (15). Our results indicate that charge reversal at this site by Glu19-Lys mutation results in a loss of inhibitory effect of PLN on SERCA activity (Figure 4.2), suggesting a significance for this residue modulating functional characteristics of PLN.

The same study identifying the Ala15-Thr PLN variant included a Pro21-Thr PLN mutation carrier who was a 60-year-old Caucasian female with a clinical diagnosis and family history of DCM (5). This variant was later identified in the analysis of high-quality exome sequence data of 60,706 individuals of diverse ethnicities and clinical genetic testing (gnomAD & ClinVar) and characterized as a VUS (18). The few Pro21 mutations that have been investigated cause partial loss of function, and Pro21 is a crucial residue in the structural dynamics of PLN (13,19,20). To the best of my knowledge, this PLN mutant identified in DCM patients has not been evaluated. Pro21-Thr resulted in a surprising gain-of-function in the form of WT-like suppression of calcium affinity (Figure 4.2 & Table 4.1). Surprisingly, the Pro21-Thr variant resulted in slight gain of function compared to wild-type PLN (K_{Ca} values of 1.05 ± 0.08 versus 0.88 ± 0.06 μM Ca^{2+}, respectively). Additionally, Pro^{21}-Thr decreased the maximal activity of SERCA, which is

opposite to the increase in the maximal activity of SERCA observed for wild-type PLN (V_{max} values of 3.2 ± 0.1 versus 4.8 ± 0.1 μmole/min/mg, respectively; 4.0 ± 0.1 μmole/min/mg for SERCA alone). This contrasts with the existing literature on other PLN Pro21 mutations (Pro21-Leu, Pro21-Ile, Pro21-Ala, Pro21-Gly)(13,20,21).

4.2.3 PLN Phosphorylation by PKA

The residues tested in the present study are near or part of the PKA recognition motif of PLN (Figure 4.1; Arg^{13}-Arg^{14}-Ala^{15}-Ser^{16}). PKA is known to prefer positively charged residues upstream (P-6, P-3, & P-2 positions) and hydrophobic residues downstream (P+1 position) of the recognition motif (22). Ile^{18} is a hydrophobic residue that may influence PKA-mediated Ser16 phosphorylation of PLN. Furthermore, it is also known that PLN structural dynamics contribute to PKA-mediated phosphorylation (23,24). For PLN structural dynamics and PKA-mediated phosphorylation, residues like Glu19 and Pro21 may be crucial. Due to these factors, we examined the full-length detergent-solubilized PLN variant's susceptibility to phosphorylation by the PKA catalytic subunit (Figure 4.3). While no known human mutations at the time of writing affect the Ser16 PKA phosphorylation site, Ala15, Thr17, Ile18, and Glu19 are included in the PKA consensus motif. We assessed each mutant's initial rate of phosphorylation in relation to wild-type PLN as well as its capacity for full phosphorylation in relation to wild-type PLN.

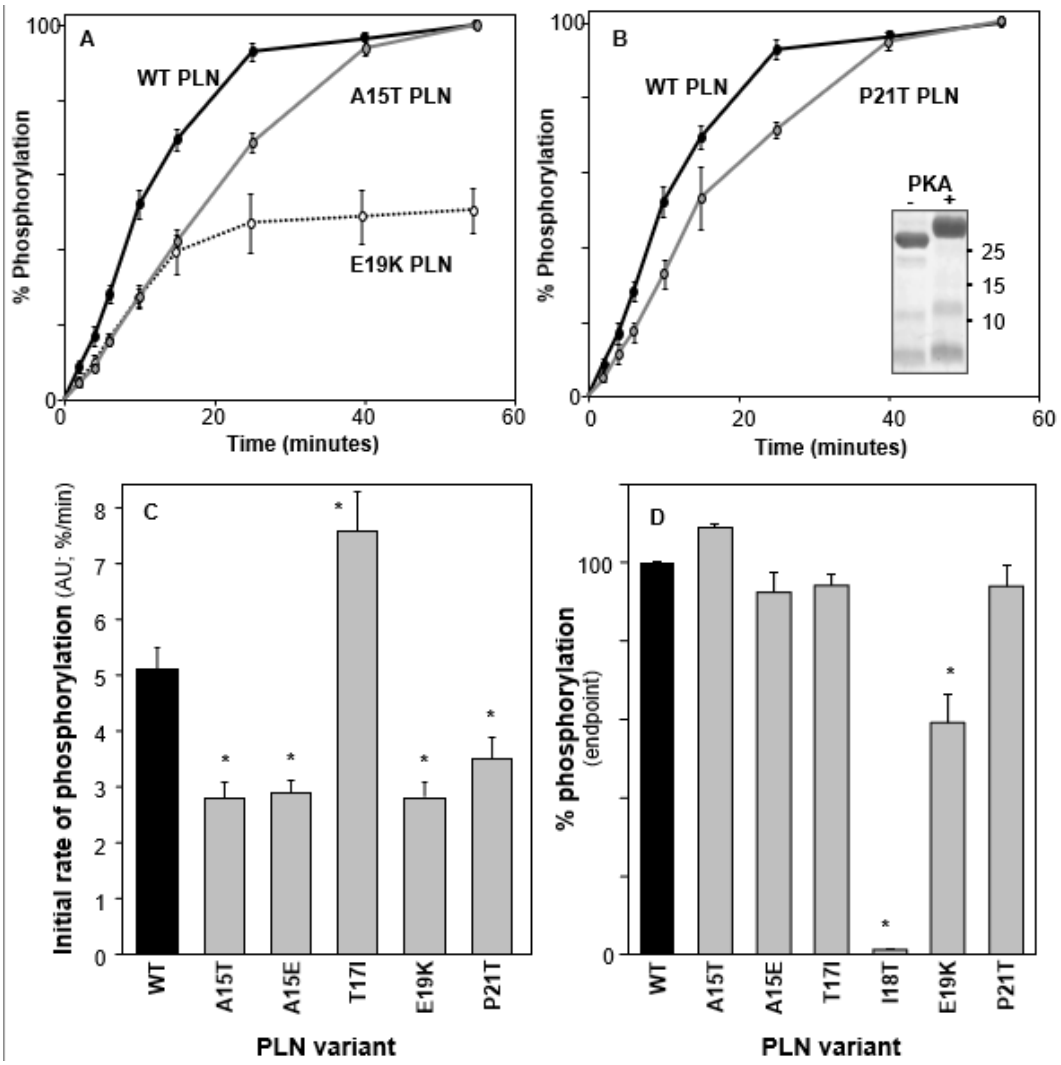

Figure 4.3: Phosphorylation of PLN by PKA. Time dependent phosphorylation of **(A)** wild-type PLN (black line), A15T PLN (top panel, grey line), E19K PLN (top panel, dashed line) **(B)** and P21T PLN (bottom panel, grey line). The PLN samples in detergent solution were phosphorylated by the catalytic subunit of PKA for 60 minutes. Each data point is the average of a minimum of three independent replicates. Inset – SDS PAGE showing increased molecular weight of phosphorylated PLN (C) The effects of PLN variants on the initial rate (within first ~10 minutes; AU) and (D) maximal phosphorylation by PKA compared to wild-type PLN (black bars). Asterisk (*) indicates $p < 0.01$ compared to wild-type PLN.

Under the experimental conditions, wild-type PKA efficiently phosphorylated wild-type full-length PLN with a half-time of approximately 10 minutes and complete phosphorylation was achieved within approximately 60 minutes (Figure 4.3, Table 4.2).

Four of the PLN variants showed slower initial rates of phosphorylation when compared to wild-type PLN which displayed an initial rate of 5.1 percent per minute (Figure 4.3 & Table 4.2). These included Ala15-Thr at 2.8% per min, Ala15-Glu at 2.9% per min, Glu19-Lys at 2.8% per min, and Pro21-Thr at 3.5% per min, indicating a defect in the rate of phosphorylation of these four mutants. The Ile18-Thr mutant did not show any phosphorylation under the experimental conditions, whereas the Thr17-Ile mutant showed a faster initial rate of phosphorylation at 7.6 % per min. The Thr^{17}-Ile and Ile^{18}-Thr variants provided an interesting opportunity in that they tested the sensitivity of PKA to hydrophobic residues downstream of the Ser^{16} phosphorylation site. The Thr^{17}-Ile variant added a hydrophobic residue and increased the initial rate of phosphorylation compared to wild-type PLN (7.6 versus 5.1% per min, respectively) while the Ile^{18}-Thr variant removed a hydrophobic residue and there was no detectable phosphorylation (Figure 4.3). These latter variants emphasize how PKA favours hydrophobic residues (at Thr17 or Ile18) that are downstream to the site of phosphorylation (Ser16). With the exception of the Glu19-Lys mutant, the PLN variations attained full phosphorylation in a manner comparable to that of wild-type PLN (Figure 4.3). The Glu19-Lys mutant also revealed another flaw in that it only reached peak phosphorylation at a saturation level of about 60%, which correlates with 3 out of 5 monomers in the context of the pentamer. The capacity of PKA to phosphorylate PLN monomers within the context of the pentamer has previously been used to explain this behaviour for some PLN variants (23).

Table 4.2: Kinetic parameters for the phosphorylation of wild-type and mutant forms of PLN by the catalytic subunit of PKA. The effects of PLN mutants on the initial rate of dephosphorylation (within first ~10 minutes; AU) and the maximum level of dephosphorylation (% of wild-type at 60 min) by PP1 compared to wild-type PLN. Asterisk (*) indicates $p < 0.01$ compared to wild-type PLN.

PLN variant	Initial rate (% per min)	Completion (% at 60 min)
Wild-type (WT)	5.1 ± 0.4	100 ± 1
Ala^{15}-Thr (A15T)	2.8 ± 0.3*	109 ± 1
Ala^{15}-Glu (A15E)	2.9 ± 0.3*	92 ± 5
Thr^{17}-Ile (T17I)	7.6 ± 0.7*	94 ± 3
Ile^{18}-Thr (I18T)	ND	1 ± 1*
Glu^{19}-Lys (E19K)	2.8 ± 0.3*	59 ± 7*
Pro^{21}-Thr (P21T)	3.5 ± 0.3*	93 ± 5

A key mechanism for reversing the SERCA inhibition caused by wild-type PLN is the phosphorylation of Ser16 by PKA. We also examined the phosphorylated PLN variants' capacity to inhibit SERCA. Ala15-Thr and Pro21-Thr PLN were the only variants that retained SERCA inhibitory activity, therefore we were only able to examine these for reversal of inhibition upon PLN phosphorylation (Figure 4.3). The calcium-dependent ATPase activities of wild-type, Ala15-Thr, and Pro21-Thr PLN were assessed after they had been phosphorylated for 60 minutes with the catalytic subunit of PKA and reconstituted into proteoliposomes with SERCA. As negative controls, phosphorylation processes were performed without ATP. The phosphorylation of all three peptides abrogated their inhibitory action. The apparent calcium affinities for SERCA in the presence of phosphorylated Ala^{15}-Thr (K_{Ca} of 0.69 ± 0.05 μM Ca^{2+}) and phosphorylated

Pro^{21}-Thr (K_{Ca} of 0.67 ± 0.03 µM Ca^{2+}) were similar to SERCA in the presence of phosphorylated wild-type PLN (K_{Ca} of 0.64 ± 0.03 µM Ca^{2+}). These results were also contrasted with those from a phosphorylation reaction followed in the absence of PLN by the reconstitution of SERCA alone into proteoliposomes (KCa of 0.54 ± 0.03 M Ca2+). These results are consistent with nearly complete reversal of SERCA inhibition by PKA-mediated phosphorylation for the PLN variants tested.

4.2.4 Effect on PP1 Activity

Full-length WT and mutant PLN were assessed in dephosphorylation studies to determine the effect of human PLN mutations on PP1 kinetics. To the best of my knowledge, the effect of PLN missense variants on dephosphorylation by PP1 has not been published. The catalytic subunit of PKA must first phosphorylate the PLN variants as a precondition. This eliminated some PLN mutants for the dephosphorylation assays (Ile^{18}-Thr & Glu^{19}-Lys; Figure 4.3). As a result, we focused on the human mutations Ala^{15}-Thr, Thr^{17}-Ile, and Pro^{21}-Thr compared to wild-type PLN. All PLN variants tested were dephosphorylated under the experimental conditions. The three human mutations Ala^{15}-Thr, Thr^{17}-Ile, and Pro^{21}-Thr exhibited slightly slower initial rates of dephosphorylation compared to WT PLN (Figure 4.4). Compared to the initial rate of dephosphorylation of wild-type PLN (10.1% per min), the PLN variants Ala^{15}-Thr (6.6% per min), Thr^{17}-Ile (4.8% per min), and Pro^{21}-Thr (5.8% per min) had slower rates of dephosphorylation (Figure 4.3). The degree of dephosphorylation was yet another intriguing characteristic (Figure 4.4) as wild-type, Ala15-Thr, and Thr17-Ile PLN were saturated at 80% dephosphorylation (20% phosphorylation was still present). This coincides with the dephosphorylation of four out of the five monomers in the context of the PLN pentamer, leaving the fifth

monomer unable to undergo dephosphorylation. The Pro21-Thr mutant plateaued at about 60% dephosphorylation (40% phosphorylation remained), which correlates with the dephosphorylation of three of the five monomers in the pentamer. These findings are consistent with the phosphorylation deficiency shown for some PLN variations (Glu19-Lys in Figure 4.3 & (18)), which saturate at about 60% phosphorylation, or three out of five PLN monomers in the pentamer.

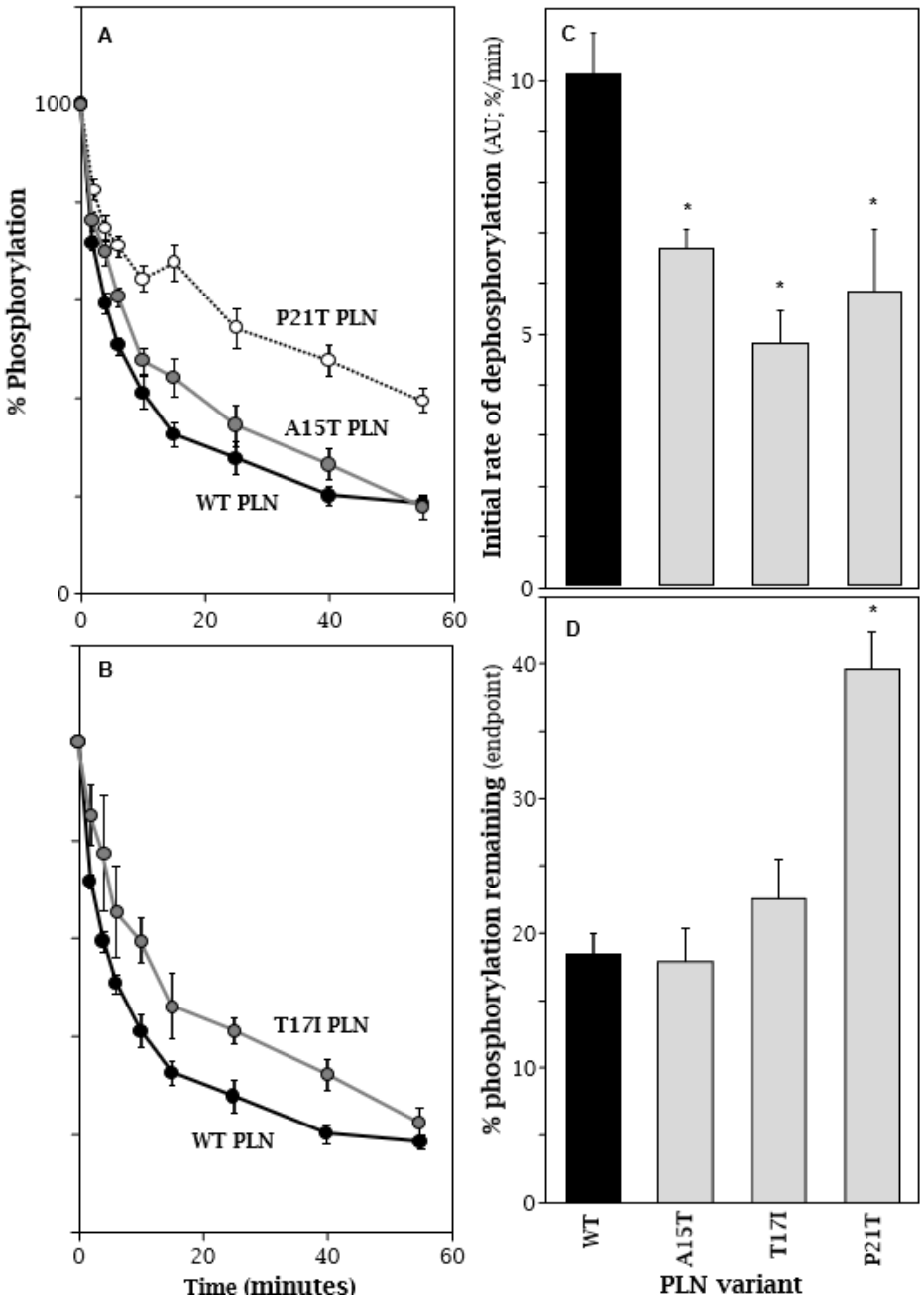

Figure 4.4: Time dependent dephosphorylation PLN. Dephosphorylation of WT PLN (black line), A15T PLN (left panel, grey line), P21T PLN (left panel, dashed line), and T17I PLN (right panel, grey line) by protein phosphatase 1 (PP1). The PLN samples in detergent solution were phosphorylated by the catalytic subunit of PKA for 60 minutes, PKA was heat inactivated, and the PLN samples were then dephosphorylated by PP1 for 60 minutes. Each data point is the average of a minimum of three independent replicates. **(C & D)** The effects of PLN mutants on the initial rate (within first ~10 minutes; AU) and maximal dephosphorylation by PP1 compared to wild-type PLN (black bars). Representative data used to calculate these parameters is shown.

4.2.5 Circular Dichroism Spectroscopy

The NMR structure of PLN consists of an N-terminal cytosolic helix (residues Glu2 to Ile18), a flexible linker region (residues Glu19 to Gln23), and a C-terminal transmembrane helix (Ala24 to Leu52) (Figure 4.5 & (25). The missense variants under investigation involve residues that lie within the N-terminal helix (Ala15, Thr17, Ile18) or within the flexible linker region of PLN (Glu19 & Pro21). These residues have the potential to change PLN's secondary structure and structural dynamics as they are located at the helix and linker region's boundary. This is especially true for Pro21, which is in the flexible linker of PLN and presumably contributes to the unwinding of this area (20). The Pro21-Thr mutant has the potential to disrupt the helical structure of PLN, contributing to defects in function, phosphorylation, and dephosphorylation. Prior work has highlighted the importance of Pro21 in the helical characteristics of PLN in the flexible hinge domain and its functional interaction with SERCA (20,21). To investigate the impact of human PLN mutations in these regions on the secondary structure of PLN, all human PLN variants were detergent solubilized and assessed by circular dichroism (CD) spectroscopy (Figures 4.5 & 4.6; Table 4.3). Two mutants – Ala15-Thr and Ile18-Thr – were similar to wild-type PLN in terms of their helical content (59%, 51%, & 57% helix respectively). Three mutants – Ala15-Glu, Thr17-Ile, & Glu19-Lys – displayed decreased helical content compared to wild-type PLN (16%, 37%, & 27% respectively; compared to 57% for wild-type PLN). Unsurprisingly, the Pro21-Thr mutant increased the helical content of PLN (83% compared to 57% for wild-type PLN). This ~26% increase in helical content correlates with a change in secondary structure of 13 residues of PLN, such that PLN adopts a largely helical structure composed of ~43 out of the 52 residues that

constitute PLN (Figure 4.6). The helical content of wild-type PLN was 57%, which correlates to ~30 residues out of the ~46 residues predicted to be helical in the NMR structure (PDB code 2KYV) and approximates previously published results (26). The structure of PLN is known to be dynamic and the data suggests the Pro21-Thr mutant promotes a change in dynamics that favors a more helical state of PLN, particularly in the linker region.

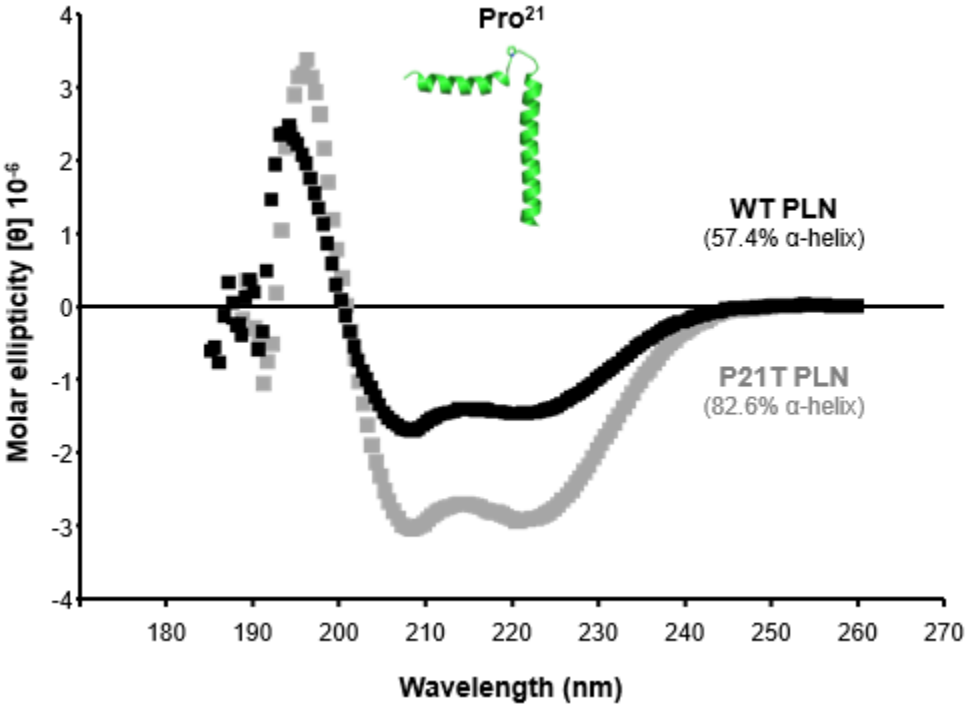

Figure 4.5: Circular dichroism spectra of wild-type PLN and PLN variants. WT PLN (black) and P21T PLN (grey). The peptides were dissolved in detergent solution and molar ellipticity was measured from 185 nm to 260 nm. The decrease in molar ellipticity at 208 nm and 222 nm is indicative of an increase in helical secondary structure content of the P21T mutant peptide. Inset – structure of the PLN monomer (PDB code 2KYV) with Pro^{21} in the linker region of PLN indicated.

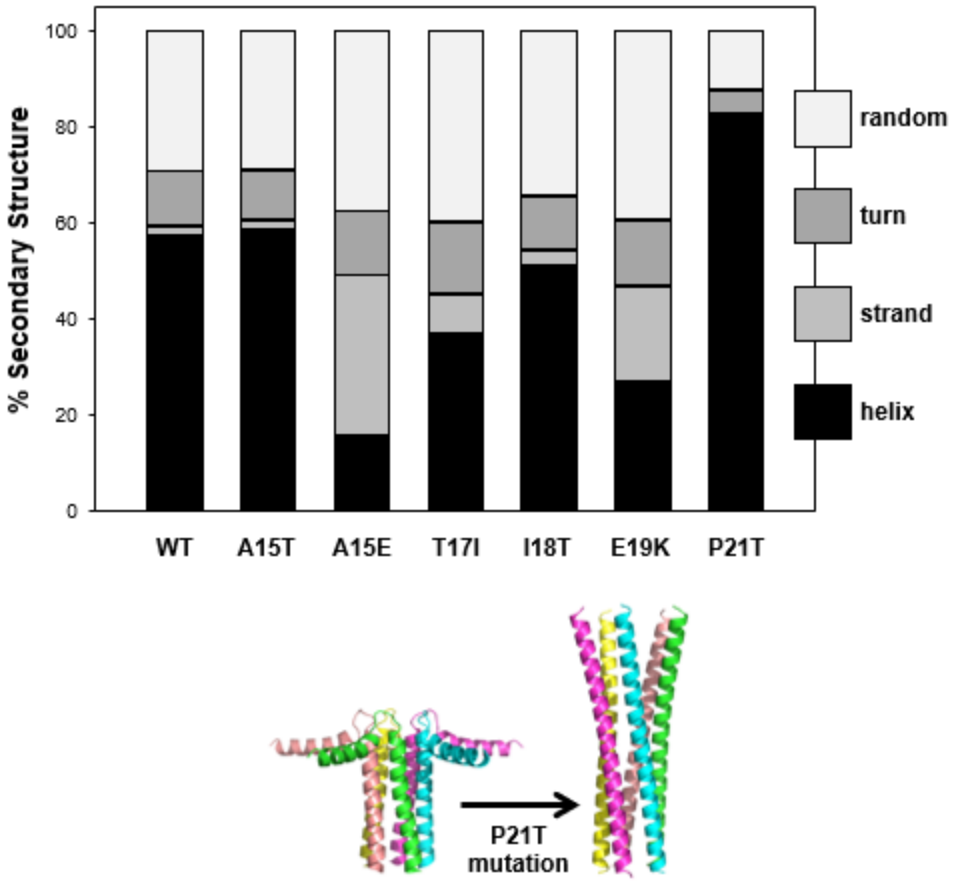

Figure 4.6: Estimation of secondary structure content for wild-type PLN and PLN variants. Representative CD spectra used to estimate secondary structure are shown in Figure 4.5. The A15T and I18T mutants were similar to wild-type PLN. A15E, T17I, and E19K had reduced helical structure compared to wild-type PLN. The P21T mutant had increased helical structure and this is shown schematically in the bottom panel.

Table 4.3. Estimation of secondary structure content from CD spectroscopy data. Representative CD spectra used to estimate secondary structure are shown in Figure 4.5. The secondary structure content (%) of the peptides was estimated from the CD spectra using DichroWeb, a website for calculating protein secondary structure from CD spectroscopic data (27,28).

PLN variant	% Helix	% Strand	% Turn	% Random
Wild-type (WT)	**57.4**	**2**	**11.4**	**29.2**
Ala^{15}-Thr (A15T)	**58.6**	**1.9**	**10.4**	**29.2**
Ala^{15}-Glu (A15E)	**15.6**	**33.5**	**13.4**	**37.5**
Thr^{17}-Ile (T17I)	**36.8**	**8.3**	**15**	**39.9**
Ile^{18}-Thr (I18T)	**51.2**	**3**	**11.3**	**34.6**
Glu^{19}-Lys (E19K)	**26.9**	**19.8**	**13.9**	**39.4**
Pro^{21}-Thr (P21T)	**82.6**	**0**	**5.1**	**12.3**

4.2.6 Correlation Between Phospholamban Structure and Function

A more helical (tense) inhibitory state and a more disordered (relaxed) non-inhibitory state are believed to be the physiologically relevant states of PLN, which relies on a dynamic helix-linker-helix structure (29). We plotted the apparent calcium affinity of SERCA (K_{Ca}) in the presence of PLN variants versus the estimated secondary structure content (α-helix) of the PLN variants to assess the relationship between PLN helical structure and its ability to inhibit SERCA. An overall trend was observed where loss of function correlated with decreased helical content (R = 0.83) (**Figure 4.7**). On the other hand, this observation might be affected by a competing influence. The K_{Ca} of SERCA may be impacted by residues that are crucial for PLN function, although the helical structure of PLN may not be significantly affected. Despite having equal amounts of helical content to wild-type PLN, the Ala15-Thr and Ile18-Thr mutations cause gain of function and partial loss of function, respectively. Despite having identical helical composition, these diverging functional results indicate that the individual residues are crucial for PLN function. The remaining PLN variations stress how important PLN helical structure is for SERCA control. The Ala15-Glu variant decreased the helical content of

PLN by ~41%, the Thr17-Ile variant decreased the helical content by ~20%, and the Glu19-Lys variant decreased the helical content by ~30%. Thus, the greatest loss-of-function mutants, Ala15-Glu, Thr17-Ile, & Glu19-Lys, were much less helical than wild-type PLN, while the gain-of-function mutant, Pro21-Thr, was much more helical than wild-type PLN.

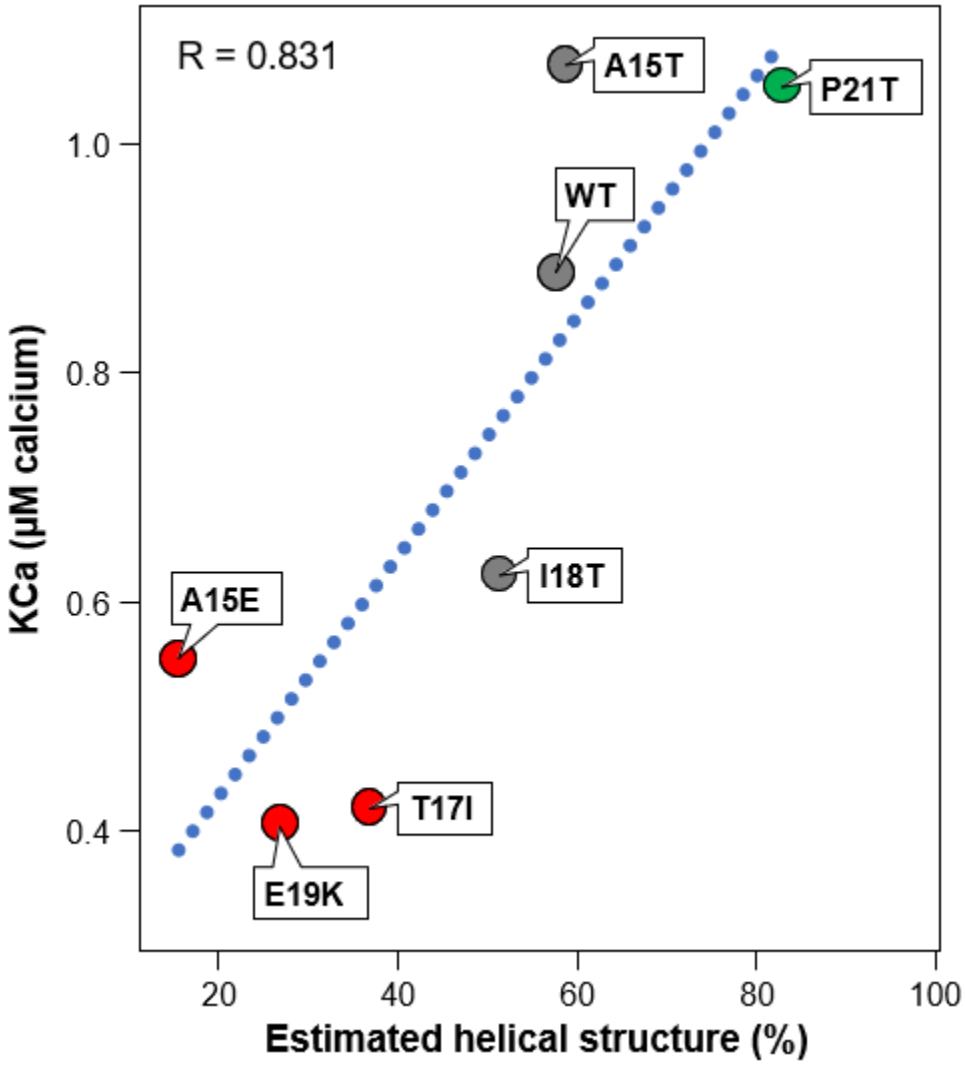

Figure 4.7: The helical structure of PLN is essential for SERCA inhibition. A plot of the apparent calcium affinity of SERCA (K_{Ca}) in the presence of wild-type and mutant forms of PLN versus the estimated helical secondary structure content of wild-type and mutant forms of PLN. Note the correlation between the helical structure of PLN and the ability to inhibit SERCA.

4.2.7 Human Mutations in Phospholamban and a Genetic Modifier in MyBPC3 (MD Simulations by L. Michel Espinoza-Fonseca)

Two important PLN missense variants characterized in this study include Ala15-Thr found in a 4-year-old female and Pro21-Thr found in a 60-year-old female, both with a family history and clinical diagnosis of DCM (5). Interestingly, both patients also harbor a Val896-Met missense mutation in MyBPC3. This Val896-Met mutation has routinely appeared in genetic screening of HCM patients, but it is categorized as a VUS and a potential genetic modifier of HCM or DCM (6,30). Due to the Ala15-Thr and Pro21-Thr mutants of PLN disrupting SERCA activity (Figure 4.2) and β-adrenergic signaling (PKA-mediated phosphorylation of PLN, Figure 4.3; PP1-mediated dephosphorylation of PLN, Figure 4.4), we speculate that calcium homeostasis and, as a result, contractility are altered in these patients. Under these conditions with PLN mutation, a normally benign mutation in MyBPC3 could exacerbate the DCM phenotype.

To evaluate this hypothesis, we performed molecular modeling and molecular dynamics (MD) simulations of the C7 domain of MyBPC3 that contains the Val896-Met mutation. MyBPC3 is a modular protein containing 8 immunoglobulin-like (Ig-like) domains and 3 fibronectin-like (FnIII-like) domains. The Val896-Met mutation is in the C7 FnIII-like domain (Figure 4.8), next to regions of MyBPC3 implicated in binding actin, myosin and titin. This mutation is near the linker region between the C6 and C7 domains. MD simulations of the wild-type and Val896-Met mutant were performed for 1 μs under solution conditions to examine the stability of the C7 domain and the changes induced by mutation. The Val896-Met mutation reduced the dynamics of the C7 domain, particularly for the N-terminal loops including residues 984-990 and 1038-1043 (Figure

4.8). This was shown from the analysis of root mean square fluctuation (RMSF) for each residue over the duration of the MD simulation. The loops consisting of residues 984-990 and residues 1038-1043 in the wild-type C7 domain are highly mobile in solution and mutation of Val896-Met reduces the mobility of these loops.

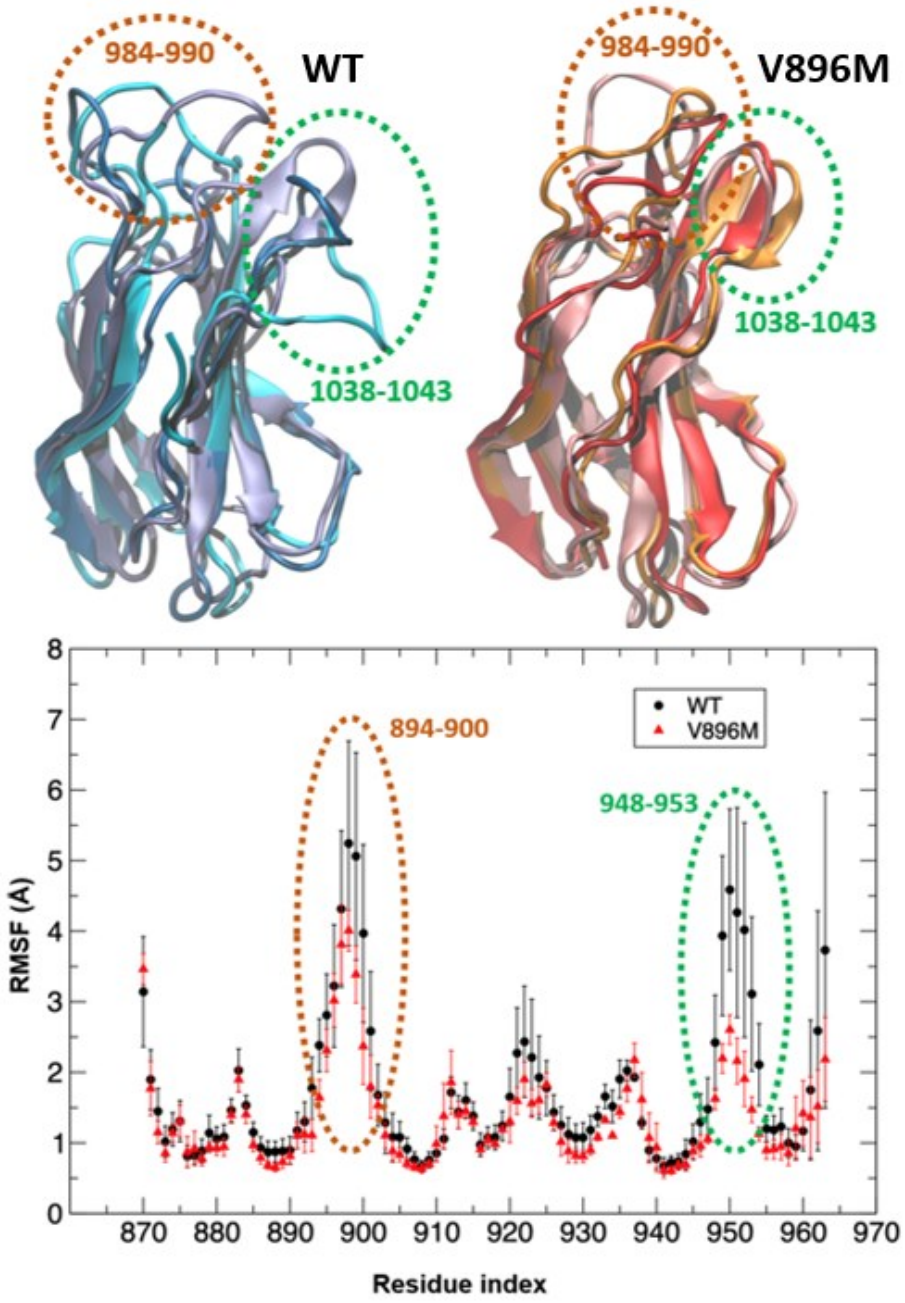

Figure 4.8: Molecular dynamics simulations of the C7 module of MyBPC3 for wild-type and the Val896-Met variant. (L. Michel Espinoza-Fonseca conducted molecular dynamics simulations of cMyBPC3). The representative structures shown are from three independent 1μs replicates for wild-type (upper left) and the variant (upper right). The Val896-Met variant impacts the dynamics of two loops encompassing residues 984-990 and 1038-1043. Lower panel - Root mean square fluctuation (RMSF) of individual residues during the time course of the simulation are plotted as RMSF versus residue number. Notice the reduced fluctuation of the two loops in the variant C7 module.

Since the two loops impacted by the Val896-Met mutation are oriented toward the C6 domain, we also performed MD simulation of the tandem C6-C7 domains (Figure 4.9). Molecular models of the C6 and C7 domains of human MyBPC3 were generated for wild-type and the Val896-Met variant using I-TASSER (31) and MD simulations of the wild-type and Val896-Met mutant were performed. The more rigid loops associated with the Val896-Met mutant translated to altered dynamics and inter-domain orientation of the tandem domains compared to wild-type. During the MD simulations, the wild-type C6-C7 tandem domains persisted in an extended conformation (inter-domain angle of ~165º), while the Val896-Met mutant persisted in a bent conformation (inter-domain angles of ~90º and ~120º).

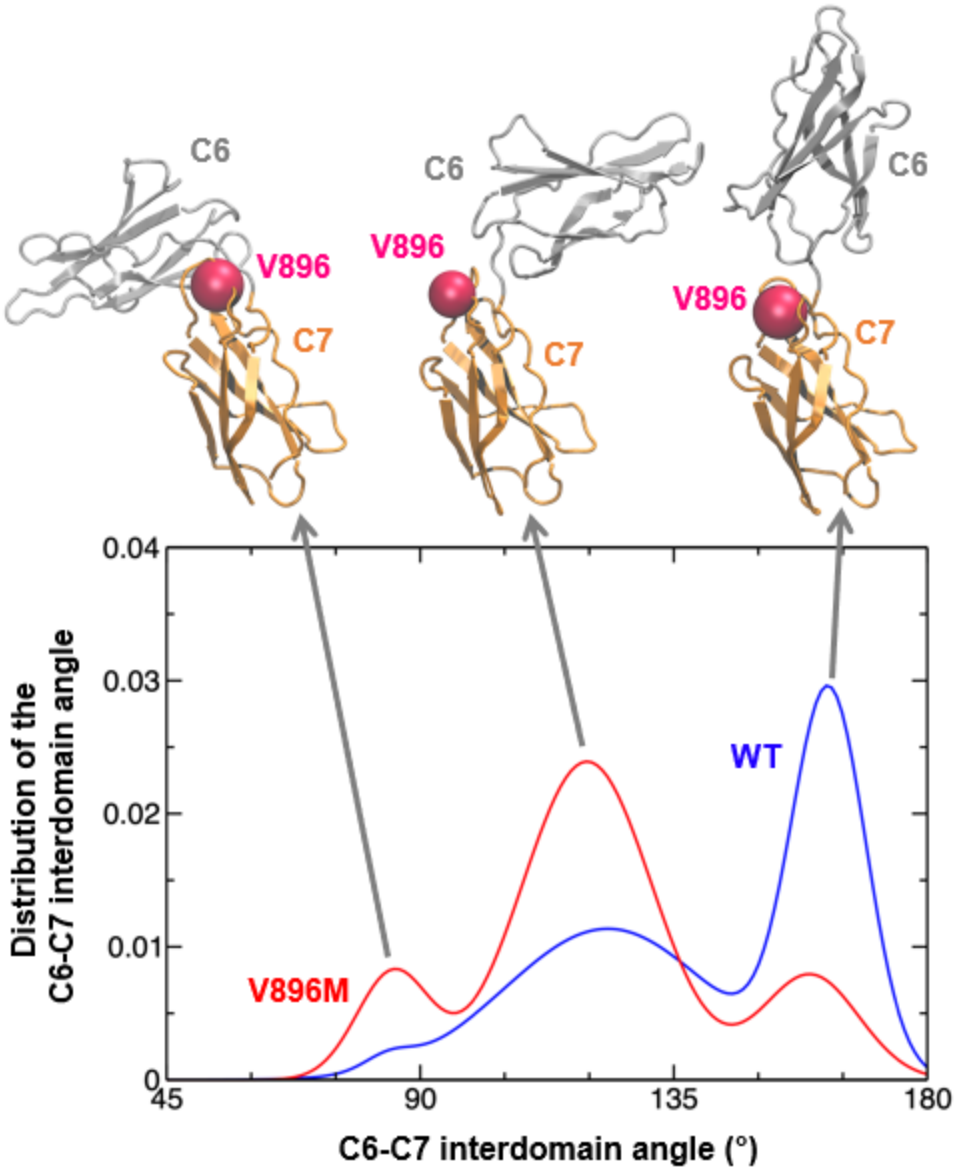

Figure 4.9: Molecular dynamics simulations of the C6-C7 tandem module of MyBPC3 for wild- type and the Val896-Met variant. (L. Michel Espinoza-Fonseca conducted molecular dynamics simulations of cMyBPC3) Representative structures of the three major conformations observed in the simulations are shown. **Lower panel** – The distribution of conformations observed during the time course of the simulations are plotted versus inter-domain angle. Notice the shift from an extended structure for the wild-type module (~165o) to bent conformations in the variant module (~90° and ~120°).

MyBPC3 is a modular, multi-domain protein that interacts with actin, myosin, and titin and acts as break on cardiac contractility. The altered inter-domain orientation of

the mutant likely impacts the function of the protein, although the available patient sequencing data suggests that it may not be directly causative in HCM or DCM.

4.3 DISCUSSION

The dysregulation of cellular calcium transport at the level of the SR, SERCA, and PLN is a common feature of heart failure despite the numerous origins of disease. In fact, single missense mutations in PLN are a recognized cause of DCM (3,32,33), and genome sequencing programs and patient genetic testing continue to uncover additional VUS. Understanding the functional characteristics of these variants is crucial since VUS are fast accumulating and could be the cause of the intricate pathological alterations that result in heart failure.

4.3.1 Missense Mutations in PLN Associated with Familial DCM

The Ala15-Thr mutation in a 4-year-old female and the Pro21-Thr mutation in a 60-year-old female, both detected in individuals with a family history and a clinical diagnosis of DCM, are the subject of the current study (5). In comparison to wild-type PLN, these mutations showed super-inhibition and decreased SERCA activity (Figure 4.2), which would cause delayed calcium reuptake and slower cardiac muscle relaxation in these patients. The lower rates of phosphorylation and dephosphorylation caused by the mutations further indicate that the cardiac contractility in these patients is less responsive to the demand for cardiac output and dynamic contractility via β-adrenergic signaling. These results parallel those with Arg25-Cys, a gain of function mutation in PLN that was previously published and found in a family with DCM and ventricular arrhythmias (32). The mutation was found to be a super-inhibitor of SERCA, which

reduced the amount of calcium in the SR, calcium transients, and contractile performance. In contrast, Arg25-Cys was discovered to be sensitive to β-adrenergic signaling. The Ala15-Thr and Pro21-Thr mutations seem to replicate the calcium handling defects associated with the Arg25-Cys mutation, with the added complication that they also perturb β-adrenergic signaling. With respect to perturbation of β-adrenergic signaling, the Arg^{14}-deletion mutation in PLN associated with both mild (34) and severe (4) DCM should be considered. This mutation prevents PLN from being phosphorylated and prevents it from responding to β-adrenergic signaling because it is located within the PKA recognition motif of PLN (35). Patients with the Arg9-Cys mutation in PLN are affected by the association between dysregulated β-adrenergic signaling and DCM (3,35). The perturbation of β-adrenergic signaling, both phosphorylation of PLN by PKA and dephosphorylation by PP1, observed for the Ala15-Thr and Pro21-Thr mutants provides another causative link to DCM, even though these mutants do not cause the severe defects in β-adrenergic signaling seen for the Arg14-deletion and Arg9-Cys variants. We categorize the Ala15-Thr and Pro21-Thr mutations as potentially pathogenic based on these factors.

4.3.2 Missense Mutations in PLN as Variants of Uncertain Significance

The Ile18-Thr missense variant of PLN was found in clinical databases (16,17) with reported clinical conditions of DCM and HCM, while the COSMIC database contained the Thr17-Ile and Glu19-Lys missense variants of PLN (15). Even though these latter mutations are somatic, certain PLN variants first showed up in the COSMIC database and then later in clinical databases (32). We also generated an Ala15-Glu missense variant to explore the role of Ala15 in the function, phosphorylation, and dephosphorylation of

PLN. While this variant has not been identified in patients, it allowed us to explore the role of this residue in mimicking the phosphorylated state of PLN. The Ile8-Thr mutant has been identified in patients, and is considered a VUS, while the Ala15-Glu, Thr17-Ile, and Glu19-Lys mutants have unknown clinical relevance. All four missense mutants resulted in loss of function in that they did not alter the apparent calcium affinity of SERCA (KC_a) as compared to wild-type PLN (Figure 4.2).

Loss-of-function PLN mutations have been associated with DCM, with the Leu39-truncation (36), Arg9-Cys (3), and Arg14-deletion (4) mutants being well-studied examples. The Leu39-truncation of PLN is considered a null form of the protein and in heterozygous patients, which represent most PLN variants identified, the truncation leads to reduced PLN levels and mild HCM which progresses to DCM later in life (32). Leu39-truncation is compared to loss of function variants of PLN. Arg9-Cys mutation results in complete loss-of-function (10), and this mutant is associated with severe DCM and death by ~25 years of age in heterozygous individuals (3). Arg14-deletion mutation results in a partial loss-of-function whereby it reduces the apparent calcium affinity of SERCA to a lesser degree than wild-type PLN (10). Arg14-deletion PLN is associated with both mild and sever DCM in heterozygous individuals, where the original heterozygous patient died at 56 years of age (4). Arg9-Cys and Arg14-deletion are also impacted negatively in PKA-mediated phosphorylation (23) contributing to our classification of all four mutants identified in this study as likely pathogenic based on their complete loss of function behavior.

PKA-mediated phosphorylation and PP1-mediated dephosphorylation of PLN via the β-adrenergic signaling pathway are critical to normal cardiac contractility and dynamic cardiac output. The phosphorylation and dephosphorylation characteristics of the identified PLN mutants was explored. The Ile18-Thr mutant could not be

phosphorylated by PKA. The Ile18-Thr mutant results in both loss of PLN function (Figure 4.2) and loss of regulatory control by phosphorylation (Figure 4.3), paralleling the well characterized Arg9-Cys mutant's functionality associated with severe, early-onset DCM. These parallels lead to our classification of the Ile18-Thr mutant as likely pathogenic. Another potentially severe mutation, Glu19-Lys, displayed both loss-of-function (Figure 4.2) and significantly reduced regulatory control by phosphorylation (Figure 4.3). This mutant is functionally in the middle between the pathogenic Leu39-truncation (null PLN) and Arg9-Cys (loss of function and phosphorylation) mutants, leading us to classify this mutant as likely pathogenic. Ala15-Glu and Thr17-Ile both exhibit more minor phosphorylation abnormalities. Ala15-Glu was phosphorylated at a slightly slower rate compared to Thr17-Ile being phosphorylated slightly faster. These two mutants are most like the Leu39-truncation (PLN null) and we classify them as likely pathogenic. The second CaMKII phosphorylation site is eliminated by the Thr17-Ile mutant. Although the phosphorylation of PLN at Ser16 by PKA via the β-adrenergic pathway appears to be the primary regulatory mechanism, the phosphorylation of Thr17 is also seen and is known to have a comparable impact on the regulation of SERCA and cardiac contractility. The Thr17-Ile variant's potential pathogenicity is likely increased as a result.

4.3.3 Structural Elements Required for PLN Function

Pro21 is an important residue in the flexible linker region separating PLN's regulatory N-terminal helix from the inhibitory transmembrane helix. Pro21 is important for coupling the two domains of PLN, and the structural changes due to phosphorylation and relief of SERCA inhibition (20,21). Thus, it is not surprising that Pro21 mutation

impacts both the helical structure and inhibitory characteristics of PLN. Investigation of Pro21 PLN relative to WT PLN (Figures 4.5, 4.6, & Table 4.3) resulted in a large change in helical content which was found to be equivalent to approximately 13 residues. The N-terminal cytoplasmic domain of PLN is dynamic (20,29,37) and the Pro21-Thr mutant appears to increase the proportion of helical secondary structure in the linker region (Figure 4.6), similar to an early entirely helical model of PLN (38).

4.3.4 A Missense Mutation in MyBPC3 as a Genetic Modifier (L. Michel Espinoza-Fonseca)

Missense mutations in MyBPC3 are associated with hypertrophic cardiomyopathy (HCM) and the two major genes associated with HCM, *MYBPC3* and *MYH7*, are involved in ~70% of familial cases. These genes encode the sarcomere proteins cardiac myosin binding protein C3 (MyBPC3) and the cardiac myosin heavy chain β isoform (MYH7). Rare variations in MyBPC3 are increasingly being found through genetic testing and high-throughput and whole-exome sequencing,. The number of variants, however, is higher than the prevalence of the disease, and many of these variants have limited penetrance and commonly arise in control populations (18,39). This is the case for the Val896-Met missense mutation, which has been found in both control and HCM cohorts. This mutation was speculated to alter the structure of the C7 domain and contribute to the development of HCM when first described in two South African HCM-affected subpopulations (30). Later investigation identified missense mutations in MYH7 and MyBPC3 that co-segregated in a small set of patients (40) and the conclusion was drawn that the nature of the Val896-Met mutant remains unclear, and that it likely acts as a

genetic modifier of disease in the presence of a MYH7 mutation classified as pathogenic or likely pathogenic (Ala355-Thr).

The PLN and MyBPC3 mutations have different effects on cardiac contractility. The PLN mutations Ala15-Thr and Pro21-Thr disrupt cellular calcium homeostasis and β-adrenergic signaling, which has the potential to be pathogenic. The Val896-Met mutation in MyBPC3 leads to structural changes at the sarcomere level, which have the potential to further worsen contractility issues. It is likely that the DCM in these patients is caused by the compounding effects of these two missense mutations.

4.3.5 Future Directions

Hypertrophic and dilated cardiomyopathies (HCM & DCM) are frequently observed in patients with a family history of heart disease. Recent advancements in genetic testing techniques, such as genetic testing panels, exome sequencing, and whole genome sequencing, have led to the identification of numerous rare genetic causes associated with HCM and DCM. Although identifying disease-causing variants is a complex task, understanding the relationship between genotype and phenotype offers the potential for personalized treatment approaches.

Currently, variants are categorized into five groups based on available evidence, including benign, likely benign, uncertain significance, likely pathogenic, or pathogenic. This classification process considers various factors like sequence characteristics, population frequency, family segregation, and functional data.

As genetic sequencing becomes more widespread, the number of variants classified as uncertain significance (VUS) will rapidly increase. Consequently, there is a pressing need to reevaluate and reclassify VUS into clinically relevant categories. To

facilitate this process, the American College of Medical Genetics and Genomics (ACMG) recommends conducting functional studies to help determine the potential pathogenicity of VUS. In this study, the functional evaluation of PLN variants is one of the essential steps in their proper classification. Additionally, ongoing genetic testing of HCM and DCM patients continues to provide valuable information regarding population frequency and clinical associations.

In conclusion, this work highlights the importance of phosphorylation on PLN and its significance in cardiac regulation. Future directions in this field offer promising avenues for investigation. One major area is to explore the interplay between insulin regulation of cardiac SERCA through Akt and the role of the protein kinase SPEG. Investigating whether SPEG phosphorylates phospholamban at Thr-17 and its potential impact on Akt/PKB activity at this site will provide valuable insights.

Additionally, further research could delve into the competitive dynamics between adrenergic signaling via Ser-16 and insulin signaling at Thr-17 in cardiac muscle, warranting a detailed molecular analysis of phospholamban. Understanding how phospholamban mutants may interfere with insulin signaling in vivo, particularly in the context of the PLN TIEM sequence's similarity to the SPEG-phosphorylated T484LEF sequence in cardiac SERCA2a, is another intriguing avenue for future exploration.

Moreover, investigating the physiological implications of SPEG phosphorylation on SERCA and PLN interactions will shed light on the regulatory mechanisms within the cardiac system. These future endeavors have the potential to advance our understanding of cardiac function and its implications for cardiovascular health and disease.

4.4 Materials & Methods

All reagents were of the highest purity available: octaethylene glycol monododecyl ether ($C_{12}E_8$; Nikko Chemicals Co., Ltd., Tokyo, Japan); egg yolk phosphatidylcholine (EYPC) and phosphatidic acid (EYPA) (Avanti Polar Lipids, Alabaster, AL); all reagents used in the coupled enzyme assay including NADH, ATP, PEP, lactate dehydrogenase, and pyruvate kinase (Sigma-Aldrich, Oakville, ON Canada).

4.4.1 Co-Reconstitution of Phospholamban Peptides with SERCA

Recombinant human PLN peptides were expressed as maltose-binding protein (MBP) fusion proteins with a TEV cleavage site for removal of MBP as previously described (12,41). The peptides were purified by a combination of organic extraction (chloroform-isopropanol-water) and reverse-phase HPLC. Purified PLN peptides were stored as lyophilized thin films (100 µg aliquots). SERCA1a was purified from rabbit skeletal muscle SR and this isoform was used for all functional measurements. For co-reconstitution, lyophilized peptide was suspended in a 100 µl mixture of trifluoroethanol-water (5:1) and mixed with lipids (360 µg EYPC & 40 µg EYPA) from stock chloroform solutions. The peptide-lipid mixture was dried to a thin film under nitrogen gas and placed under vacuum overnight. The peptide-lipid mixture was rehydrated in buffer (20 mM imidazole pH 7.0; 100 mM NaCl; 0.02% NaN_3) at 50˚C for 15 min. After cooling to room temperature, the peptide-lipid mixture was solubilized in detergent (0.2 % $C_{12}E_8$). Detergent-solubilized SERCA1a was added (300 µg at a final concentration of 1 mg/ml) and the reconstitution was stirred gently at room temperature. Detergent was slowly removed by the addition of SM-2 Bio-Beads (Bio-Rad, Hercules, CA) over a 4-hour time course (final weight ratio of 25 Bio-Beads to 1 detergent). Following detergent removal, the reconstitution was centrifuged over a

sucrose step-gradient (20% & 50% layers) for 1 h at 100,000g. The reconstituted proteoliposomes at the 20%-50% gradient interface were removed, flash-frozen in liquid-nitrogen, and stored at -80 ˚C. The final molar ratios ranged from 2-5 peptides per SERCA.

4.4.2 Calcium-Dependent ATPase Activity Assays

The reconstituted proteoliposomes contain a high density of SERCA and PLN peptides (lipid-to-protein ratio of ~100:1) designed to mimic native SR membranes (11,12). The resultant proteoliposomes allow the measurement of steady-state calcium-dependent ATPase activity (e.g. (10,42,43)). In this study, the calcium-dependent ATPase activity of the co-reconstituted proteoliposomes was measured by a coupled-enzyme assay as previously described. Absorbance was measured at 340 nm wavelength to monitor the conversion of NADH to NAD^+ as ATP was hydrolyzed by SERCA (44). Samples were run in a 96-well format with a well volume of 155 µl containing 10-20 nM SERCA and various concentrations of calcium ranging from 0.1 to 10 µM (30˚C; data points were collected every ~30 seconds for 20 minutes). The reactions were initiated by the addition of proteoliposomes to each well of assay solution. The V_{max} (maximal activity) and K_{Ca} (apparent calcium affinity) were determined based on non-linear least-squares fitting of the activity data to the Hill equation (Sigma Plot software, SPSS Inc., Chicago, IL). Errors were calculated as the standard error of the mean for a minimum of four independent reconstitutions. Comparison of K_{Ca} and V_{max} was carried out using one-way analysis of variance (between subjects), followed by the Holm-Sidak test for pairwise comparisons.

4.4.3 Phosphorylation Assays

PLN was phosphorylated in detergent solution by the catalytic subunit of PKA (MilliporeSigma, Canada) in the absence of SERCA as previously described (12,35). PLN was phosphorylated in the presence of ATP spiked with [γ-^{32}P]ATP (~0.1 µCi/µl). At various time points, the reactions were stopped by the addition of TCA, incubated on ice for 10 min, washed several times with 10% TCA and water, and counted in 1 ml of liquid scintillant (Perkin-Elmer) for 1 min in a scintillation counter. All of the values were corrected for a negative control by subtracting background counts per minute from samples containing no PKA. The values were compared to a positive control consisting of wild-type PLN fully phosphorylated for 60 minutes at 30˚C. Errors were calculated as the standard error of the mean for a minimum of three independent experiments. Comparison of phosphorylation levels was carried out using one-way analysis of variance (between subjects), followed by the Holm-Sidak test for pairwise comparisons.

4.4.4 Dephosphorylation Assays

Protein phosphatase-1cα (PP1) was expressed and purified as described (45,46). PLN was phosphorylated in detergent solution by the catalytic subunit of PKA in the absence of SERCA for 60 minutes at 30˚C as described above. After 60 minutes, the samples were heated to 60˚C to inactivate the catalytic subunit of PKA. The samples were cooled to 30˚C and PP1 was added. The reactions were stopped by the addition of TCA, incubated on ice for 10 min, washed several times with 10% TCA and water, and counted in 1 ml of liquid scintillant (Perkin-Elmer) for 1 min in a scintillation counter. All of the values were compared to a negative control consisting of samples containing no PP1 and a positive control consisting of wild-type PLN fully phosphorylated for 60 minutes at 30˚C followed by dephosphorylation by PP1 for 60 minutes at 30˚C. Errors were

calculated as the standard error of the mean for a minimum of three independent experiments. Comparison of dephosphorylation levels was carried out using one-way analysis of variance (between subjects), followed by the Holm-Sidak test for pairwise comparisons.

4.4.5 Circular Dichroism (CD) Spectroscopy

Peptide concentrations were 1 mg/ml in detergent solution (10 mM Tris-HCl pH 7.5, 2.5% dodecylmaltoside (DDM), 0.5 mM DTT). Peptide samples were stirred overnight and centrifuged the following day to remove any precipitate. The concentration of the supernatant was measured via a Pierce BCA protein assay (ThermoFisher Scientific). CD spectra were recorded at 20˚C on a Jasco J-500C spectropolarimeter (Jasco, Easton, MD). The data were collected at 0.1 nm resolution with a scan speed of 50 nm/min from 260 to 190 nm in quartz cells with a path length of 0.02 cm. A simple spline curve of the data was generated with Sigma Plot software (SPSS Inc., Chicago, IL). The secondary structure content of the peptides was estimated from the CD spectra using DichroWeb, a website for calculating protein secondary structure from CD spectroscopic data (27,28).

4.4.6 Molecular modeling and molecular dynamics simulations of **MyBPC3 (L. Michel Espinoza-Fonseca conducted molecular dynamics simulations of cMyBPC3, Sara Amidian piloted initial MD simulation feasibility studies (data not shown))**

Molecular models of the C7 domain (residues 870-963) and the C6-C7 tandem domains (residues 772-963) of human MyBPC3 were generated for wild-type and the Val^{896}-Met variant using I-TASSER (31). The molecular models generated were based on a FnIII tandem of titin (PDB code 3LPW; RMSD 1.2Å). The final models of the proteins were

solvated using TIP3P water molecules with a minimum margin of 20 Å between the edges of the periodic box and the protein, and K^+ and Cl^- ions were added to neutralize the system and to produce a KCl concentration of ~100 mM. Preparation of the systems was done using the CHARMM-GUI web interface (47). We performed the molecular simulations with AMBER20 on Tesla V100 GPUs (48) using the AMBER ff19SB force field (49). We maintained a temperature of 310 K with a Langevin thermostat and a pressure of 1.0 bar with the Monte Carlo barostat. We used the SHAKE algorithm to constrain all bonds involving hydrogens and allow a time step of 2 fs. We first performed 5000 steps of steepest-descent energy minimization followed by equilibration as follows: two 25-ps MD simulations using a canonical ensemble (NVT), one 25-ps MD simulation using an isothermal–isobaric ensemble (NPT), and two 500-ps MD simulations using the NPT ensemble. The equilibrated systems were used as a starting point to perform three independent 1µs replicates of the WT protein, and three independent 1µs replicates of the V896 variant. We analyzed the MD trajectories using VMD (50) (Humphrey et al., 1996). Rendering of structures was performed with VMD (50), and RMSF plots were created using QtGrace (https://sourceforge.net/projects/qtgrace/).

Chapter 4 References

1. Haghighi K, Bidwell P, Kranias EG. Phospholamban interactome in cardiac contractility and survival: A new vision of an old friend. J Mol Cell Cardiol [Internet]. 2014;77:160–7. Available from: http://linkinghub.elsevier.com/retrieve/pii/S0022282814003253

2. van der Zwaag PA, van Rijsingen IAW, Asimaki A, Jongbloed JDH, van Veldhuisen DJ, Wiesfeld ACP, et al. Phospholamban R14del mutation in patients diagnosed with dilated cardiomyopathy or arrhythmogenic right ventricular cardiomyopathy: evidence supporting the concept of arrhythmogenic cardiomyopathy. Eur J Heart Fail [Internet]. 2012 Nov [cited 2022 Sep 30];14(11):1199–207. Available from: https://pubmed.ncbi.nlm.nih.gov/22820313/

3. Schmitt JP, Kamisago M, Asahi M, Li GH, Ahmad F, Mende U, et al. Dilated cardiomyopathy and heart failure caused by a mutation in phospholamban. Science. 2003;299(February):1410–3.

4. Haghighi K, Kolokathis F, Gramolini AO, Waggoner JR, Pater L, Lynch RA, et al. A mutation in the human phospholamban gene, deleting arginine 14, results in lethal, hereditary cardiomyopathy. Proceedings of the National Academy of Sciences [Internet]. 2006 Jan;103(5):1388 LP – 1393. Available from: http://www.pnas.org/content/103/5/1388.abstract

5. Pugh TJ, Kelly MA, Gowrisankar S, Hynes E, Seidman MA, Baxter SM, et al. The landscape of genetic variation in dilated cardiomyopathy as surveyed by clinical DNA sequencing. Genetics in Medicine. 2014;16(8):601–8.

6. Jääskeläinen P, Heliö T, Aalto-Setälä K, Kaartinen M, Ilveskoski E, Hämäläinen L, et al. A new common mutation in the cardiac beta-myosin heavy chain gene in Finnish patients with hypertrophic cardiomyopathy. Ann Med [Internet]. 2014 Sep 1 [cited 2022 Sep 30];46(6):424–9. Available from: https://pubmed.ncbi.nlm.nih.gov/24888384/

7. Kimura Y, Kurzydlowski K, Tada M, MacLennan DH. Phospholamban Inhibitory Function Is Activated by Depolymerization. Journal of Biological Chemistry [Internet]. 1997 Jun;272(24):15061–4. Available from: http://www.jbc.org/content/272/24/15061.abstract

8. Adams PD, Arkin IT, Engelman DM, Brünger AT. Computational searching and mutagenesis suggest a structure for the pentameric transmembrane domain of phospholamban. Nature Structural Biology 1995 2:2 [Internet]. 1995 [cited 2022 Sep 30];2(2):154–62. Available from: https://www.nature.com/articles/nsb0295-154

9. Simmerman HKB, Kobayashi YM, Autry JM, Jones LR. A leucine zipper stabilizes the pentameric membrane domain of phospholamban and forms a coiled-coil pore structure. Journal of Biological Chemistry. 1996;271(10):5941–6.

10. Ceholski DK, Trieber C a., Young HS. Hydrophobic imbalance in the cytoplasmic domain of phospholamban is a determinant for lethal dilated cardiomyopathy. Journal of Biological Chemistry. 2012;287(20):16521–9.

11. Trieber CA, Afara M, Young HS. Effects of Phospholamban Transmembrane Mutants on the Calcium Affinity, Maximal Activity, and Cooperativity of the Sarcoplasmic Reticulum Calcium Pump. Biochemistry [Internet]. 2009 Oct;48(39):9287–96. Available from: https://doi.org/10.1021/bi900852m

12. Trieber CA, Douglas JL, Afara M, Young HS. The Effects of Mutation on the Regulatory Properties of Phospholamban in Co-Reconstituted Membranes†. Biochemistry [Internet]. 2005 Mar;44(9):3289–97. Available from: http://dx.doi.org/10.1021/bi047878d

13. Kimura Y, Asahi M, Kurzydlowski K, Tada M, MacLennan DH. Phospholamban Domain Ib Mutations Influence Functional Interactions with the Ca2+-ATPase Isoform of Cardiac Sarcoplasmic Reticulum. Journal of Biological Chemistry [Internet]. 1998 Jun;273(23):14238–41. Available from: http://www.jbc.org/content/273/23/14238.abstract

14. Glaves JP, Trieber C a., Ceholski DK, Stokes DL, Young HS. Phosphorylation and mutation of phospholamban alter physical interactions with the sarcoplasmic reticulum calcium pump. J Mol Biol [Internet]. 2011;405(3):707–23. Available from: http://dx.doi.org/10.1016/j.jmb.2010.11.014

15. Bamford S, Dawson E, Forbes S, Clements J, Pettett R, Dogan A, et al. The COSMIC (Catalogue of Somatic Mutations in Cancer) database and website. Br J Cancer [Internet]. 2004 Jul 19 [cited 2022 Sep 30];91(2):355–8. Available from: https://pubmed.ncbi.nlm.nih.gov/15188009/

16. Howe KL, Achuthan P, Allen J, Allen J, Alvarez-Jarreta J, Ridwan Amode M, et al. Ensembl 2021. Nucleic Acids Res [Internet]. 2021 Jan 8 [cited 2022 Sep 30];49(D1):D884–91. Available from: https://pubmed.ncbi.nlm.nih.gov/33137190/

17. Landrum MJ, Chitipiralla S, Brown GR, Chen C, Gu B, Hart J, et al. ClinVar: improvements to accessing data. Nucleic Acids Res [Internet]. 2020 Jan 1 [cited 2022 Sep 30];48(D1):D835–44. Available from: https://pubmed.ncbi.nlm.nih.gov/31777943/

18. Walsh R, Thomson KL, Ware JS, Funke BH, Woodley J, McGuire KJ, et al. Reassessment of Mendelian gene pathogenicity using 7,855 cardiomyopathy cases and 60,706 reference samples. Genet Med [Internet]. 2017 Feb 1 [cited 2022 Sep 30];19(2):192–203. Available from: https://pubmed.ncbi.nlm.nih.gov/27532257/

19. Li J, Boschek CB, Xiong Y, Sacksteder C a, Squier TC, Bigelow DJ. Essential Role for Pro in Phospholamban for Optimal Inhibition of the Ca-ATPase Essential Role for Pro 21 in Phospholamban for Optimal Inhibition of the. Society. 2005;16181–91.

20. Ha KN, Traaseth NJ, Verardi R, Zamoon J, Cembran A, Karim CB, et al. Controlling the inhibition of the sarcoplasmic Ca2+-ATPase by tuning phospholamban structural dynamics. J Biol Chem [Internet]. 2007 Dec 21 [cited 2022 Sep 28];282(51):37205–14. Available from: https://pubmed.ncbi.nlm.nih.gov/17908690/

21. Li J, Boschek CB, Xiong Y, Sacksteder CA, Squier TC, Bigelow DJ. Essential role for Pro21 in phospholamban for optimal inhibition of the Ca-ATPase. Biochemistry. 2005;44(49):16181–91.

22. Moore MJ, Adams JA, Taylor SS. Structural basis for peptide binding in protein kinase A. Role of glutamic acid 203 and tyrosine 204 in the peptide-positioning loop. J Biol Chem [Internet]. 2003 Mar 21 [cited 2022 Oct 1];278(12):10613–8. Available from: https://pubmed.ncbi.nlm.nih.gov/12499371/

23. Ceholski DK, Trieber CA, Holmes CFB, Young HS. Lethal, Hereditary Mutants of Phospholamban Elude Phosphorylation by Protein Kinase A. Journal of Biological Chemistry [Internet]. 2012 Aug;287(32):26596–605. Available from: http://www.jbc.org/content/287/32/26596.abstract

24. Masterson LR, Cheng C, Yu T, Tonelli M, Kornev A, Taylor SS, et al. Dynamics connect substrate recognition to catalysis in protein kinase A. Nat Chem Biol [Internet]. 2010 Oct;6:821. Available from: https://doi.org/10.1038/nchembio.452

25. Verardi R, Shi L, Traaseth NJ, Walsh N, Veglia G. Structural topology of phospholamban pentamer in lipid bilayers by a hybrid solution and solid-state NMR method. Proc Natl Acad Sci U S A [Internet]. 2011 May 31 [cited 2022 Oct 1];108(22):9101–6. Available from: https://www.pnas.org/doi/abs/10.1073/pnas.1016535108

26. Simmerman HKB, Jones LR. Phospholamban: Protein structure, mechanism of action, and role in cardiac function. Physiol Rev [Internet]. 1998 [cited 2022 Oct 1];78(4):921–47. Available from: https://journals.physiology.org/doi/10.1152/physrev.1998.78.4.921

27. Whitmore L, Wallace BA. Protein secondary structure analyses from circular dichroism spectroscopy: methods and reference databases. Biopolymers [Internet]. 2008 May [cited 2023 Apr 19];89(5):392–400. Available from: https://pubmed.ncbi.nlm.nih.gov/17896349/

28. Miles AJ, Ramalli SG, Wallace BA. DichroWeb, a website for calculating protein secondary structure from circular dichroism spectroscopic data. Protein Science

[Internet]. 2022 Jan 1 [cited 2023 Apr 19];31(1):37–46. Available from: https://onlinelibrary.wiley.com/doi/full/10.1002/pro.4153

29. Gustavsson M, Verardi R, Mullen DG, Mote KR, Traaseth NJ, Gopinath T, et al. Allosteric regulation of SERCA by phosphorylation-mediated conformational shift of phospholamban. Proc Natl Acad Sci U S A [Internet]. 2013;110(43):17338–43. Available from: http://www.pubmedcentral.nih.gov/articlerender.fcgi?artid=3808617&tool=pmcentrez&rendertype=abstract

30. Moolman-Smook JC, de Lange WJ, Bruwer ECD, Brink PA, Corfield VA. The origins of hypertrophic cardiomyopathy-causing mutations in two South African subpopulations: a unique profile of both independent and founder events. Am J Hum Genet [Internet]. 1999 [cited 2022 Oct 1];65(5):1308–20. Available from: https://pubmed.ncbi.nlm.nih.gov/10521296/

31. Yang J, Yan R, Roy A, Xu D, Poisson J, Zhang Y. The I-TASSER Suite: protein structure and function prediction. Nature Methods 2015 12:1 [Internet]. 2014 Dec 30 [cited 2022 Oct 1];12(1):7–8. Available from: https://www.nature.com/articles/nmeth.3213

32. Liu GS, Morales A, Vafiadaki E, Lam CK, Cai WF, Haghighi K, et al. A novel human R25C-phospholamban mutation is associated with super-inhibition of calcium cycling and ventricular arrhythmia. Cardiovasc Res [Internet]. 2015 Jul 1 [cited 2022 Oct 2];107(1):164–74. Available from: https://pubmed.ncbi.nlm.nih.gov/25852082/

33. Medeiros A, Biagi DG, Sobreira TJP, de Oliveira PSL, Negrão CE, Mansur AJ, et al. Mutations in the human phospholamban gene in patients with heart failure. Am Heart J [Internet]. 2011;162(6):1088-1095.e1. Available from: http://dx.doi.org/10.1016/j.ahj.2011.07.028

34. DeWitt MM, MacLeod HM, Soliven B, McNally EM. Phospholamban R14 Deletion Results in Late-Onset, Mild, Hereditary Dilated Cardiomyopathy. J Am Coll Cardiol [Internet]. 2006;48(7):1396–8. Available from: http://www.sciencedirect.com/science/article/pii/S0735109706018377

35. Ceholski DK, Trieber C a., Holmes CFB, Young HS. Lethal, hereditary mutants of phospholamban elude phosphorylation by protein kinase A. Journal of Biological Chemistry. 2012;287:26596–605.

36. Haghighi K, Kolokathis F, Pater L, Lynch RA, Asahi M, Gramolini AO, et al. Human phospholamban null results in lethal dilated cardiomyopathy revealing a critical difference between mouse and human. J Clin Invest [Internet]. 2003 Mar;111(6):869–76. Available from: https://doi.org/10.1172/JCI17892

37. Seidel K, Andronesi OC, Krebs J, Griesinger C, Young HS, Becker S, et al. Structural Characterization of Ca2+-ATPase-Bound Phospholamban in Lipid Bilayers by Solid-State Nuclear Magnetic Resonance (NMR) Spectroscopy,. Biochemistry [Internet]. 2008 Apr;47(15):4369–76. Available from: https://doi.org/10.1021/bi7024194

38. Arkin IT, Rothman M, Ludlam CFC, Aimoto S, Engelman DM, Rothschild KJ, et al. Structural model of the phospholamban ion channel complex in phospholipid

membranes. J Mol Biol [Internet]. 1995 May 12 [cited 2022 Sep 28];248(4):824–34. Available from: https://pubmed.ncbi.nlm.nih.gov/7752243/

39. Sabater-Molina M, Pérez-Sánchez I, Hernández del Rincón JP, Gimeno JR. Genetics of hypertrophic cardiomyopathy: A review of current state. Clin Genet [Internet]. 2018 Jan 1 [cited 2022 Oct 3];93(1):3–14. Available from: https://pubmed.ncbi.nlm.nih.gov/28369730/

40. Richard P, Charron P, Carrier L, Ledeuil C, Cheav T, Pichereau C, et al. Hypertrophic cardiomyopathy: distribution of disease genes, spectrum of mutations, and implications for a molecular diagnosis strategy. Circulation [Internet]. 2003 May 6 [cited 2022 Oct 3];107(17):2227–32. Available from: https://pubmed.ncbi.nlm.nih.gov/12707239/

41. Douglas JL, Trieber C a., Afara M, Young HS. Rapid, high-yield expression and purification of Ca2+-ATPase regulatory proteins for high-resolution structural studies. Protein Expr Purif [Internet]. 2005 Mar;40(1):118–25. Available from: http://www.sciencedirect.com/science/article/pii/S1046592804004036

42. Fisher ME, Bovo E, Aguayo-Ortiz R, Cho EE, Pribadi MP, Dalton MP, et al. Dwarf open reading frame (Dworf) is a direct activator of the sarcoplasmic reticulum calcium pump serca. Elife. 2021 Jun 1;10.

43. Smeazzetto S, Armanious GP, Moncelli MR, Bak JJ, Lemieux MJ, Young HS, et al. Conformational memory in the association of the transmembrane protein phospholamban with the sarcoplasmic reticulum calcium pump SERCA. Journal of Biological Chemistry. 2017;292(52):21330–9.

44. Warren GB, Toon P a, Birdsall NJ, Lee a G, Metcalfe JC. Reconstitution of a calcium pump using defined membrane components. Proc Natl Acad Sci U S A. 1974;71(3):622–6.

45. Skene-Arnold TD, Luu HA, Uhrig RG, De Wever V, Nimick M, Maynes J, et al. Molecular mechanisms underlying the interaction of protein phosphatase-1c with ASPP proteins. Biochem J [Internet]. 2013 Feb 1 [cited 2023 Apr 19];449(3):649–59. Available from: https://pubmed.ncbi.nlm.nih.gov/23088536/

46. Zhou Y, Millott R, Kim HJ, Peng S, Edwards RA, Skene-Arnold T, et al. Flexible Tethering of ASPP Proteins Facilitates PP-1c Catalysis. Structure [Internet]. 2019 Oct 1 [cited 2023 Apr 19];27(10):1485-1496.e4. Available from: https://pubmed.ncbi.nlm.nih.gov/31402222/

47. Jo S, Kim T, Iyer VG, Im W. CHARMM-GUI: a web-based graphical user interface for CHARMM. J Comput Chem [Internet]. 2008 Aug [cited 2023 Apr 19];29(11):1859–65. Available from: https://pubmed.ncbi.nlm.nih.gov/18351591/

48. Salomon-Ferrer R, Götz AW, Poole D, Le Grand S, Walker RC. Routine microsecond molecular dynamics simulations with AMBER on GPUs. 2. Explicit solvent particle mesh ewald. J Chem Theory Comput [Internet]. 2013 Sep 10 [cited 2023 Apr 19];9(9):3878–88. Available from: https://pubs.acs.org/doi/abs/10.1021/ct400314y

49. Tian C, Kasavajhala K, Belfon KAA, Raguette L, Huang H, Migues AN, et al. ff19SB: Amino-Acid-Specific Protein Backbone Parameters Trained against Quantum Mechanics Energy Surfaces in Solution. J Chem Theory Comput [Internet]. 2020 Jan 14 [cited 2023 Apr 19];16(1):528–52. Available from: https://pubmed.ncbi.nlm.nih.gov/31714766/

50. Humphrey W, Dalke A, Schulten K. VMD: Visual molecular dynamics. J Mol Graph [Internet]. 1996 [cited 2023 Apr 19];14(1):33–8. Available from: https://pubmed.ncbi.nlm.nih.gov/8744570/

Bibliography (Comprehensive)

Chapter 1 Works Cited

1. Carafoli E, Krebs J. Why Calcium? How Calcium Became the Best Communicator. Journal of Biological Chemistry [Internet]. 2016 Sep;291(40):20849–57. Available from: http://www.jbc.org/content/291/40/20849.abstract

2. Crichton RR. Calcium – Cellular Signalling. Biological Inorganic Chemistry. 2012 Jan 1;215–28.

3. Ripa R, George T, Sattar Y. Physiology, Cardiac Muscle. StatPearls [Internet]. 2022 Jun 2 [cited 2022 Oct 29]; Available from: https://www.ncbi.nlm.nih.gov/books/NBK572070/

4. Thompson BR, Metzger JM. Cell biology of sarcomeric protein engineering: disease modeling and therapeutic potential. Anat Rec (Hoboken) [Internet]. 2014 [cited 2022 Oct 29];297(9):1663–9. Available from: https://pubmed.ncbi.nlm.nih.gov/25125179/

5. staff Blausen com, staff Blausen com. [[WikiJournal of Medicine/Medical gallery of Blausen Medical 2014|Medical gallery of Blausen Medical 2014]]. [[WikiJournal of Medicine|WikiJournal of Medicine]]. 2014;1(2).

6. Creative Commons Legal Code [Internet]. [cited 2023 Mar 11]. Available from: https://creativecommons.org/licenses/by/3.0/legalcode

7. Meissner G. Ryanodine receptor/Ca2+ release channels and their regulation by endogenous effectors. Annu Rev Physiol [Internet]. 1994 [cited 2022 Nov 4];56:485–508. Available from: https://pubmed.ncbi.nlm.nih.gov/7516645/

8. Franzini-Armstrong C, Protasi F, Ramesh V. Shape, size, and distribution of Ca(2+) release units and couplons in skeletal and cardiac muscles. Biophys J [Internet]. 1999 [cited 2022 Nov 4];77(3):1528–39. Available from: https://pubmed.ncbi.nlm.nih.gov/10465763/

9. Bers DM. Cardiac excitation-contraction coupling. Nature [Internet]. 2002 Jan 10 [cited 2022 Nov 4];415(6868):198–205. Available from: https://pubmed.ncbi.nlm.nih.gov/11805843/

10. Doroudgar S, Glembotski CC. New concepts of endoplasmic reticulum function in the heart: Programmed to conserve. J Mol Cell Cardiol [Internet]. 2013;55:85–91. Available from: http://www.sciencedirect.com/science/article/pii/S0022282812003744

11. Palmgren MG, Nissen P. P-Type ATPases. Annu Rev Biophys [Internet]. 2011 May;40(1):243–66. Available from: https://doi.org/10.1146/annurev.biophys.093008.131331

12. Toyoshima C. Ion pumping by calcium ATPase of sarcoplasmic reticulum. Adv Exp Med Biol [Internet]. 2007 [cited 2022 Nov 4];592:295–303. Available from: https://link.springer.com/chapter/10.1007/978-4-431-38453-3_25

13. Møller J v, Olesen C, Winther AML, Nissen P. The sarcoplasmic Ca2+-ATPase: design of a perfect chemi-osmotic pump. Q Rev Biophys [Internet]. 2010;43(4):501–66.

Available from: https://www.cambridge.org/core/product/712917B2C432A2C19D12749FF667D772

14. Dally S, Corvazier E, Bredoux R, Bobe R, Enouf J. Multiple and diverse coexpression, location, and regulation of additional SERCA2 and SERCA3 isoforms in nonfailing and failing human heart. J Mol Cell Cardiol [Internet]. 2010;48(4):633–44. Available from: http://www.sciencedirect.com/science/article/pii/S0022282809004878

15. Wuytack F, Raeymaekers L, Missiaen L. Molecular physiology of the SERCA and SPCA pumps. Cell Calcium [Internet]. 2002;32(5):279–305. Available from: http://www.sciencedirect.com/science/article/pii/S0143416002001847

16. Kósa M, Brinyiczki K, van Damme P, Goemans N, Hancsák K, Mendler L, et al. The neonatal sarcoplasmic reticulum Ca2+-ATPase gives a clue to development and pathology in human muscles. J Muscle Res Cell Motil [Internet]. 2015;36(2):195–203. Available from: https://doi.org/10.1007/s10974-014-9403-z

17. Vangheluwe P, Raeymaekers L, Dode L, Wuytack F. Modulating sarco(endo)plasmic reticulum Ca2+ ATPase 2 (SERCA2) activity: Cell biological implications. Cell Calcium [Internet]. 2005;38(3):291–302. Available from: http://www.sciencedirect.com/science/article/pii/S014341600500120X

18. Gorski P a., Trieber C a., Larivière E, Schuermans M, Wuytack F, Young HS, et al. Transmembrane helix 11 is a genuine regulator of the endoplasmic reticulum Ca2+ pump and acts as a functional parallel of β-subunit on α-Na+,K+-ATPase. Journal of Biological Chemistry. 2012;287(24):19876–85.

19. Gélébart P, Martin V, Enouf J, Papp B. Identification of a new SERCA2 splice variant regulated during monocytic differentiation. Biochem Biophys Res Commun [Internet]. 2003;303(2):676–84. Available from: http://www.sciencedirect.com/science/article/pii/S0006291X03004054

20. Chemaly ER, Bobe R, Adnot S, Hajjar RJ, Lipskaia L. Sarco (Endo) Plasmic Reticulum Calcium Atpases (SERCA) Isoforms in the Normal and Diseased Cardiac, Vascular and Skeletal Muscle. 2013;

21. Sagara Y, Fernandez-Belda F, de Meis L, Inesi G. Characterization of the inhibition of intracellular Ca2+ transport ATPases by thapsigargin. Journal of Biological Chemistry [Internet]. 1992 Jun;267(18):12606–13. Available from: http://www.jbc.org/content/267/18/12606.abstract

22. Vandecaetsbeek I, Trekels M, de Maeyer M, Ceulemans H, Lescrinier E, Raeymaekers L, et al. Structural basis for the high Ca2+ affinity of the ubiquitous SERCA2b Ca2+ pump. Proc Natl Acad Sci U S A. 2009;106(20102):18533–8.

23. Reddy LG, Jones LR, Pace RC, Stokes DL. Purified, Reconstituted Cardiac Ca2+-ATPase Is Regulated by Phospholamban but Not by Direct Phosphorylation with Ca2+/Calmodulin-dependent Protein Kinase. Journal of Biological Chemistry [Internet]. 1996 Jun;271(25):14964–70. Available from: http://www.jbc.org/content/271/25/14964.abstract

24. Toyoshima C, Nakasako M, Nomura H, Ogawa H. Crystal structure of the calcium pump of sarcoplasmic reticulum at 2.6 A resolution. Nature. 2000;405(M):647–55.

25. Kühlbrandt W. Biology, structure and mechanism of P-type ATPases. Nat Rev Mol Cell Biol. 2004;5(April):282–95.

26. Apell HJ. How do P-Type ATPases transport ions? [cited 2022 Nov 4]; Available from: www.elsevier.com/locate/bioelechem

27. Toyoshima C. How Ca2+-ATPase pumps ions across the sarcoplasmic reticulum membrane. Biochimica et Biophysica Acta (BBA) - Molecular Cell Research [Internet]. 2009;1793(6):941–6. Available from: http://www.sciencedirect.com/science/article/pii/S0167488908003558

28. Kirchberber MA, Tada M, Katz AM. Phospholamban: a regulatory protein of the cardiac sarcoplasmic reticulum. Recent Adv Stud Cardiac Struct Metab. 1975;5:103–15.

29. Odermatt a, Becker S, Khanna VK, Kurzydlowski K, Leisner E, Pette D, et al. Sarcolipin regulates the activity of SERCA1, the fast-twitch skeletal muscle sarcoplasmic reticulum Ca2+-ATPase. J Biol Chem. 1998;273(20):12360–9.

30. Wawrzynow A, Theibert JL, Murphy C, Jona I, Martonosi A, Collins JH. Sarcolipin, the “proteolipid” of skeletal muscle sarcoplasmic reticulum, is a unique, amphipathic, 31-residue peptide. Arch Biochem Biophys. 1992 Nov;298(2):620–3.

31. Simmerman HKB, Collins JH, Theibert JL, Wegener a. D, Jones LR. Sequence analysis of phospholamban. Identification of phosphorylation sites and two major structural domains. Journal of Biological Chemistry. 1986;261(28):13333–41.

32. Stokes DL. Keeping Calcium in its Place: Ca2+ ATPase and Phospholamban. Curr Opin Struct Biol. 1997;7:550–6.

33. Anderson DM, Makarewich CA, Anderson KM, Shelton JM, Bezprozvannaya S, Bassel-Duby R, et al. Widespread control of calcium signaling by a family of SERCA-inhibiting micropeptides. Sci Signal [Internet]. 2016 Dec;9(457):ra119 LP-ra119. Available from: http://stke.sciencemag.org/content/9/457/ra119.abstract

34. Rathod N, Bak JJ, Primeau JO, Fisher ME, Espinoza-fonseca LM, Lemieux MJ, et al. Nothing regular about the regulins: Distinct functional properties of SERCA transmembrane peptide regulatory subunits. Int J Mol Sci [Internet]. 2021 Aug 2 [cited 2023 Mar 11];22(16):22. Available from: /pmc/articles/PMC8396278/

35. KATZ AM. Discovery of Phospholamban: A Personal History. Ann N Y Acad Sci [Internet]. 1998 Sep;853(1):9–19. Available from: https://doi.org/10.1111/j.1749-6632.1998.tb08252.x

36. Simmerman HKB, Collins JH, Theibert JL, Wegener AD, Jones LR. Sequence analysis of phospholamban. Identification of phosphorylation sites and two major structural domains. Journal of Biological Chemistry. 1986 Oct 5;261(28):13333–41.

37. Asahi M, Mckenna E, Kurzydlowski K, Tada M, Maclennan DH. Physical Interactions between Phospholamban and Sarco (endo) plasmic Reticulum Ca 2 ⁺ - ATPases Are Dissociated by Elevated Ca 2 ⁺ , but Not by Phospholamban Phosphorylation , Vanadate , or Thapsigargin , and Are Enhanced by ATP *. 2000;275(20):15034–8.

38. Kimura Y, Kurzydlowski K, Tada M, MacLennan DH. Phospholamban Inhibitory Function Is Activated by Depolymerization. Journal of Biological Chemistry [Internet].

1997 Jun;272(24):15061–4. Available from: http://www.jbc.org/content/272/24/15061.abstract

39. Tada M, Inui M, Yamada M, Kadoma M aki, Kuzuya T, Abe H, et al. Effects of phospholamban phosphorylation catalyzed by adenosine 3′:5′-monophosphate- and calmodulin-dependent protein kinases on calcium transport ATPase of cardiac sarcoplasmic reticulum. J Mol Cell Cardiol [Internet]. 1983;15(5):335–46. Available from: http://www.sciencedirect.com/science/article/pii/0022282883913457

40. Cornea RL, Jones LR, Autry JM, Thomas DD. Mutation and Phosphorylation Change the Oligomeric Structure of Phospholamban in Lipid Bilayers. Biochemistry [Internet]. 1997 Mar;36(10):2960–7. Available from: https://doi.org/10.1021/bi961955q

41. Chu G, Li L, Sato Y, Harrer JM, Kadambi VJ, Hoit BD, et al. Pentameric assembly of phospholamban facilitates inhibition of cardiac function in vivo. Journal of Biological Chemistry. 1998;273(50):33674–80.

42. Glaves JP, Trieber C a., Ceholski DK, Stokes DL, Young HS. Phosphorylation and mutation of phospholamban alter physical interactions with the sarcoplasmic reticulum calcium pump. J Mol Biol [Internet]. 2011;405(3):707–23. Available from: http://dx.doi.org/10.1016/j.jmb.2010.11.014

43. Stokes DL, Pomfret AJ, Rice WJ, Glaves JP, Young HS. Interactions between Ca2+-ATPase and the pentameric form of phospholamban in two-dimensional co-crystals. Biophys J. 2006;90(June):4213–23.

44. Tada M, Kirchberger MA, Katz AM. Regulation of calcium transport in cardiac sarcoplasmic reticulum by cyclic AMP-dependent protein kinase. Recent Adv Stud Cardiac Struct Metab. 1976;9:225–39.

45. Tada M, Kirchberger MA, Repke DI, Katz AM. The Stimulation of Calcium Transport in Cardiac Sarcoplasmic Reticulum by Adenosine 3':5'-Monophosphate-dependent Protein Kinase. Journal of Biological Chemistry [Internet]. 1974 Oct;249(19):6174–80. Available from: http://www.jbc.org/content/249/19/6174.abstract

46. Catalucci D, Latronico MVG, Ceci M, Rusconi F, Young HS, Gallo P, et al. Akt Increases Sarcoplasmic Reticulum Ca2+ Cycling by Direct Phosphorylation of Phospholamban at Thr17. Journal of Biological Chemistry [Internet]. 2009 Oct;284(41):28180–7. Available from: http://www.jbc.org/content/284/41/28180.abstract

47. Bartel S, Vetter D, Schlegel WP, Wallukat G, Krause EG, Karczewski P. Phosphorylation of Phospholamban at Threonine-17 in the Absence and Presence of β -Adrenergic Stimulation in Neonatal Rat Cardiomyocytes. J Mol Cell Cardiol [Internet]. 2000;32(12):2173–85. Available from: http://www.sciencedirect.com/science/article/pii/S0022282800912434

48. Haghighi K, Kolokathis F, Pater L, Lynch RA, Asahi M, Gramolini AO, et al. Human phospholamban null results in lethal dilated cardiomyopathy revealing a critical difference between mouse and human. J Clin Invest [Internet]. 2003 Mar;111(6):869–76. Available from: https://doi.org/10.1172/JCI17892

49. Landstrom AP, Adekola BA, Bos JM, Ommen SR, Ackerman MJ. PLN-encoded phospholamban mutation in a large cohort of hypertrophic cardiomyopathy cases: Summary of the literature and implications for genetic testing. Am Heart J [Internet]. 2011;161(1):165–71. Available from: http://www.sciencedirect.com/science/article/pii/S0002870310006757

50. Schmitt JP, Kamisago M, Asahi M, Li GH, Ahmad F, Mende U, et al. Dilated cardiomyopathy and heart failure caused by a mutation in phospholamban. Science. 2003;299(February):1410–3.

51. P. SJ, Ferhaan A, Kristina L, Lutz H, Stefan S, Michio A, et al. Alterations of Phospholamban Function Can Exhibit Cardiotoxic Effects Independent of Excessive Sarcoplasmic Reticulum Ca2+-ATPase Inhibition. Circulation [Internet]. 2009 Jan;119(3):436–44. Available from: https://doi.org/10.1161/CIRCULATIONAHA.108.783506

52. DeWitt MM, MacLeod HM, Soliven B, McNally EM. Phospholamban R14 Deletion Results in Late-Onset, Mild, Hereditary Dilated Cardiomyopathy. J Am Coll Cardiol [Internet]. 2006;48(7):1396–8. Available from: http://www.sciencedirect.com/science/article/pii/S0735109706018377

53. Haghighi K, Kolokathis F, Gramolini AO, Waggoner JR, Pater L, Lynch RA, et al. A mutation in the human phospholamban gene, deleting arginine 14, results in lethal, hereditary cardiomyopathy. Proceedings of the National Academy of Sciences [Internet]. 2006 Jan;103(5):1388 LP – 1393. Available from: http://www.pnas.org/content/103/5/1388.abstract

54. Toyofuku T, Kurzydlowski K, Tada M, MacLennan DH. Amino acids Glu2 to Ile18 in the cytoplasmic domain of phospholamban are essential for functional association with the Ca(2+)-ATPase of sarcoplasmic reticulum. Journal of Biological Chemistry [Internet]. 1994 Jan;269(4):3088–94. Available from: http://www.jbc.org/content/269/4/3088.abstract

55. Trieber CA, Afara M, Young HS. Effects of Phospholamban Transmembrane Mutants on the Calcium Affinity, Maximal Activity, and Cooperativity of the Sarcoplasmic Reticulum Calcium Pump. Biochemistry [Internet]. 2009 Oct;48(39):9287–96. Available from: https://doi.org/10.1021/bi900852m

56. Autry JM, Jones LR. Functional Co-expression of the Canine Cardiac Ca2+Pump and Phospholamban in Spodoptera frugiperda (Sf21) Cells Reveals New Insights on ATPase Regulation. Journal of Biological Chemistry [Internet]. 1997 Jun;272(25):15872–80. Available from: http://www.jbc.org/content/272/25/15872.abstract

57. Sugita Y, Miyashita N, Yoda T, Ikeguchi M, Toyoshima C. Structural changes in the cytoplasmic domain of phospholamban by phosphorylation at Ser16: A molecular dynamics study. Biochemistry. 2006 Oct 3;45(39):11752–61.

58. Gustavsson M, Verardi R, Mullen DG, Mote KR, Traaseth NJ, Gopinath T, et al. Allosteric regulation of SERCA by phosphorylation-mediated conformational shift of phospholamban. Proc Natl Acad Sci U S A [Internet]. 2013;110(43):17338–43. Available from: http://www.pubmedcentral.nih.gov/articlerender.fcgi?artid=3808617&tool=pmcentrez&rendertype=abstract

59. Karim CB, Zhang Z, Howard EC, Torgersen KD, Thomas DD. Phosphorylation-dependent conformational switch in spin-labeled phospholamban bound to SERCA. J Mol Biol [Internet]. 2006 May;358(4):1032–40. Available from: http://www.sciencedirect.com/science/article/pii/S0022283606002506

60. Ceholski DK, Trieber C a., Holmes CFB, Young HS. Lethal, hereditary mutants of phospholamban elude phosphorylation by protein kinase A. Journal of Biological Chemistry. 2012;287:26596–605.

61. Wittmann T, Lohse MJ, Schmitt JP. Phospholamban pentamers attenuate PKA-dependent phosphorylation of monomers. J Mol Cell Cardiol [Internet]. 2015 Jan;80C:90–7. Available from: http://www.sciencedirect.com/science/article/pii/S0022282814004325

62. Masterson LR, Cheng C, Yu T, Tonelli M, Kornev A, Taylor SS, et al. Dynamics connect substrate recognition to catalysis in protein kinase A. Nat Chem Biol [Internet]. 2010 Oct;6:821. Available from: https://doi.org/10.1038/nchembio.452

63. Kemp BE, Bylund DB, Huang TS, Krebs EG. Substrate specificity of the cyclic AMP-dependent protein kinase. Proc Natl Acad Sci U S A [Internet]. 1975 Sep;72(9):3448–52. Available from: https://www.ncbi.nlm.nih.gov/pubmed/1059131

64. MACDOUGALL LK, JONES LR, COHEN P. Identification of the major protein phosphatases in mammalian cardiac muscle which dephosphorylate phospholamban. Eur J Biochem [Internet]. 1991 Mar;196(3):725–34. Available from: https://doi.org/10.1111/j.1432-1033.1991.tb15871.x

65. Steenaart NAE, Ganim JR, Di Salvo J, Kranias EG. The phospholamban phosphatase associated with cardiac sarcoplasmic reticulum is a type 1 enzyme. Arch Biochem Biophys [Internet]. 1992;293(1):17–24. Available from: http://www.sciencedirect.com/science/article/pii/0003986192903595

66. Winther AML, Bublitz M, Karlsen JL, Møller J V, Hansen JB, Nissen P, et al. The sarcolipin-bound calcium pump stabilizes calcium sites exposed to the cytoplasm. Nature [Internet]. 2013;495(7440):265–9. Available from: http://www.ncbi.nlm.nih.gov/pubmed/23455424

67. Toyoshima C, Iwasawa S, Ogawa H, Hirata A, Tsueda J, Inesi G. Crystal structures of the calcium pump and sarcolipin in the Mg2+-bound E1 state. Nature [Internet]. 2013 Mar;495:260. Available from: https://doi.org/10.1038/nature11899

68. Gorski PA, Glaves JP, Vangheluwe P, Young HS. Sarco(endo)plasmic Reticulum Calcium ATPase (SERCA) Inhibition by Sarcolipin Is Encoded in Its Luminal Tail. Journal of Biological Chemistry [Internet]. 2013 Mar;288(12):8456–67. Available from: http://www.jbc.org/content/288/12/8456.abstract

69. Sahoo SK, Shaikh S a., Sopariwala DH, Bal NC, Periasamy M. Sarcolipin protein interaction with Sarco(endo)plasmic reticulum CA 2+ ATPase (SERCA) Is distinct from phospholamban protein,and only sarcolipin can promote uncoupling of the serca pump. Journal of Biological Chemistry. 2013;288:6881–9.

70. Reddy LG, Cornea RL, Winters DL, McKenna E, Thomas DD. Defining the Molecular Components of Calcium Transport Regulation in a Reconstituted Membrane System.

Biochemistry [Internet]. 2003 Apr;42(15):4585–92. Available from: https://doi.org/10.1021/bi026995a

71. Ceholski DK, Trieber C a., Young HS. Hydrophobic imbalance in the cytoplasmic domain of phospholamban is a determinant for lethal dilated cardiomyopathy. Journal of Biological Chemistry. 2012;287(20):16521–9.

72. Trieber CA, Douglas JL, Afara M, Young HS. The Effects of Mutation on the Regulatory Properties of Phospholamban in Co-Reconstituted Membranes†. Biochemistry [Internet]. 2005 Mar;44(9):3289–97. Available from: http://dx.doi.org/10.1021/bi047878d

73. Bal NC, Maurya SK, Sopariwala DH, Sahoo SK, Gupta SC, Shaikh S a, et al. Sarcolipin is a newly identified regulator of muscle-based thermogenesis in mammals. Nat Med [Internet]. 2012;18(10):1575–9. Available from: http://dx.doi.org/10.1038/nm.2897

74. Pant M, Bal NC, Periasamy M. Sarcolipin: A Key Thermogenic and Metabolic Regulator in Skeletal Muscle. Trends in Endocrinology and Metabolism. 2016.

75. Campbell KL, Dicke AA. Sarcolipin Makes Heat, but Is It Adaptive Thermogenesis? Front Physiol [Internet]. 2018 Jun;9:714. Available from: https://www.ncbi.nlm.nih.gov/pubmed/29962960

76. Bal NC, Sahoo SK, Maurya SK, Periasamy M. The Role of Sarcolipin in Muscle Non-shivering Thermogenesis [Internet]. Vol. 9, Frontiers in Physiology. 2018. p. 1217. Available from: https://www.frontiersin.org/article/10.3389/fphys.2018.01217

77. Gamu D, Bombardier E, Smith IC, Fajardo VA, Tupling AR. Sarcolipin Provides a Novel Muscle-Based Mechanism for Adaptive Thermogenesis. Exerc Sport Sci Rev. 2014;42(3):136–42.

78. Bal NC, Maurya SK, Sopariwala DH, Sahoo SK, Gupta SC, Shaikh S a, et al. Sarcolipin is a newly identified regulator of muscle-based thermogenesis in mammals. Nat Med [Internet]. 2012;18(10):1575–9. Available from: http://dx.doi.org/10.1038/nm.2897

79. MacLennan DH, Asahi M, Tupling AR. The regulation of SERCA-type pumps by phospholamban and sarcolipin. Ann N Y Acad Sci. 2003 Apr;986:472–80.

80. Bhupathy P, Babu GJ, Ito M, Periasamy M. Threonine-5 at the N-terminus can modulate sarcolipin function in cardiac myocytes. J Mol Cell Cardiol [Internet]. 2009;47(5):723–9. Available from: http://dx.doi.org/10.1016/j.yjmcc.2009.07.014

81. Magny EG, Pueyo JI, Pearl FMG, Cespedes M a., Niven JE, Bishop S a., et al. Conserved Regulation of Cardiac Calcium Uptake by Peptides Encoded in Small Open Reading Frames. Science (1979) [Internet]. 2013;341:1116–20. Available from: http://www.sciencemag.org/cgi/doi/10.1126/science.1238802

82. Nelson BR, Catherine A. Makarewich Benjamin R. Winders Constantine D. Troupes Fenfen Wu DMA, Reese AL, McAnally JR, Chen X, Kavalali ET, et al. A peptide encoded by a transcript annotated as long noncoding RNA enhances SERCA activity in muscle. Science (1979). 2016;351(6270).

83. Anderson DM, Anderson KM, Bassel-duby R, Olson EN, Mcanally JR, Kasaragod P, et al. A Micropeptide Encoded by a Putative Long Noncoding RNA Regulates Muscle Performance Article A Micropeptide Encoded by a Putative Long Noncoding RNA

Regulates Muscle Performance. Cell [Internet]. 2015;160:1–12. Available from: http://dx.doi.org/10.1016/j.cell.2015.01.009

84. Magny EG, Pueyo JI, Pearl FMG, Cespedes MA, Niven JE, Bishop SA, et al. Conserved regulation of cardiac calcium uptake by peptides encoded in small open reading frames. Science [Internet]. 2013 [cited 2023 Mar 11];341(6150):1116–20. Available from: https://pubmed.ncbi.nlm.nih.gov/23970561/

Chapter 2 Works Cited

1. Roger VL. The Heart Failure Epidemic. International Journal of Environmental Research and Public Health 2010, Vol 7, Pages 1807-1830 [Internet]. 2010 Apr 19 [cited 2022 Oct 5];7(4):1807–30. Available from: https://www.mdpi.com/1660-4601/7/4/1807/htm

2. Towbin JA, Bowles NE. Molecular diagnosis of myocardial disease. Expert Rev Mol Diagn [Internet]. 2002 Nov [cited 2022 Oct 5];2(6):587–602. Available from: https://pubmed.ncbi.nlm.nih.gov/12465455/

3. Kimura A. Molecular etiology and pathogenesis of hereditary cardiomyopathy. Circ J [Internet]. 2008 [cited 2022 Oct 5];72 Suppl A(SUPPL. A). Available from: https://pubmed.ncbi.nlm.nih.gov/18772524/

4. te Rijdt WP, van der Klooster ZJ, Hoorntje ET, Jongbloed JDH, van der Zwaag PA, Asselbergs FW, et al. Phospholamban immunostaining is a highly sensitive and specific

method for diagnosing phospholamban p.Arg14del cardiomyopathy. Cardiovasc Pathol [Internet]. 2017 Sep 1 [cited 2022 Oct 5];30:23–6. Available from: https://pubmed.ncbi.nlm.nih.gov/28759816/

5. te Rijdt WP, van Tintelen JP, Vink A, van der Wal AC, de Boer RA, van den Berg MP, et al. Phospholamban p.Arg14del cardiomyopathy is characterized by phospholamban aggregates, aggresomes, and autophagic degradation. Histopathology [Internet]. 2016 Oct 1 [cited 2022 Oct 5];69(4):542–50. Available from: https://pubmed.ncbi.nlm.nih.gov/26970417/

6. te Rijdt WP, ten Sande JN, Gorter TM, van der Zwaag PA, van Rijsingen IA, Boekholdt SM, et al. Myocardial fibrosis as an early feature in phospholamban p.Arg14del mutation carriers: phenotypic insights from cardiovascular magnetic resonance imaging. Eur Heart J Cardiovasc Imaging [Internet]. 2019 Jan 1 [cited 2022 Oct 5];20(1):92–100. Available from: https://pubmed.ncbi.nlm.nih.gov/29635323/

7. van Rijsingen IAW, van der Zwaag PA, Groeneweg JA, Nannenberg EA, Jongbloed JDH, Zwinderman AH, et al. Outcome in phospholamban R14del carriers: results of a large multicentre cohort study. Circ Cardiovasc Genet [Internet]. 2014 Aug 1 [cited 2022 Oct 5];7(4):455–65. Available from: https://pubmed.ncbi.nlm.nih.gov/24909667/

8. van der Zwaag PA, van Rijsingen IAW, Asimaki A, Jongbloed JDH, van Veldhuisen DJ, Wiesfeld ACP, et al. Phospholamban R14del mutation in patients diagnosed with dilated cardiomyopathy or arrhythmogenic right ventricular cardiomyopathy: evidence supporting the concept of arrhythmogenic cardiomyopathy. Eur J Heart Fail [Internet]. 2012 Nov [cited 2022 Sep 30];14(11):1199–207. Available from: https://pubmed.ncbi.nlm.nih.gov/22820313/

9. Posch MG, Perrot A, Geier C, Boldt LH, Schmidt G, Lehmkuhl HB, et al. Genetic deletion of arginine 14 in phospholamban causes dilated cardiomyopathy with attenuated electrocardiographic R amplitudes. Heart Rhythm [Internet]. 2009 Jan 18 [cited 2022 Oct 2];6(4):480–6. Available from: http://europepmc.org/article/MED/19324307

10. DeWitt MM, MacLeod HM, Soliven B, McNally EM. Phospholamban R14 Deletion Results in Late-Onset, Mild, Hereditary Dilated Cardiomyopathy. J Am Coll Cardiol [Internet]. 2006;48(7):1396–8. Available from: http://www.sciencedirect.com/science/article/pii/S0735109706018377

11. Haghighi K, Kolokathis F, Gramolini AO, Waggoner JR, Pater L, Lynch RA, et al. A mutation in the human phospholamban gene, deleting arginine 14, results in lethal, hereditary cardiomyopathy. Proceedings of the National Academy of Sciences [Internet]. 2006 Jan;103(5):1388 LP – 1393. Available from: http://www.pnas.org/content/103/5/1388.abstract

12. Ha KN, Mastersona LR, Hou Z, Verardi R, Walsh N, Veglia G, et al. Lethal Arg9Cys phospholamban mutation hinders Ca2+-ATPase regulation and phosphorylation by protein kinase A. Proc Natl Acad Sci U S A [Internet]. 2011 Feb 15 [cited 2022 Oct 5];108(7):2735–40. Available from: https://www.pnas.org/doi/abs/10.1073/pnas.1013987108

13. Schmitt JP, Kamisago M, Asahi M, Li GH, Ahmad F, Mende U, et al. Dilated cardiomyopathy and heart failure caused by a mutation in phospholamban. Science. 2003;299(February):1410–3.

14. Pugh TJ, Kelly MA, Gowrisankar S, Hynes E, Seidman MA, Baxter SM, et al. The landscape of genetic variation in dilated cardiomyopathy as surveyed by clinical DNA sequencing. Genetics in Medicine. 2014;16(8):601–8.

15. Landstrom AP, Adekola BA, Bos JM, Ommen SR, Ackerman MJ. PLN-encoded phospholamban mutation in a large cohort of hypertrophic cardiomyopathy cases: Summary of the literature and implications for genetic testing. Am Heart J [Internet]. 2011;161(1):165–71. Available from: http://www.sciencedirect.com/science/article/pii/S0002870310006757

16. Chiu C, Tebo M, Ingles J, Yeates L, Arthur JW, Lind JM, et al. Genetic screening of calcium regulation genes in familial hypertrophic cardiomyopathy. J Mol Cell Cardiol. 2007 Sep 1;43(3):337–43.

17. Mollanoori H, Naderi N, Amin A, Hassani B, Shahraki H, Teimourian S. A novel human T17N-phospholamban variation in idiopathic dilated cardiomyopathy. Gene Rep [Internet]. 2018;12(June):122–7. Available from: https://doi.org/10.1016/j.genrep.2018.06.014

18. Haghighi K, Kolokathis F, Pater L, Lynch RA, Asahi M, Gramolini AO, et al. Human phospholamban null results in lethal dilated cardiomyopathy revealing a critical difference between mouse and human. J Clin Invest [Internet]. 2003 Mar;111(6):869–76. Available from: https://doi.org/10.1172/JCI17892

19. Medeiros A, Biagi DG, Sobreira TJP, de Oliveira PSL, Negrão CE, Mansur AJ, et al. Mutations in the human phospholamban gene in patients with heart failure. Am Heart J

[Internet]. 2011;162(6):1088-1095.e1. Available from: http://dx.doi.org/10.1016/j.ahj.2011.07.028

20. Kimura Y, Kurzydlowski K, Tada M, MacLennan DH. Phospholamban Inhibitory Function Is Activated by Depolymerization. Journal of Biological Chemistry [Internet]. 1997 Jun;272(24):15061–4. Available from: http://www.jbc.org/content/272/24/15061.abstract

21. Simmerman HKB, Jones LR. Phospholamban: Protein structure, mechanism of action, and role in cardiac function. Physiol Rev [Internet]. 1998 [cited 2022 Oct 1];78(4):921–47. Available from: https://journals.physiology.org/doi/10.1152/physrev.1998.78.4.921

22. Robia SL, Campbell KS, Kelly EM, Hou Z, Winters DL, Thomas DD. Förster Transfer Recovery Reveals That Phospholamban Exchanges Slowly From Pentamers but Rapidly From the SERCA Regulatory Complex. Circ Res [Internet]. 2007 Nov;101(11):1123–9. Available from: https://www.ahajournals.org/doi/10.1161/CIRCRESAHA.107.159947

23. Karim CB, Stamm JD, Karim J, Jones LR, Thomas DD. Cysteine Reactivity and Oligomeric Structures of Phospholamban and Its Mutants†. Biochemistry [Internet]. 1998 Sep 1 [cited 2022 Oct 5];37(35):12074–81. Available from: https://pubs.acs.org/doi/abs/10.1021/bi980642n

24. Zvaritch E, Backx PH, Jirik F, Kimura Y, de Leon S, Schmidt AG, et al. The transgenic expression of highly inhibitory monomeric forms of phospholamban in mouse heart impairs cardiac contractility. J Biol Chem [Internet]. 2000 May 19 [cited 2022 Oct 5];275(20):14985–91. Available from: https://pubmed.ncbi.nlm.nih.gov/10809743/

25. Bluhm WF, Kranias EG, Dillmann WH, Meyer M. Phospholamban: A major determinant of the cardiac force-frequency relationship. Am J Physiol Heart Circ Physiol [Internet]. 2000 [cited 2022 Oct 10];278(1 47-1). Available from: https://journals.physiology.org/doi/10.1152/ajpheart.2000.278.1.H249

26. Haghighi K, Schmidt AG, Hoit BD, Brittsan AG, Yatani A, Lester JW, et al. Superinhibition of sarcoplasmic reticulum function by phospholamban induces cardiac contractile failure. J Biol Chem [Internet]. 2001 Jun 29 [cited 2022 Oct 10];276(26):24145–52. Available from: https://pubmed.ncbi.nlm.nih.gov/11328820/

27. MacLennan DH, Kranias EG. Phospholamban: a crucial regulator of cardiac contractility. Nat Rev Mol Cell Biol [Internet]. 2003 Jul;4(7):566–77. Available from: http://www.nature.com/articles/nrm1151

28. Kranias EG, Hajjar RJ. Modulation of cardiac contractility by the phopholamban/SERCA2a regulatome. Circ Res. 2012;110(12):1646–60.

29. Park WJ, Oh JG. SERCA2a: a prime target for modulation of cardiac contractility during heart failure. BMB Rep [Internet]. 2013 [cited 2022 Oct 10];46(5):237–43. Available from: https://pubmed.ncbi.nlm.nih.gov/23710633/

30. Zamoon J, Mascioni A, Thomas DD, Veglia G. NMR Solution Structure and Topological Orientation of Monomeric Phospholamban in Dodecylphosphocholine Micelles. Biophys J [Internet]. 2003 Oct 1 [cited 2022 Oct 10];85(4):2589. Available from: /pmc/articles/PMC1303482/

31. Verardi R, Shi L, Traaseth NJ, Walsh N, Veglia G. Structural topology of phospholamban pentamer in lipid bilayers by a hybrid solution and solid-state NMR

method. Proc Natl Acad Sci U S A [Internet]. 2011 May 31 [cited 2022 Oct 1];108(22):9101–6. Available from: https://www.pnas.org/doi/abs/10.1073/pnas.1016535108

32. Kimura Y, Kurzydlowski K, Tada M, MacLennan DH. Phospholamban regulates the Ca2+-ATPase through intramembrane interactions. J Biol Chem [Internet]. 1996 [cited 2022 Oct 10];271(36):21726–31. Available from: https://pubmed.ncbi.nlm.nih.gov/8702967/

33. Simmerman HKB, Kobayashi YM, Autry JM, Jones LR. A leucine zipper stabilizes the pentameric membrane domain of phospholamban and forms a coiled-coil pore structure. Journal of Biological Chemistry. 1996;271(10):5941–6.

34. Fujii J, Maruyama K, Tada M, MacLennan DH. Expression and Site-specific Mutagenesis of Phospholamban: Studies of Residues Involved in Phosphorylation and Pentamer Formation. Journal of Biological Chemistry. 1989 Aug 5;264(22):12950–5.

35. Kelly EM, Hou Z, Bossuyt J, Bers DM, Robia SL. Phospholamban oligomerization, quaternary structure, and sarco(endo)plasmic reticulum calcium ATPase binding measured by fluorescence resonance energy transfer in living cells. Journal of Biological Chemistry. 2008;283:12202–11.

36. Trieber CA, Afara M, Young HS. Effects of Phospholamban Transmembrane Mutants on the Calcium Affinity, Maximal Activity, and Cooperativity of the Sarcoplasmic Reticulum Calcium Pump. Biochemistry [Internet]. 2009 Oct;48(39):9287–96. Available from: https://doi.org/10.1021/bi900852m

37. Ceholski DK, Trieber C a., Young HS. Hydrophobic imbalance in the cytoplasmic domain of phospholamban is a determinant for lethal dilated cardiomyopathy. Journal of Biological Chemistry. 2012;287(20):16521–9.

38. Hou Z, Kelly EM, Robia SL. Phosphomimetic Mutations Increase Phospholamban Oligomerization and Alter the Structure of Its Regulatory Complex. Journal of Biological Chemistry [Internet]. 2008 Oct;283(43):28996–9003. Available from: http://www.jbc.org/lookup/doi/10.1074/jbc.M804782200

39. Butler J, Lee AG, Wilson DI, Spalluto C, Hanley NA, East JM. Phospholamban and sarcolipin are maintained in the endoplasmic reticulum by retrieval from the ER-Golgi intermediate compartment. Cardiovasc Res [Internet]. 2007 Apr 1 [cited 2022 Oct 10];74(1):114–23. Available from: https://pubmed.ncbi.nlm.nih.gov/17307155/

40. Gramolini AO, Kislinger T, Asahi M, Li W, Emili A, MacLennan DH. Sarcolipin retention in the endoplasmic reticulum depends on its C-terminal RSYQY sequence and its interaction with sarco(endo)plasmic Ca(2+)-ATPases. Proc Natl Acad Sci U S A [Internet]. 2004 Nov 30 [cited 2022 Oct 10];101(48):16807–12. Available from: https://pubmed.ncbi.nlm.nih.gov/15556994/

41. Gorski PA, Glaves JP, Vangheluwe P, Young HS. Sarco(endo)plasmic Reticulum Calcium ATPase (SERCA) Inhibition by Sarcolipin Is Encoded in Its Luminal Tail. Journal of Biological Chemistry [Internet]. 2013 Mar;288(12):8456–67. Available from: http://www.jbc.org/content/288/12/8456.abstract

42. Abrol N, Smolin N, Armanious G, Ceholski DK, Trieber CA, Young HS, et al. Phospholamban C-terminal Residues Are Critical Determinants of the Structure and

Function of the Calcium ATPase Regulatory Complex. J Biol Chem [Internet]. 2014 Sep 9 [cited 2022 Oct 12];289(37):25855. Available from: /pmc/articles/PMC4162186/

43. Karim CB, Zhang Z, Howard EC, Torgersen KD, Thomas DD. Phosphorylation-dependent conformational switch in spin-labeled phospholamban bound to SERCA. J Mol Biol [Internet]. 2006 May;358(4):1032–40. Available from: http://www.sciencedirect.com/science/article/pii/S0022283606002506

44. Traaseth NJ, Thomas DD, Veglia G. Effects of Ser16 phosphorylation on the allosteric transitions of phospholamban/Ca(2+)-ATPase complex. J Mol Biol [Internet]. 2006 May 12 [cited 2022 Oct 12];358(4):1041–50. Available from: https://pubmed.ncbi.nlm.nih.gov/16564056/

45. Stenoien DL, Knyushko T v., Londono MP, Opresko LK, Mayer MU, Brady ST, et al. Cellular trafficking of phospholamban and formation of functional sarcoplasmic reticulum during myocyte differentiation. Am J Physiol Cell Physiol [Internet]. 2007 Jun [cited 2022 Oct 12];292(6). Available from: https://pubmed.ncbi.nlm.nih.gov/17287364/

46. Pallikkuth S, Blackwell DJ, Hu Z, Hou Z, Zieman DT, Svensson B, et al. Phosphorylated phospholamban stabilizes a compact conformation of the cardiac calcium-ATPase. Biophys J [Internet]. 2013;105(8):1812–21. Available from: http://dx.doi.org/10.1016/j.bpj.2013.08.045

47. Bidwell P, Blackwell DJ, Hou Z, Zima A v, Robia SL. Phospholamban Binds with Differential Affinity to Calcium Pump Conformers. Journal of Biological Chemistry [Internet]. 2011 Oct;286(40):35044–50. Available from: http://www.jbc.org/content/286/40/35044.abstract

48. Mueller B, Karim CB, Negrashov I v, Kutchai H, Thomas DD. Direct Detection of Phospholamban and Sarcoplasmic Reticulum Ca-ATPase Interaction in Membranes Using Fluorescence Resonance Energy Transfer. Biochemistry [Internet]. 2004 Jul;43(27):8754–65. Available from: https://doi.org/10.1021/bi049732k

49. Li J, Bigelow DJ, Squier TC. Conformational Changes within the Cytosolic Portion of Phospholamban upon Release of Ca-ATPase Inhibition. Biochemistry [Internet]. 2004 Apr;43(13):3870–9. Available from: https://doi.org/10.1021/bi036183u

50. Li J, Bigelow DJ, Squier TC. Conformational Changes within the Cytosolic Portion of Phospholamban upon Release of Ca-ATPase Inhibition†. Biochemistry [Internet]. 2004 Apr 6 [cited 2022 Oct 12];43(13):3870–9. Available from: https://pubs.acs.org/doi/abs/10.1021/bi036183u

51. Akin BL, Hurley TD, Chen Z, Jones LR. The structural basis for phospholamban inhibition of the calcium pump in sarcoplasmic reticulum. Journal of Biological Chemistry. 2013;288(42):30181–91.

52. Chen Z, Akin BL, Stokes DL, Jones LR. Cross-linking of C-terminal residues of phospholamban to the Ca 2+ pump of cardiac sarcoplasmic reticulum to probe spatial and functional interactions within the transmembrane domain. Journal of Biological Chemistry. 2006;281(20):14163–72.

53. Trieber CA, Douglas JL, Afara M, Young HS. The Effects of Mutation on the Regulatory Properties of Phospholamban in Co-Reconstituted Membranes†. Biochemistry [Internet]. 2005 Mar;44(9):3289–97. Available from: http://dx.doi.org/10.1021/bi047878d

54. Eletr S, Inesi G. Phospholipid orientation in sarcoplasmic membranes: spin-label ESR and proton MNR studies. Biochim Biophys Acta. 1972 Sep;282(1):174–9.

55. Stokes DL, Green NM. Three-dimensional crystals of CaATPase from sarcoplasmic reticulum. Symmetry and molecular packing. Biophys J. 1990;57(January):1–14.

56. Young HS, Jones LR, Stokes DL. Locating phospholamban in co-crystals with Ca(2+)-ATPase by cryoelectron microscopy. Biophys J. 2001;81(May):884–94.

57. Young HS, Rigaud JL, Lacapère JJ, Reddy LG, Stokes DL. How to make tubular crystals by reconstitution of detergent-solubilized Ca2(+)-ATPase. Biophys J [Internet]. 1997;72(6):2545–58. Available from: http://www.sciencedirect.com/science/article/pii/S0006349597788982

58. Warren GB, Toon P a, Birdsall NJ, Lee a G, Metcalfe JC. Reconstitution of a calcium pump using defined membrane components. Proc Natl Acad Sci U S A. 1974;71(3):622–6.

Chapter 3 Works Cited

1. Smeazzetto S, Armanious GP, Moncelli MR, Bak JJ, Lemieux MJ, Young HS, et al. Conformational memory in the association of the transmembrane protein phospholamban with the sarcoplasmic reticulum calcium pump SERCA. Journal of Biological Chemistry. 2017;292(52):21330–9.

2. Toyoshima C. How Ca2+-ATPase pumps ions across the sarcoplasmic reticulum membrane. Biochimica et Biophysica Acta (BBA) - Molecular Cell Research [Internet].

2009;1793(6):941–6. Available from: http://www.sciencedirect.com/science/article/pii/S0167488908003558

3. Toyoshima C, Cornelius F. New crystal structures of PII-type ATPases: excitement continues. Curr Opin Struct Biol [Internet]. 2013 Aug [cited 2022 Oct 17];23(4):507–14. Available from: https://pubmed.ncbi.nlm.nih.gov/23871101/

4. Møller J v, Olesen C, Winther AML, Nissen P. The sarcoplasmic Ca2+-ATPase: design of a perfect chemi-osmotic pump. Q Rev Biophys [Internet]. 2010;43(4):501–66. Available from: https://www.cambridge.org/core/product/712917B2C432A2C19D12749FF667D772

5. de Meis L, Vianna AL. Energy interconversion by the Ca2+-dependent ATPase of the sarcoplasmic reticulum. Annu Rev Biochem. 1979;48:275–92.

6. Jones LR, Cornea RL, Chen Z. Close proximity between residue 30 of phospholamban and cysteine 318 of the cardiac Ca2+ pump revealed by intermolecular thiol cross-linking. Journal of Biological Chemistry. 2002;277:28319–29.

7. Toyoshima C, Asahi M, Sugita Y, Khanna R, Tsuda T, MacLennan DH. Modeling of the inhibitory interaction of phospholamban with the Ca2+ ATPase. Proc Natl Acad Sci U S A. 2003;100:467–72.

8. Seidel K, Andronesi OC, Krebs J, Griesinger C, Young HS, Becker S, et al. Structural Characterization of Ca2+-ATPase-Bound Phospholamban in Lipid Bilayers by Solid-State Nuclear Magnetic Resonance (NMR) Spectroscopy,. Biochemistry [Internet]. 2008 Apr;47(15):4369–76. Available from: https://doi.org/10.1021/bi7024194

9. Gustavsson M, Traaseth NJ, Veglia G. ACTIVATING AND DEACTIVATING ROLES OF LIPID BILAYERS ON THE CA2+-ATPASE/PHOSPHOLAMBAN COMPLEX. Biochemistry [Internet]. 2011 Nov 11 [cited 2022 Oct 21];50(47):10367. Available from: /pmc/articles/PMC3487395/

10. Winther AML, Bublitz M, Karlsen JL, Møller J V, Hansen JB, Nissen P, et al. The sarcolipin-bound calcium pump stabilizes calcium sites exposed to the cytoplasm. Nature [Internet]. 2013;495(7440):265–9. Available from: http://www.ncbi.nlm.nih.gov/pubmed/23455424

11. Toyoshima C, Iwasawa S, Ogawa H, Hirata A, Tsueda J, Inesi G. Crystal structures of the calcium pump and sarcolipin in the Mg2+-bound E1 state. Nature [Internet]. 2013 Mar;495:260. Available from: https://doi.org/10.1038/nature11899

12. Akin BL, Hurley TD, Chen Z, Jones LR. The structural basis for phospholamban inhibition of the calcium pump in sarcoplasmic reticulum. Journal of Biological Chemistry. 2013;288(42):30181–91.

13. Tada M, Kirchberger MA, Katz AM. Regulation of calcium transport in cardiac sarcoplasmic reticulum by cyclic AMP-dependent protein kinase. Recent Adv Stud Cardiac Struct Metab. 1976;9:225–39.

14. Bilezikjian LM, Kranias EG, Potter JD, Schwartz A. Studies on phosphorylation of canine cardiac sarcoplasmic reticulum by calmodulin-dependent protein kinase. Circ Res [Internet]. 1981 [cited 2022 Oct 21];49(6):1356–62. Available from: https://pubmed.ncbi.nlm.nih.gov/6273007/

15. Chu G, Li L, Sato Y, Harrer JM, Kadambi VJ, Hoit BD, et al. Pentameric assembly of phospholamban facilitates inhibition of cardiac function in vivo. Journal of Biological Chemistry. 1998;273(50):33674–80.

16. Glaves JP, Trieber C a., Ceholski DK, Stokes DL, Young HS. Phosphorylation and mutation of phospholamban alter physical interactions with the sarcoplasmic reticulum calcium pump. J Mol Biol [Internet]. 2011;405(3):707–23. Available from: http://dx.doi.org/10.1016/j.jmb.2010.11.014

17. Bidwell P, Blackwell DJ, Hou Z, Zima A v, Robia SL. Phospholamban Binds with Differential Affinity to Calcium Pump Conformers. Journal of Biological Chemistry [Internet]. 2011 Oct;286(40):35044–50. Available from: http://www.jbc.org/content/286/40/35044.abstract

18. Li J, James ZM, Dong X, Karim CB, Thomas DD. Structural and Functional Dynamics of an Integral Membrane Protein Complex Modulated by Lipid Headgroup Charge. J Mol Biol [Internet]. 2012 May 5 [cited 2022 Oct 21];418(5):379. Available from: /pmc/articles/PMC3327772/

19. Gustavsson M, Verardi R, Mullen DG, Mote KR, Traaseth NJ, Gopinath T, et al. Allosteric regulation of SERCA by phosphorylation-mediated conformational shift of phospholamban. Proc Natl Acad Sci U S A [Internet]. 2013;110(43):17338–43. Available from: http://www.pubmedcentral.nih.gov/articlerender.fcgi?artid=3808617&tool=pmcentrez&rendertype=abstract

20. Trieber CA, Afara M, Young HS. Effects of Phospholamban Transmembrane Mutants on the Calcium Affinity, Maximal Activity, and Cooperativity of the Sarcoplasmic Reticulum Calcium Pump. Biochemistry [Internet]. 2009 Oct;48(39):9287–96. Available from: https://doi.org/10.1021/bi900852m

21. Ceholski DK, Trieber C a., Young HS. Hydrophobic imbalance in the cytoplasmic domain of phospholamban is a determinant for lethal dilated cardiomyopathy. Journal of Biological Chemistry. 2012;287(20):16521–9.

22. Schörner M, Beyer SR, Southall J, Cogdell RJ, Köhler J. Conformational Memory of a Protein Revealed by Single-Molecule Spectroscopy. Journal of Physical Chemistry B. 2015;119(44):13964–70.

23. Trieber CA, Douglas JL, Afara M, Young HS. The Effects of Mutation on the Regulatory Properties of Phospholamban in Co-Reconstituted Membranes†. Biochemistry [Internet]. 2005 Mar;44(9):3289–97. Available from: http://dx.doi.org/10.1021/bi047878d

24. Toyoshima C, Nomura H. Structural changes in the calcium pump accompanying the dissociation of calcium. Nature. 2002 Aug;418(6898):605–11.

25. Toyoshima C, Nakasako M, Nomura H, Ogawa H. Crystal structure of the calcium pump of sarcoplasmic reticulum at 2.6 A resolution. Nature. 2000;405(M):647–55.

26. Toyoshima C, Yonekura SI, Tsueda J, Iwasawa S. Trinitrophenyl derivatives bind differently from parent adenine nucleotides to Ca2+-ATPase in the absence of Ca2+. Proc Natl Acad Sci U S A [Internet]. 2011/01/14. 2011 Feb;108(5):1833–8. Available from: https://www.ncbi.nlm.nih.gov/pubmed/21239683

27. Blackwell DJ, Zak TJ, Robia SL. Cardiac Calcium ATPase Dimerization Measured by Cross-Linking and Fluorescence Energy Transfer. Biophys J [Internet]. 2016;111(6):1192–202. Available from: http://www.sciencedirect.com/science/article/pii/S0006349516306622

28. Douglas JL, Trieber C a., Afara M, Young HS. Rapid, high-yield expression and purification of Ca2+-ATPase regulatory proteins for high-resolution structural studies. Protein Expr Purif [Internet]. 2005 Mar;40(1):118–25. Available from: http://www.sciencedirect.com/science/article/pii/S1046592804004036

29. Eletr S, Inesi G. Phospholipid orientation in sarcoplasmic membranes: spin-label ESR and proton MNR studies. Biochim Biophys Acta. 1972 Sep;282(1):174–9.

30. Stokes DL, Green NM. Three-dimensional crystals of CaATPase from sarcoplasmic reticulum. Symmetry and molecular packing. Biophys J. 1990;57(January):1–14.

31. Gorski PA, Glaves JP, Vangheluwe P, Young HS. Sarco(endo)plasmic Reticulum Calcium ATPase (SERCA) Inhibition by Sarcolipin Is Encoded in Its Luminal Tail. Journal of Biological Chemistry [Internet]. 2013 Mar;288(12):8456–67. Available from: http://www.jbc.org/content/288/12/8456.abstract

32. Young HS, Jones LR, Stokes DL. Locating phospholamban in co-crystals with Ca(2+)-ATPase by cryoelectron microscopy. Biophys J. 2001;81(May):884–94.

33. Warren GB, Toon P a, Birdsall NJ, Lee a G, Metcalfe JC. Reconstitution of a calcium pump using defined membrane components. Proc Natl Acad Sci U S A. 1974;71(3):622–6.

Chapter 4 Works Cited

1. Haghighi K, Bidwell P, Kranias EG. Phospholamban interactome in cardiac contractility and survival: A new vision of an old friend. J Mol Cell Cardiol [Internet]. 2014;77:160–7. Available from: http://linkinghub.elsevier.com/retrieve/pii/S0022282814003253

2. van der Zwaag PA, van Rijsingen IAW, Asimaki A, Jongbloed JDH, van Veldhuisen DJ, Wiesfeld ACP, et al. Phospholamban R14del mutation in patients diagnosed with dilated cardiomyopathy or arrhythmogenic right ventricular cardiomyopathy: evidence supporting the concept of arrhythmogenic cardiomyopathy. Eur J Heart Fail [Internet]. 2012 Nov [cited 2022 Sep 30];14(11):1199–207. Available from: https://pubmed.ncbi.nlm.nih.gov/22820313/

3. Schmitt JP, Kamisago M, Asahi M, Li GH, Ahmad F, Mende U, et al. Dilated cardiomyopathy and heart failure caused by a mutation in phospholamban. Science. 2003;299(February):1410–3.

4. Haghighi K, Kolokathis F, Gramolini AO, Waggoner JR, Pater L, Lynch RA, et al. A mutation in the human phospholamban gene, deleting arginine 14, results in lethal, hereditary cardiomyopathy. Proceedings of the National Academy of Sciences [Internet]. 2006 Jan;103(5):1388 LP – 1393. Available from: http://www.pnas.org/content/103/5/1388.abstract

5. Pugh TJ, Kelly MA, Gowrisankar S, Hynes E, Seidman MA, Baxter SM, et al. The landscape of genetic variation in dilated cardiomyopathy as surveyed by clinical DNA sequencing. Genetics in Medicine. 2014;16(8):601–8.

6. Jääskeläinen P, Heliö T, Aalto-Setälä K, Kaartinen M, Ilveskoski E, Hämäläinen L, et al. A new common mutation in the cardiac beta-myosin heavy chain gene in Finnish patients with hypertrophic cardiomyopathy. Ann Med [Internet]. 2014 Sep 1 [cited 2022 Sep 30];46(6):424–9. Available from: https://pubmed.ncbi.nlm.nih.gov/24888384/

7. Kimura Y, Kurzydlowski K, Tada M, MacLennan DH. Phospholamban Inhibitory Function Is Activated by Depolymerization. Journal of Biological Chemistry [Internet]. 1997 Jun;272(24):15061–4. Available from: http://www.jbc.org/content/272/24/15061.abstract

8. Adams PD, Arkin IT, Engelman DM, Brünger AT. Computational searching and mutagenesis suggest a structure for the pentameric transmembrane domain of phospholamban. Nature Structural Biology 1995 2:2 [Internet]. 1995 [cited 2022 Sep 30];2(2):154–62. Available from: https://www.nature.com/articles/nsb0295-154

9. Simmerman HKB, Kobayashi YM, Autry JM, Jones LR. A leucine zipper stabilizes the pentameric membrane domain of phospholamban and forms a coiled-coil pore structure. Journal of Biological Chemistry. 1996;271(10):5941–6.

10. Ceholski DK, Trieber C a., Young HS. Hydrophobic imbalance in the cytoplasmic domain of phospholamban is a determinant for lethal dilated cardiomyopathy. Journal of Biological Chemistry. 2012;287(20):16521–9.

11. Trieber CA, Afara M, Young HS. Effects of Phospholamban Transmembrane Mutants on the Calcium Affinity, Maximal Activity, and Cooperativity of the Sarcoplasmic Reticulum Calcium Pump. Biochemistry [Internet]. 2009 Oct;48(39):9287–96. Available from: https://doi.org/10.1021/bi900852m

12. Trieber CA, Douglas JL, Afara M, Young HS. The Effects of Mutation on the Regulatory Properties of Phospholamban in Co-Reconstituted Membranes†. Biochemistry [Internet]. 2005 Mar;44(9):3289–97. Available from: http://dx.doi.org/10.1021/bi047878d

13. Kimura Y, Asahi M, Kurzydlowski K, Tada M, MacLennan DH. Phospholamban Domain Ib Mutations Influence Functional Interactions with the Ca2+-ATPase Isoform of Cardiac Sarcoplasmic Reticulum. Journal of Biological Chemistry [Internet]. 1998 Jun;273(23):14238–41. Available from: http://www.jbc.org/content/273/23/14238.abstract

14. Glaves JP, Trieber C a., Ceholski DK, Stokes DL, Young HS. Phosphorylation and mutation of phospholamban alter physical interactions with the sarcoplasmic reticulum calcium pump. J Mol Biol [Internet]. 2011;405(3):707–23. Available from: http://dx.doi.org/10.1016/j.jmb.2010.11.014

15. Bamford S, Dawson E, Forbes S, Clements J, Pettett R, Dogan A, et al. The COSMIC (Catalogue of Somatic Mutations in Cancer) database and website. Br J Cancer [Internet]. 2004 Jul 19 [cited 2022 Sep 30];91(2):355–8. Available from: https://pubmed.ncbi.nlm.nih.gov/15188009/

16. Howe KL, Achuthan P, Allen J, Allen J, Alvarez-Jarreta J, Ridwan Amode M, et al. Ensembl 2021. Nucleic Acids Res [Internet]. 2021 Jan 8 [cited 2022 Sep 30];49(D1):D884–91. Available from: https://pubmed.ncbi.nlm.nih.gov/33137190/

17. Landrum MJ, Chitipiralla S, Brown GR, Chen C, Gu B, Hart J, et al. ClinVar: improvements to accessing data. Nucleic Acids Res [Internet]. 2020 Jan 1 [cited 2022 Sep 30];48(D1):D835–44. Available from: https://pubmed.ncbi.nlm.nih.gov/31777943/

18. Walsh R, Thomson KL, Ware JS, Funke BH, Woodley J, McGuire KJ, et al. Reassessment of Mendelian gene pathogenicity using 7,855 cardiomyopathy cases and 60,706 reference samples. Genet Med [Internet]. 2017 Feb 1 [cited 2022 Sep 30];19(2):192–203. Available from: https://pubmed.ncbi.nlm.nih.gov/27532257/

19. Li J, Boschek CB, Xiong Y, Sacksteder C a, Squier TC, Bigelow DJ. Essential Role for Pro in Phospholamban for Optimal Inhibition of the Ca-ATPase Essential Role for Pro 21 in Phospholamban for Optimal Inhibition of the. Society. 2005;16181–91.

20. Ha KN, Traaseth NJ, Verardi R, Zamoon J, Cembran A, Karim CB, et al. Controlling the inhibition of the sarcoplasmic Ca2+-ATPase by tuning phospholamban structural dynamics. J Biol Chem [Internet]. 2007 Dec 21 [cited 2022 Sep 28];282(51):37205–14. Available from: https://pubmed.ncbi.nlm.nih.gov/17908690/

21. Li J, Boschek CB, Xiong Y, Sacksteder CA, Squier TC, Bigelow DJ. Essential role for Pro21 in phospholamban for optimal inhibition of the Ca-ATPase. Biochemistry. 2005;44(49):16181–91.

22. Moore MJ, Adams JA, Taylor SS. Structural basis for peptide binding in protein kinase A. Role of glutamic acid 203 and tyrosine 204 in the peptide-positioning loop. J

Biol Chem [Internet]. 2003 Mar 21 [cited 2022 Oct 1];278(12):10613–8. Available from: https://pubmed.ncbi.nlm.nih.gov/12499371/

23. Ceholski DK, Trieber CA, Holmes CFB, Young HS. Lethal, Hereditary Mutants of Phospholamban Elude Phosphorylation by Protein Kinase A. Journal of Biological Chemistry [Internet]. 2012 Aug;287(32):26596–605. Available from: http://www.jbc.org/content/287/32/26596.abstract

24. Masterson LR, Cheng C, Yu T, Tonelli M, Kornev A, Taylor SS, et al. Dynamics connect substrate recognition to catalysis in protein kinase A. Nat Chem Biol [Internet]. 2010 Oct;6:821. Available from: https://doi.org/10.1038/nchembio.452

25. Verardi R, Shi L, Traaseth NJ, Walsh N, Veglia G. Structural topology of phospholamban pentamer in lipid bilayers by a hybrid solution and solid-state NMR method. Proc Natl Acad Sci U S A [Internet]. 2011 May 31 [cited 2022 Oct 1];108(22):9101–6. Available from: https://www.pnas.org/doi/abs/10.1073/pnas.1016535108

26. Simmerman HKB, Jones LR. Phospholamban: Protein structure, mechanism of action, and role in cardiac function. Physiol Rev [Internet]. 1998 [cited 2022 Oct 1];78(4):921–47. Available from: https://journals.physiology.org/doi/10.1152/physrev.1998.78.4.921

27. Whitmore L, Wallace BA. Protein secondary structure analyses from circular dichroism spectroscopy: methods and reference databases. Biopolymers [Internet]. 2008 May [cited 2023 Apr 19];89(5):392–400. Available from: https://pubmed.ncbi.nlm.nih.gov/17896349/

28. Miles AJ, Ramalli SG, Wallace BA. DichroWeb, a website for calculating protein secondary structure from circular dichroism spectroscopic data. Protein Science [Internet]. 2022 Jan 1 [cited 2023 Apr 19];31(1):37–46. Available from: https://onlinelibrary.wiley.com/doi/full/10.1002/pro.4153

29. Gustavsson M, Verardi R, Mullen DG, Mote KR, Traaseth NJ, Gopinath T, et al. Allosteric regulation of SERCA by phosphorylation-mediated conformational shift of phospholamban. Proc Natl Acad Sci U S A [Internet]. 2013;110(43):17338–43. Available from: http://www.pubmedcentral.nih.gov/articlerender.fcgi?artid=3808617&tool=pmcentrez&rendertype=abstract

30. Moolman-Smook JC, de Lange WJ, Bruwer ECD, Brink PA, Corfield VA. The origins of hypertrophic cardiomyopathy-causing mutations in two South African subpopulations: a unique profile of both independent and founder events. Am J Hum Genet [Internet]. 1999 [cited 2022 Oct 1];65(5):1308–20. Available from: https://pubmed.ncbi.nlm.nih.gov/10521296/

31. Yang J, Yan R, Roy A, Xu D, Poisson J, Zhang Y. The I-TASSER Suite: protein structure and function prediction. Nature Methods 2015 12:1 [Internet]. 2014 Dec 30 [cited 2022 Oct 1];12(1):7–8. Available from: https://www.nature.com/articles/nmeth.3213

32. Liu GS, Morales A, Vafiadaki E, Lam CK, Cai WF, Haghighi K, et al. A novel human R25C-phospholamban mutation is associated with super-inhibition of calcium cycling and ventricular arrhythmia. Cardiovasc Res [Internet]. 2015 Jul 1 [cited 2022 Oct 2];107(1):164–74. Available from: https://pubmed.ncbi.nlm.nih.gov/25852082/

33. Medeiros A, Biagi DG, Sobreira TJP, de Oliveira PSL, Negrão CE, Mansur AJ, et al. Mutations in the human phospholamban gene in patients with heart failure. Am Heart J [Internet]. 2011;162(6):1088-1095.e1. Available from: http://dx.doi.org/10.1016/j.ahj.2011.07.028

34. DeWitt MM, MacLeod HM, Soliven B, McNally EM. Phospholamban R14 Deletion Results in Late-Onset, Mild, Hereditary Dilated Cardiomyopathy. J Am Coll Cardiol [Internet]. 2006;48(7):1396–8. Available from: http://www.sciencedirect.com/science/article/pii/S0735109706018377

35. Ceholski DK, Trieber C a., Holmes CFB, Young HS. Lethal, hereditary mutants of phospholamban elude phosphorylation by protein kinase A. Journal of Biological Chemistry. 2012;287:26596–605.

36. Haghighi K, Kolokathis F, Pater L, Lynch RA, Asahi M, Gramolini AO, et al. Human phospholamban null results in lethal dilated cardiomyopathy revealing a critical difference between mouse and human. J Clin Invest [Internet]. 2003 Mar;111(6):869–76. Available from: https://doi.org/10.1172/JCI17892

37. Seidel K, Andronesi OC, Krebs J, Griesinger C, Young HS, Becker S, et al. Structural Characterization of Ca2+-ATPase-Bound Phospholamban in Lipid Bilayers by Solid-State Nuclear Magnetic Resonance (NMR) Spectroscopy,. Biochemistry [Internet]. 2008 Apr;47(15):4369–76. Available from: https://doi.org/10.1021/bi7024194

38. Arkin IT, Rothman M, Ludlam CFC, Aimoto S, Engelman DM, Rothschild KJ, et al. Structural model of the phospholamban ion channel complex in phospholipid

membranes. J Mol Biol [Internet]. 1995 May 12 [cited 2022 Sep 28];248(4):824–34. Available from: https://pubmed.ncbi.nlm.nih.gov/7752243/

39. Sabater-Molina M, Pérez-Sánchez I, Hernández del Rincón JP, Gimeno JR. Genetics of hypertrophic cardiomyopathy: A review of current state. Clin Genet [Internet]. 2018 Jan 1 [cited 2022 Oct 3];93(1):3–14. Available from: https://pubmed.ncbi.nlm.nih.gov/28369730/

40. Richard P, Charron P, Carrier L, Ledeuil C, Cheav T, Pichereau C, et al. Hypertrophic cardiomyopathy: distribution of disease genes, spectrum of mutations, and implications for a molecular diagnosis strategy. Circulation [Internet]. 2003 May 6 [cited 2022 Oct 3];107(17):2227–32. Available from: https://pubmed.ncbi.nlm.nih.gov/12707239/

41. Douglas JL, Trieber C a., Afara M, Young HS. Rapid, high-yield expression and purification of Ca2+-ATPase regulatory proteins for high-resolution structural studies. Protein Expr Purif [Internet]. 2005 Mar;40(1):118–25. Available from: http://www.sciencedirect.com/science/article/pii/S1046592804004036

42. Fisher ME, Bovo E, Aguayo-Ortiz R, Cho EE, Pribadi MP, Dalton MP, et al. Dwarf open reading frame (Dworf) is a direct activator of the sarcoplasmic reticulum calcium pump serca. Elife. 2021 Jun 1;10.

43. Smeazzetto S, Armanious GP, Moncelli MR, Bak JJ, Lemieux MJ, Young HS, et al. Conformational memory in the association of the transmembrane protein phospholamban with the sarcoplasmic reticulum calcium pump SERCA. Journal of Biological Chemistry. 2017;292(52):21330–9.

44. Warren GB, Toon P a, Birdsall NJ, Lee a G, Metcalfe JC. Reconstitution of a calcium pump using defined membrane components. Proc Natl Acad Sci U S A. 1974;71(3):622–6.

45. Skene-Arnold TD, Luu HA, Uhrig RG, De Wever V, Nimick M, Maynes J, et al. Molecular mechanisms underlying the interaction of protein phosphatase-1c with ASPP proteins. Biochem J [Internet]. 2013 Feb 1 [cited 2023 Apr 19];449(3):649–59. Available from: https://pubmed.ncbi.nlm.nih.gov/23088536/

46. Zhou Y, Millott R, Kim HJ, Peng S, Edwards RA, Skene-Arnold T, et al. Flexible Tethering of ASPP Proteins Facilitates PP-1c Catalysis. Structure [Internet]. 2019 Oct 1 [cited 2023 Apr 19];27(10):1485-1496.e4. Available from: https://pubmed.ncbi.nlm.nih.gov/31402222/

47. Jo S, Kim T, Iyer VG, Im W. CHARMM-GUI: a web-based graphical user interface for CHARMM. J Comput Chem [Internet]. 2008 Aug [cited 2023 Apr 19];29(11):1859–65. Available from: https://pubmed.ncbi.nlm.nih.gov/18351591/

48. Salomon-Ferrer R, Götz AW, Poole D, Le Grand S, Walker RC. Routine microsecond molecular dynamics simulations with AMBER on GPUs. 2. Explicit solvent particle mesh ewald. J Chem Theory Comput [Internet]. 2013 Sep 10 [cited 2023 Apr 19];9(9):3878–88. Available from: https://pubs.acs.org/doi/abs/10.1021/ct400314y

49. Tian C, Kasavajhala K, Belfon KAA, Raguette L, Huang H, Migues AN, et al. ff19SB: Amino-Acid-Specific Protein Backbone Parameters Trained against Quantum Mechanics Energy Surfaces in Solution. J Chem Theory Comput [Internet]. 2020 Jan 14 [cited 2023 Apr 19];16(1):528–52. Available from: https://pubmed.ncbi.nlm.nih.gov/31714766/

50. Humphrey W, Dalke A, Schulten K. VMD: Visual molecular dynamics. J Mol Graph [Internet]. 1996 [cited 2023 Apr 19];14(1):33–8. Available from: https://pubmed.ncbi.nlm.nih.gov/8744570/